Tomas Bata University in Zlín

Doctoral thesis

Tailoring of polylactide properties and its degradation behaviour through various modification approaches

Úprava vlastností a degradačního chování polylaktidu pomocí různých modifikačních přístupů

Author: **Ing. Gabriela Jandíková**

Study program:P2808 / Chemistry and material technology

Study course:2808V009 / Chemistry and material technology

Supervisor:doc. Ing. Vladimír Sedlařík, Ph.D.

Consultant:Ing. Petr Stloukal, Ph.D.

August 2016, Zlín

Klíčová slova: *biodegradabilní polymery, testování biorozložitelnosti, modifikace vlastností a stability PLA*

Keywords: *biodegradable polymers, biodegradability testing. PLA properties and stability testing*

Plná verze disertační práce je dostupná v Knihovně UTB ve Zlíně.

TABLE OF CONTENS

ACKNOWLEDGEMENTS

I would like to thank all people who helped me through my doctoral studies.

First of all, I would like to thank to my supervisor Assoc. prof. Vladimír Sedlařík, for his professional leading and for giving me the base ideas of this work

My sincere acknowledgement also belong to my consultant Ing. Petr Stloukal, Ph.D., who guided me through the polymer degradation issue and provided me with valuable advices.

My special thanks belong also to all of my colleagues for very friendly working environment.

Finally, I am deeply grateful to my family and my best friends for their support during my studies.

ABSTRAKT

Tato práce se zaměřuje na úpravu materiálových vlastností a degradačního chování polyesterů na bázi polylaktidu prostřednictvím modifikace polymerní matrice pomocí specifických přísad. Teoretická část práce přináší přehled současného stavu poznání v oblasti degradovatelných polymerů, mechanismu jejich degradace a metodologii testování biodegradace. Experimentální část se pak soustředí na tři způsoby úpravy degradačního chování polylaktidu prostřednictvím jeho modifikace s antihydrolytickým činidlem, chemicky povrchově upravenými přírodními vlákny a hybridními plnivy. Nová metoda pro popis degradačního chování polylaktidu pomocí dielektrické relaxační spektroskopie byla v rámci této práce také testována a optimalizována.

ABSTRACT

Tailoring of the material properties and degradation behaviour of polylactide based polyesters through their modifications with specific compounds or the addition of the specific fillers were objectives of this work. The theoretical part brings state of art in the field of environmentally degradable polymers, degradation mechanisms and methodology of the biodegradation testing. Experimental part aims at three approaches for polylactide degradation behaviour through its modification with anti-hydrolysis agent, surface chemically treated natural fibres and hybrid fillers. The novel method for polylactide degradation process characterization by using dielectric relaxation spectroscopy was also tested and optimized within the experimental part.

THEORETICAL BACKGROUND

Introduction

Biodegradable polymers are natural (bio-based) or synthetic polymers that are decomposed in environment by action of microorganism. They generally possess comparable physicochemical properties and processability with conventional petroleum-based polymers. Therefore, in the last decades a significant progress in biodegradable polymers has been observed and the polymers have been widely investigated as a replacement of conventional plastic in various applications, especially in short-term usage in agriculture (mulching films), packaging, disposal dishes and area of medicine (e.g. drug delivery systems, sutures, implants). However, there is an effort to extend the range of utilization in industry sectors such as electronics and automotive. These applications require materials with good stability and thermal and mechanical properties, which can be supplied by various modifications of polymer matrix.

The polymer stability or degradability represents one of the crucial parameter for products end-use. Polymers are during processing and also during life time exposed to many types of factors, which can caused changes in chemical and physical properties. Therefore, the knowledge of the degradable processes can enable the prediction of the material behaviour during processing and usage.

The theoretical part brings an overview of the current state in a field of biodegradable polymers, biodegradability estimation techniques and possibilities in modification of environmental stability of polymers. Experimental part aims at three approaches for polylactide degradation behaviour through its modification with anti-hydrolysis agent, surface chemically treated natural fibres and hybrid fillers. The novel method for polylactide degradation process characterization by using dielectric relaxation spectroscopy was also tested and optimized within the experimental part.

1. Environmentally degradable polymers

Environmentally degradable polymers may be described according to the standard ISO 472 as a material which is designed to undergo a significant change in its chemical structure under specific environmental conditions. These changes resulting in a loss of properties. The degradation can be carried out in two ways according to factors, which initiate the process. The first one is abiotic mechanism, where the disintegration is caused by moisture, light, temperature, mechanical impact etc. [1, 2, 3, 4]. The second mechanism is based on the action of living organisms. However, both mechanisms are in close synergy and usually the abiotic degradation is the pre-step, where the molar mass is reduced and further more easily metabolisable fragments are formed [3, 5].

1.1. Biodegradable polymers

Biodegradable polymers are designed to degrade by the action of microorganisms (e.g. bacteria, fungi) with the resulting products CO_2, CH_4, water and biomass. Biodegradable polymers can be classified as natural or synthetic biodegradable polymers according to their origin [6]. The way of the catalysis of biodegradation process may also vary. In particular, the polymers synthesized from natural resources are sensitive to enzymatic degradation and synthetic polymers can be usually considered as the hydrolytically degradable polymers [7]. Nowadays, biodegradable polymers have been extensively investigated as a replacement of conventional polymers in various applications in packaging, agriculture and medical field.

1.1.1.Natural biodegradable polymers

Polymers, which are synthesized or formed in natural environment during the growth cycles of organisms, are referred as natural polymers [8]. Those polymers contain labile bonds that are degradable directly with action of enzymes [3]. Microbial biopolymers are produced either directly via fermentation or by chemical polymerisation of monomers, which are produced through fermentation [9]. Many biopolymers are biocompatible and have no adverse effects on biological systems. Therefore, their utilization is mainly in biomedical applications [7]. Biopolymers can be divided into three major classes according to their chemical structure: polysaccharides, polypeptides and bacterial polyesters.

Polysaccharides are carbohydrate polymers formed from more than 2 monosaccharide units (Figure 1) linked together by glycosidic linkages. They play critical roles in a wide range of biological, biochemical, and physical processes, including cellular metabolism, signalling and adhesion [10]. Cellulose, starch and their derivatives have been the major focus of interest. They represent an interesting alternative for synthetic polymers where long-term durability is not desirable and rapid degradation is an advantage [11]. Starch is composed of two structural units: linear amylose and branched amylopectin. Cellulose is the most widespread polymer on the earth. It is recovered from wood after removal of hemicellulose and lignin. Starch and cellulose based materials can be used in a wide range of applications such as disposal products, packaging, personal care etc. However, the increasing attention is being paid to the polysaccharides, which are produced by living organisms, such as hyaluronic acid, chitin, chitosan, xanthan, etc. [6, 12]. For instance, chitosan, which is obtained by deacetylation of chitin, represents promising antibacterial substance with natural origin.
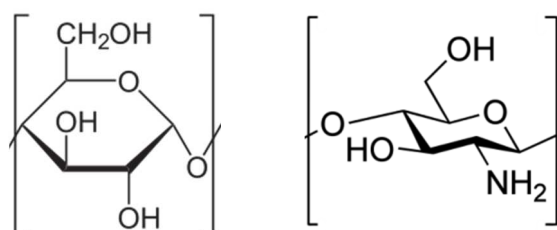

Figure 1 – From the left: stuctural units of cellulose/starch and chitosan.

Proteins are polymers composed by regularly arranged different types of alfa amino acids which are connected with peptide bond (formed according to reaction in Figure 2) and are folded into a three-dimensional structure. The proteins play several functions in the nature: structural (collagen, keratin, elastin), transport and storage function (hemoglobin), catalytic (enzymes, hormones) and protection (immunoglobulin). Being a major component of many tissues, proteins are preferably used in pharmaceutical and biomedical applications as a material for scaffolds for tissue engineering, sutures and drug delivery systems [6, 7]. Well-known and most utilized proteins are e.g. collagen/gelatin, casein, albumin, soy protein, zein [11, 12].

amino acid
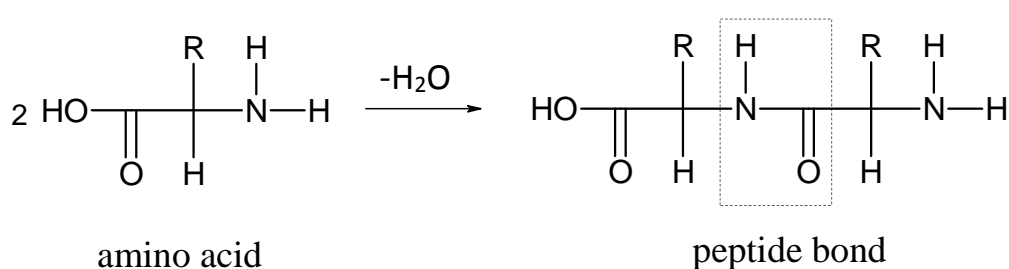
peptide bond

Figure 2 – Polycondensation of amino acids resulting peptide bond.

The third class of biopolymers are **poly(β-hydroxyalkanoate)s (PHAs)**, the natural polyesters, which are synthesized biochemically by microbial fermentation. In Figure 3 is a schematic structure of PHA where R can be substituted by e.g. methyl and ethyl groups representing Poly(β-hydroxybutyrate) (PHB) and poly(-hydroxyvalerate) (PHV), respectively. One of the most investigated member of the PHAs, Poly(β-hydroxybutyrate), occurs in bacteria cells as a carbon and energy storage compound in wide variety of bacteria. PHB has potential in applications as degradable plastics. However, its high crystallinity, which causes the brittleness, limits the usage. Therefore, copolymers containing other hydroxyalkanoate units are preferred [11, 13].
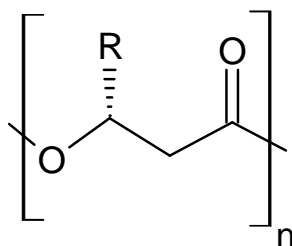
Figure 3 - Structure of poly(β-hydroxyalkanoate)s PHAs.

1.1.2. Synthetic biodegradable polymers

Opposite to natural polymers, synthetic biodegradable polymers possess biological inertness and more predictable properties, which can be better tailored to give a wider range of applications [14]. Moreover, a batch-to-batch uniformity is obtained [7]. These properties make synthetic biodegradable polymers suitable for more versatile and diverse biomedical applications [15]. Biodegradation has been accomplished by scission of hydrolytically unstable linkages in the backbone, like esters, amides, anhydrides and urethanes [14].

Polyesters are thermoplastic polymers with aliphatic ester linkages in their backbone, which are generally easily hydrolyzed. Polyesters can be obtained from wide range of monomers via ring-opening and condensation polymerization [7]. Due to their biodegradability, bioresorbability, and biocompatibility, the polyesters represent the most extensively and the most widely used biodegradable material in medicine [7, 16]. Several polyesters, such as poly(lactic acid) (PLA), poly(glycolic acid) (PGA), poly(ε-caprolactone) (PCL) and their copolymers, are produced on semi-commercial scale. The broad field of usage of polyesters has been defined, from disposable products (cutlery, cups, plates), packaging up to drug delivery systems, tissue engineering and medical products (implants, sutures) [16, 17, 18, 19].
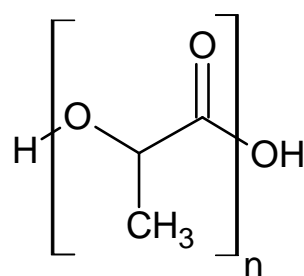

Figure 4 - Chemical structure of PLA.

Nowadays, PLA is one of the most utilized and investigated polymer in the group of polyesters. It is a linear polyester synthesized either from lactic acid by condensation reaction or by ring-opening of cyclic lactide. According to monomer, two products are then synthesized, poly(lactic acid) or polylactide. To simplify this, both products are called PLA. The lactic acid exhibits two optical activities: L(+) and D(-). Resulting poly(L-lactic acid) (PLLA) and poly(D-lactic acid) (PDLA) are semicrystalline polymers with relatively slow rate of hydrolysis. However, poly(D,L-lactic acid) (PDLLA) has an amorphous structure with better ability to hydrolysis. [20, 21, 22]

The group of biodegradable *polyurethanes* usually exhibits good mechanical properties and desirable biocompatibility, which are expected to be important characteristics for biomedical materials [23, 24]. Polyurethanes are generally comprised of two chemically different parts connected with urethane linkages: soft segment based on easily hydrolyzable polyols (PCL, PGA, PLA) and the diisocyanate with chain extender (rigid segment) [23, 25]. The rigid part provides polymer strength and lower ability to degrade than the soft part due to better susceptibility of ester bones to hydrolytic degradation than the urethane bonds. Therefore, physicochemical properties and the rate of the degradation can be tailored by the ratio of soft to rigid segment and chemistries of the soft segments. [26]

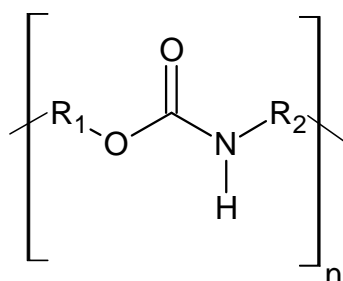*Figure 5 – Scheme of chemical structure of polyurethanes.*

The biodegradability of polyurethanes can be possibly provided if the natural biopolyols have been used for their synthesis. The biopolyols are derived from vegetable oils and thus, they are classified as biobased material. However, the natural origin of these polyols may not guarantee the biodegradability of the resulting polyurethane. [27, 28]

Polyamides may be also very useful for medical purposes [29]. They dispose excellent mechanical properties. Well-known polyamides are polyamide 6 and 66. However, they are limited with the low rate of biodegradation, which is related to their high crystallinity and hydrophobicity [6, 30]. They are often classified as nondegradable polymers. Nevertheless, in the recent years, sustained efforts have been devoted to increase the ability of polyamides to degrade. The solution is polyamide 4 (PA 4), a polymer of γ-aminobutyric acid which has been described as a biodegradable polymer [31]. Yamano et al. have tested the PA 4 biodegradability in active sludge [32], Hashimoto et al. in soil [33] and Kawasaki et al. described the biodegradation of branched PA 4 [31]. Moreover, composites including amide and ester groups are suggested and investigated as polymers with good properties and degradability, where the degradability of copolymers is increasing with ester bonds contents [7, 11].
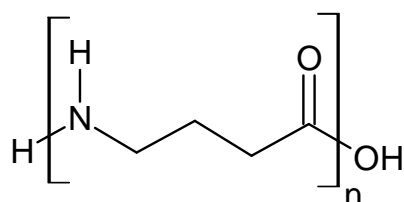
Figure 6 - Chemical structure of Polyamide 4.

As a biodegradable polymers are reported also ***polyanhydrides***, which are classified as most hydrolytically labile polymers due to their aliphatic anhydride bonds in the backbone [7]. Mechanism of the degradation is based mainly on the surface erosion and degrades uniformly into non-toxic metabolites that are non-mutagenic, non-cytotoxic and non-inflammatory [34]. Owing to those properties, polyanhydrides are widely used for drug delivery systems preparation [6].

Figure 7 - Scheme of chemical structure of polyanhydrides.

1.2. Oxo-biodegradable polymers

Special group of the biodeagradable materials are oxo-biodegradable polymers, which may represent the solution between affordable (in comparison with intrinsically biodegradable polymers) and environmentally friendly materials. These materials are based on 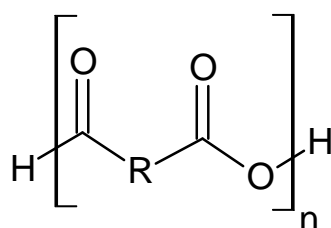the commonly used synthetic polymers, such as polyethylene (PE), containing substances with prodegradant activity, known as pro-oxidants [35]. The most commonly used pro-oxidants are transition metal ion (e.g. Fe, Co, Mn, Ti, Zn, Cu) complexes which promote the abiotic (photo or thermal) oxidation in order to accelerate fragmentation, reduction of the molar mass and to form oxygenated groups, which are then easily metabolized by microorganisms [3, 36]. The oxo-biodegradable materials are already commercially available especially in food packaging (e.g. shopping bags) and in agriculture as mulching foils [36, 37].

However, the ability of these plastics to fully biodegrade is still questionable. For example, Yashchuk et al. investigated polyethylene film with commercial pro-oxidant when the complete mineralization had not been achieved after 90 days of incubation at 55 °C [38]. On the other hand, Mehmood et al. suggested modified LDPE with dye sensitized titania and starch blend as environmentally friendly material which could be degraded at an accelerated pace in a real environment [39].

2. Degradation mechanisms

The degradation mechanism of polymer matrix is characterized by changes in polymer structure caused by chemical, physical or biological effects which lead to chain scission and formation of new functional groups. These changes may be reflected in changes in optical, mechanical and electrical properties of material. [40]

Degradation of polymers may be promoted by different mechanisms initiated by action of environmental factors (see Figure 8) and their combination. According to initiators, two ways of degradation are established: abiotic and biotic degradation.

Figure 8 - Environmental factors influencing polymer degradation.
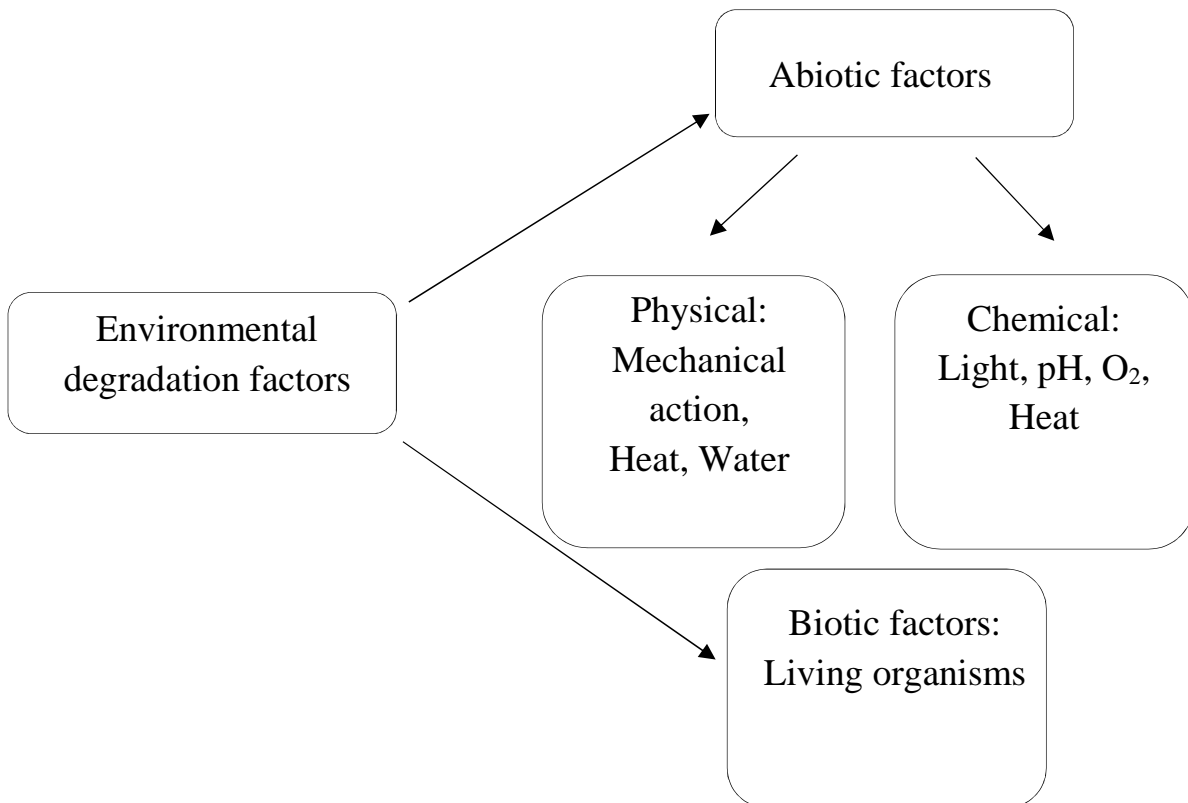
Figure 8 - Environmental factors influencing polymer degradation.

2.1. Abiotic degradation

As mentioned in the scheme above, the abiotic degradation may be caused by two factors: physical and chemical. However, practically these processes are often in close synergy and the action of only one factor occurs only rarely. There are several environmental factors that can initiate the degradation, e.g. moisture, light, temperature and pH. Generally, the abiotic degradation is based on distortion without microorganism contribution.

2.1.1. Physical degradation

Physical mechanisms of abiotic degradation are considered as processes where the decomposition is based on an action causing only physical changes in the polymer structure, such as melting, dissolution, swelling, etc. Physical changes can be induced by action of water, mechanical loading (compression, tension, shear force) or increasing temperature. The degradation may principally lead to decrease of end-use properties of products (shape changes, surface erosion, weight loss). [40, 41, 42]

2.1.2. Chemical degradation

The mechanism of the chemical degradation is based on processes where chemical changes in the polymer structure occur. These changes can be characterized by reduction of MW and transformation of chemical composition due to chain scission. Chemical degradation may be triggered by the exposure to e.g. electromagnetic irradiation, heat, atmospheric form of oxygen and specific chemicals. [1, 5, 12] However, the effects of irradiation, heat and oxygen are often in close synergy. Therefore, the degradation by irradiation and heat often takes place with the participation of oxygen and photooxidation and thermooxidation, are proposed to be the main mechanisms during the degradations.

Photodegradation

The action of electromagnetic radiation, especially of the light radiation, is one of the most important parameters of abiotic degradation. Following radiations with characteristic wavelength (λ) play the significant role in the polymer photodegradation:

- Infrared radiation ($\lambda \sim 760$ nm – 1 mm)
- Visible light ($\lambda \sim 400$–750 nm)
- UV radiation ($\lambda \sim 10$–400 nm)
- X-ray radiation ($\lambda \sim 0.01$–10 nm)
- γ-radiation ($\lambda < 0.01$ nm)

However, many polymers, such as polyolefins, when exposed to light have tendency to absorb the UV-B and UV-A radiation [5]. Moreover, only the UV-B (~ 295–315 nm) and UV-A (~ 315–400 nm) radiation induce direct photolysis or photooxidation of polymers, whereas the visible light and infrared radiation are generally responsible for acceleration of thermal oxidation [40]. The depolymerisation is initiated by absorption of photons energy (E), which is characterized (Equation 1) by direct relation to Planck constant ($h = 6.626 \cdot 10^{-34}$ J·s) and frequency (v, s^{-1}):

$$E = h \cdot v \tag{1}$$

The absorbed energy is responsible for the creation of unstable states in molecules, free radicals initiate further breakdown of the polymeric bonds. The polymer photodegradation may be ascribed mainly to oxidative reaction, where free radicals (P•) react with oxygen to produce a polymer peroxy radical (POO•). Further the chain propagation is carried out by reaction of peroxy radical with another polymer chain to generate polymer hydroperoxide (POOH) and a new polymer alkyl radical (P•). This process is schematically depicted in Figure 9. [43]

Norrish reactions may also describe the photolysis mechanism (see Figure 3). According to Norrish I, free radicals are generated or chain scission of the polymers is caused, which is known as Norrish II mechanism [1, 44]. The Norrish II has been described e.g. during the polyethylene and polylactide photodegradation [2, 45].

$$P \xrightarrow{h v/\text{heat}/O_2} 2P \cdot$$
$$P \cdot + O_2 \rightarrow POO \cdot$$
$$POO \cdot + PH \rightarrow POOH + P \cdot$$
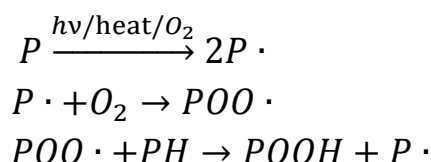
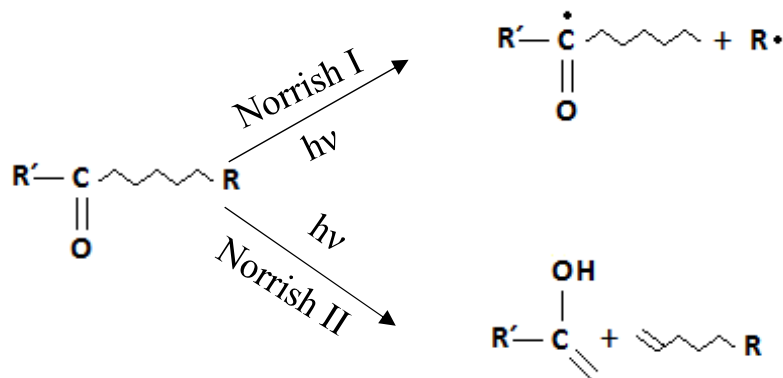*Figure 9 - Simplified scheme of photooxidation of polymer.*

Figure 10 - Mechanism of the Norrish reactions.

Sensitivity to photodegrade may be significantly increased by impurities that are present in manufactured products and also by blending with the light-absorbing species like carbonyl groups, hydroperoxides, dienes, trienes and aromatic compounds [2]. Besides these factors, the additives based on the transition metal ions (Fe^{3+}, Ti^{4+}, Zn^{2+}) are widely used as prooxidants. [5, 36, 46] They initiate the decomposition of peroxides to form free radicals for reaction initiation:

$$ROOH + Me^+ \rightarrow RO \cdot + HO^- + Me^{2+}$$
$$ROOH + Me^{2+} \rightarrow ROO \cdot + H^+ + Me^+.$$
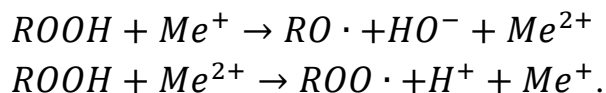
Thermal degradation

Thermal degradation of polymers can be characterized by a molecular deterioration as a result of overheating. The direct chain scission, thermolysis, is caused usually by higher temperatures (T > 400 °C). However, the thermal degradation usually occurs during polymer processing, when the melt temperature (100–200 °C) is reached and the components of long chain backbone break down by molecular scission leading to decrease in molar mass. [47]

The scission during the lower temperatures is attributed to thermooxidative reaction. The mechanism of oxidation initiated by heat is similar to photo-oxidation (Figure 9) with only one difference in the initiator. The extreme case of thermal oxidation is combustion which leads to low molecular products or up to carbon. [48]

The rate of thermal degradation can be also increased by prooxidants on the transition metal ions principle. Suitable for thermooxidation are e.g. ions of Co, Mn [49].
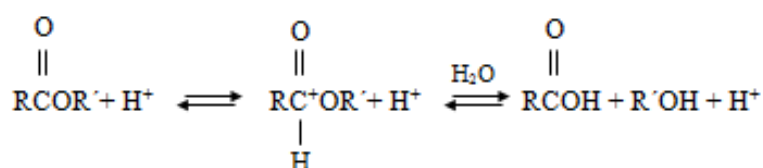
Oxidative degradation

There are two types of polymers oxidation, direct oxidation caused by reaction with acids and oxidising agents and the process of auto oxidation which is provoked by atmospheric forms of oxygen (O_2, O_3). During the autooxidation, the oxygen attacks peroxides bonds producing free radicals. These oxidations can be contributing or synergic to light degradation to produce free radicals. Resulting peroxyl radicals can further lead to crosslinking reactions and chain scission. However, the autooxidation has several limitations, such as diffusion of the oxygen. [1, 40]

Hydrolysis

Abiotic hydrolysis is carried out by reaction with H_2O. Therefore, the degradation takes place if the polymer contains hydrolysable bonds (e.g. ester, ether, anhydride, amide, urethane etc.) [1]. Hydrolysis is dependent on factors like hydrophilicity of polymer, temperature, pH and time [50].

Hydrolysis is divided according to initiators of the reaction into depolymerisations in alkaline or acidic environment [1]. Both principles are illustrated in the simple scheme below (Figure 4).

Acidic hydrolysis:

$$\underset{\text{RCOR'}}{\overset{\overset{\displaystyle O}{\|}}{}} + H^+ \rightleftharpoons \underset{\substack{| \\ H}}{\overset{\overset{\displaystyle O}{\|}}{RC^+OR'}} + H^+ \overset{H_2O}{\rightleftharpoons} \overset{\overset{\displaystyle O}{\|}}{RCOH} + R'OH + H^+$$

Alkaline hydrolysis:

$$\underset{\text{RCOR'}}{\overset{\overset{\displaystyle O}{\|}}{}} + {}^-OH \rightleftharpoons \underset{\substack{| \\ OH}}{\overset{\overset{\displaystyle O}{|}}{RC^-OR'}} + H^+ \overset{H_2O}{\rightleftharpoons} \overset{\overset{\displaystyle O}{\|}}{RCOH} + R'OH + {}^-OH$$
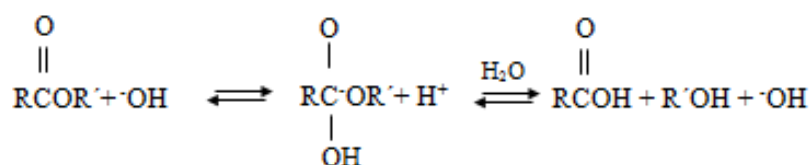
Figure 11 - Scheme of acidic and alkaline hydrolysis of polymers.

2.2. Biotic degradation

Biodegradation is defined as a decomposition of organic substances by the action of microorganisms. Particularly two types of microorganism participate on the degradation of polymers: bacteria and fungi. Their action leads to the polymer mineralisation with main end-products including new biomass, water, carbon dioxide and methane. [6] According to availability of the oxygen, there are two metabolic processes of the substrate (polymer) mineralization:

Aerobic

$$C_{substrate} + O_2 \longrightarrow CO_2 + H_2O + C_{biomass}$$

Anaerobic

$$C_{substrate} \longrightarrow CO_2 + H_2O + CH_4 + C_{biomass}$$
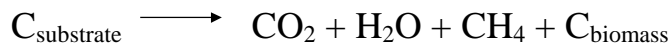
The biodegradation is generally considered as a heterogeneous process including several steps.

2.2.1. Extracellular depolymerisation – fragmentation

Polymers are generally molecules with high molecular weight unable to cross the cell wall and/or cytoplasmic membrane. Therefore, the first step is the depolymerisation of the large macromolecules outside the cells into the oligomers and monomers. It is called extracellular depolymerisation and it is a necessary phenomenon for the subsequent step called assimilation. The fragmentation is performed, in many cases, by the microorganism excreted extracellular enzymes. [1]

The enzymes are divided according to their function as follows:

- Oxidoreductases – catalyse the transfer of electrons
- Transferases – enable transfer of specific groups
- Hydrolases – catalyse the hydrolysis
- Lyases – catalyse the breaking of various bonds (other than hydrolysis or oxidation)
- Isomerases – catalyse isomeric reactions
- Ligases – catalyse bonding of two molecules by covalent bonds.

Nevertheless, the oxidoreductases and the hydrolases take place in most cases of biofragmentation of polymers [6].

Besides the enzymes action during the extracellular depolymerisation, abiotic physical and chemical effects, such as hydrolysis, thermal degradation, oxidation or photodegradation, can also initiate the cleavage of the polymer chains. For instance, biodegradation of PLA is directly initiated by hydrolysis without contribution of microorganisms [17]. Photooxidation has been investigated to initiate the biodegradation of polyethylene [38]. In these cases, usually, the prooxidants are added into the polyethylene matrix.

The polymer fragments can pass the cellular membranes in two ways: passive or active. Diffusion of small pieces or their transport inside the cell through the specific membrane carriers are considered as a passive transport.

Active transport is described as biotransformation reactions, where the transported molecules are modified into the suitable molecules, which can passed inside the cell. They are generally oxidised through catabolic pathways that lead to the production of adenosine diphosphate (ADP) and phosphates by adenosine triphosphate (ATP) hydrolysis. The transport of the bigger molecules is mediated by vesicular transport. [1, 6] Exocytosis is known as transport from

the cell to extracellular environment. When the molecules move in, the process is called endocytosis and there are two types [51]:

- pinocytosis – transfer of liquids and small molecules, implemented by every cell
- phagocytosis – transfer of solids, implemented by e.g. macrophage.
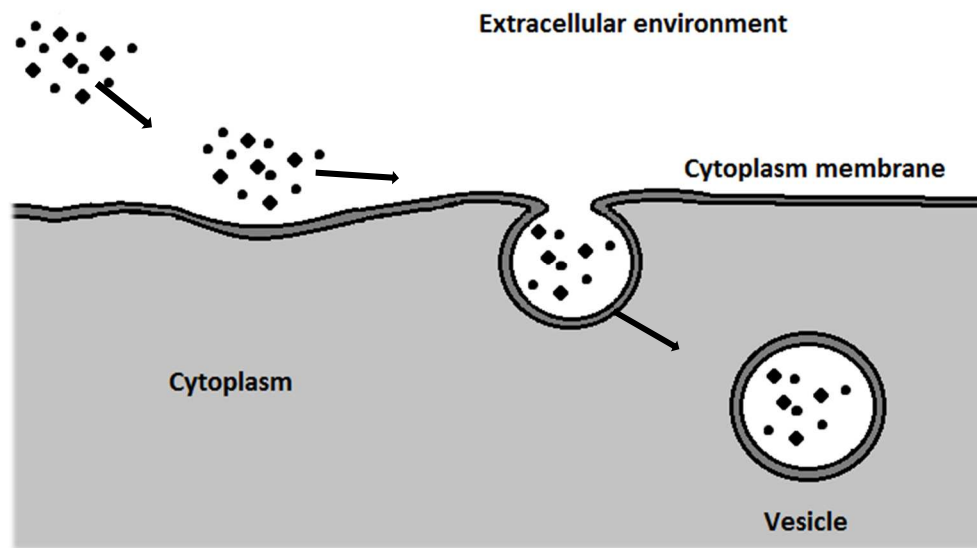
Figure 12 - Scheme of pinocytosis mechanism.

2.2.2. Intracellular processes

The process of mineralisation takes place inside the cell and poses a source of energy, electrons and elements, which are important for microorganism growth and reproduction. The microorganisms can utilize the substrate (polymer) by processes of dissimilation (cells respiration, fermentation) and assimilation (nutrients supplying, production of new biomass) which are conducted by various biochemical cycles in the cell (e.g. Krebs cycle, pentose phosphate or glycolysis cycle, etc.). The end-products of these intracellular processes are energy, CO_2, H_2O and new biomass. [1]

3. Biodegradability estimation techniques

As described in previous chapters, polymers are during the biodegradation subjected to physical and chemical changes that influence their properties. Therefore, the rate of polymer biodegradation can be characterized by evaluation of these changes by several estimation techniques.

3.1. Monitoring of polymer biodegradability

Many parameters influence the biodegradation process, not only parameters influencing the ability of polymers to degrade but also crucial factors affecting the microbial activity. Factors, such as humidity, temperature, pH, presence/absence of oxygen and the supply of different nutrients significantly affect the rate of polymers biodegradation. Therefore, these conditions must be considered during the determination of plastics biodegradability. [6, 40]

According to the presence of oxygen, the biodegradation processes can be divided into aerobic and anaerobic. Aerobic processes are involved in decomposition in wastewater, surface water, in organic waste (compost, landfill). Anaerobic mechanisms take place during degradation processes in e.g. anaerobic sediments and anaerobic sludge.

The biodegradability testing can be conducted under laboratory conditions (in vitro) or in the natural environment. There are several advantages of laboratory investigations, such as good results reproduction, easily observed physical and chemical properties and the acceleration of usually long-term degradation (by increasing temperature). On the other hand, the testing in real environment gives the actual results about product behaviour in natural environment. However, testing in natural conditions has some drawbacks (unstable climate, long lasting experiment, unpredictable conditions, etc.). [52]

The biodegradability examination can be carried out using several types of medium. The most frequently used are:

- Test in aqueous environment – sewage, liquids simulating in vivo conditions, aqueous medium with specific enzymes

- Controlled composting test – aerobic process of conversion of organic substrate to compost

- Active composting – specific conditions (temperature 58 °C, humidity 50 %)
- Passive composting – long term experiment, lower temperature (30 °C)
- Composting in natural way

- Soil burial test – decomposition of products in soil

- In vivo testing

Biodegradation can be estimated by several methods: those pertaining to the polymer (substrate), to the microorganisms, or to the reaction products. Therefore, the biodegradation process can be, for common purposes, studied and evaluated according to the following parameters:
- Changes in polymer properties
- Depletion of substrate (polymer)
- Microbial growth
- Reaction products

3.1.1. Visual observations

The method of visual observation can be considered as first indication of a microbial attack. Visible changes caused by degradation include surface roughening, changes in colour, formation of holes and cracks, formation of biofilm on the surface. The more detailed observation of these effects can be obtained using scanning electron microscopy (SEM) or atomic force microscopy (AFM). In the picture below (Figure 5), there can be seen the sample of PLA after the biodegradation with clearly visible colonies of bacteria on its surface indicating microbial activity.
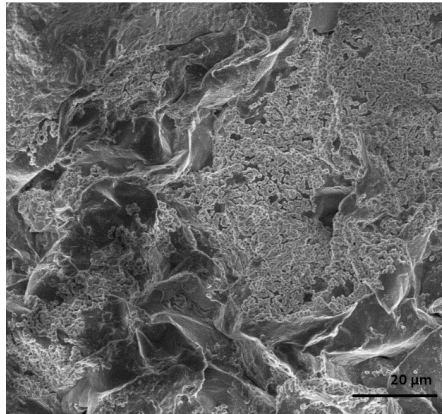
Figure 13 - SEM micrograph of PLA after biodegradation.

3.1.2. Monitoring of physical and chemical properties

Changes in physical properties are closely related with chemical changes in polymer structure. For instance, mechanical properties such as tensile strength depend very closely on changes in molar mass of polymers. This can be also applied for thermal properties and thermal stability. [52]

However, if the polymer is subjected to abiotic degradation in the first stage of biodegradation, the depolymerisation often takes place in bulk and can be indicated directly with tensile strength measurement. This type of measurement is often used for materials where the abiotic processes take place, such as PLA hydrolysis or polyethylene oxidation.

Besides the reduction of the molar mass, the degradation can be characterized also by changes in composition (creation of new bonds and end groups) or/and in amount of total organic carbon, which is during the degradation consumed by microorganisms or released into the surrounding environment. The reduction of polymer molar mass is usually accompanied by weight loss caused by microbial metabolism of low-molecular products (erosion). Analytical methods, which are commonly used for determination of these changes, are listed below.

Methods for determination of physical properties:
- Mechanical tests
- Thermal analysis
    - Differential scanning calorimetry (DSC)
    - Thermogravimetric analysis (TGA)

Methods for determination of chemical composition and structure:
- Chromatography
    - Gel permeation chromatography (GPC)
    - Gas chromatography (GC)
    - High performance liquid chromatography (HPLC)

- Spectroscopy
    - Fourier transform infrared spectroscopy (FTIR)
    - Nuclear magnetic resonance (NMR)

- Elemental analysis
    - Total organic carbon analysis (TOC)

3.1.3. Monitoring of microbial growth

Testing of the microbial activity can also point out the biodegradability of material. The method is based on the clear zone technique. It is a very simple method where the polymer is dispersed to create a fine suspension in an agar gel as the sole carbon source (opaque appearance). After inoculation and incubation with microorganisms, a clear zone appears in surrounding of the inoculum, which indicates the polymer utilization (depolymerisation) by microorganisms. [53]

Figure 14 - Formation of clear zone after incubation.

3.1.4. Analysis of reaction products

During the polymer mineralisation, the process of dissimilation is carried out. It is based usually on oxygen consumption (aerobic systems) or evolution of metabolic end-products in gas state (CO_2, CH_4). Analysis of these products can be considered a good biodegradation indicator. For this purpose, respiration tests (Chapter 3.2.) are the most often used methods to measure biodegradation in laboratory conditions.

3.1.5. Other methods

Some other analytical methods to monitor biodegradability can be applied [40, 52]:

- Radiolabelling – Measurement of slowly degradable materials. Process based on incorporation of radioactive ^{14}C in polymers and comparison of the amount of produced radioactive $^{14}CO_2$ and $^{14}CH_4$ to the original radioactivity of the labelled polymer.

- Dissolved carbon measurement – determination of dissolved organic carbon content in medium.

- pH measurement – estimation of changes in pH caused by formation of free acids through enzymatic polyester cleavage.

- Dielectric spectroscopy - a very useful tool to study the changes in polymer structure caused by the biodegradation. By the observation of relaxation spectra (dielectric permittivity $\varepsilon´$ and $\varepsilon´´$) can be described changes in dynamics of various relaxation processes. α relaxation generally relates to the Brown motion of the main chain, which caused the glass transition and β relaxations can be associated with rotation of side groups or with local movements of main chain. Reduction of molar mass enables better mobility of the chains due to more free volume, which is reflected then in the relaxation processes. [54, 55]

3.2. Respiration tests

Aerobic microbial activity is typically characterized by *the utilisation of oxygen.* Thus, a measurement of the amount of utilized oxygen, defined as the biochemical oxygen demand (BOD), can express the degree of biodegradation. The closed bottle BOD measurements have been designed to determine the biodegradability of chemicals in water. Recently, it has been adapted in applications in nonwater-soluble materials, such as plastics. The most often used method is dilution method 5-day BOD test. The standard method consists of filling with sample, to overflowing, an airtight bottle of the specified size and incubating it at the specified temperature for 5 days. Dissolved oxygen (DO) is measured initially and after incubation, and the BOD is computed from the difference between initial and final DO. [52, 53]

The evolution of carbon dioxide or methane from substrate represents a direct parameter for mineralisation. Gas evolution tests can also be important tools to determine the polymer biodegradability. Therefore, a number of standards for aerobic and anaerobic degradation tests have been specified. Aerobic degradation can be tested in an aqueous medium according to e.g. ISO 9439, ISO 14852, EN 14047, or under controlled composting conditions (ASTM D5338-98, ISO 14855, EN 14046, DIN V 54900). Anaerobic tests have been described as sludge test (ASTM D5210-92, ISO 11734) and digestion test (ASTM D5511-02). However, these methods are all based on the same principle, which differs in medium composition, inoculum, introduction of substrate and in the measurement technique of the gas. The principle of the ISO 14855 method is described in Figure 15. [52, 53]

Besides the conventional trapping of CO_2 to $Ba(OH)_2$ solution followed by manual titration, infrared gas sensors can also be used. It can be applied for continuously and also for noncontinuously aerated systems. Moreover, for noncontinuous systems, the analysis of CO_2 directly in the headspace can be used (using GC analysis). [40]
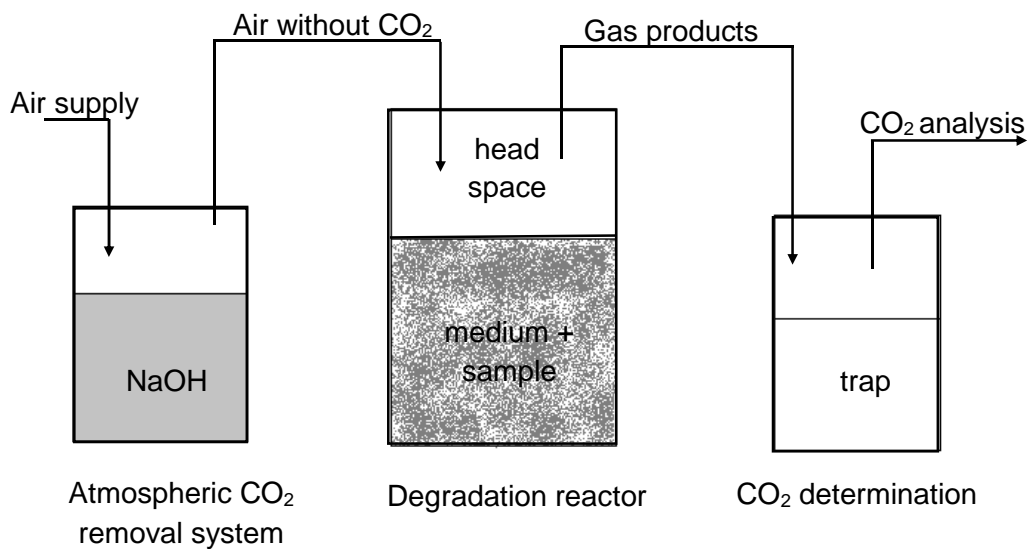
Figure 15 - Principle of biodegradation determination according to ISO 14855.

The degree of biodegradation is generally expressed by equation:

$$D_t(\%) = \frac{(CO_2)_T - (CO_2)_B}{ThCO_2} \cdot 100 \tag{2}$$

where $(CO_2)_T$ represents cumulative amount (g) of CO_2 from flask with sample, $(CO_2)_B$ represents cumulative amount (g) of CO_2 of blank (without sample) and $ThCO_2$ is theoretical amount of CO_2 in sample (determined by e.g. TOC analysis). The polymer can be generally considered as degradable only when the carbon conversion to CO_2 achieved 60% within 28 days.

Biodegradability of plastics has been widely investigated and number of methods have been standardised. Frequently used standards are summarised in Table 1.

Table 1 - Summary of ISO standards for polymer biodegradation testing. [56]

ISO No.	Title	Conditions
14851	Determination of the ultimate aerobic biodegradability of plastic materials in an aqueous medium - Method by measuring the oxygen demand in a closed respirometer	aqueous
14852	Determination of the ultimate aerobic biodegradability of plastic materials in an aqueous medium - Method by analysis of evolved carbon dioxide	
14855-1	Determination of the ultimate aerobic biodegradability of plastic materials under controlled composting conditions - Method by analysis of evolved carbon dioxide Part 1: General method	compost
14855-2	Determination of the ultimate aerobic biodegradability of plastic materials under controlled composting conditions-Method by analysis of evolved carbon dioxide Part 2: Gravimetric measurement of carbon dioxide evolved in a laboratory-scale test	
16929	Plastics - Determination of the degree of disintegration of plastic materials under defined composting conditions in a pilot-scale test	disintegration
20200	Plastics - Determination of the degree of disintegration of plastic materials under simulated composting conditions in a laboratory-scale test	
17556	Plastics - Determination of the ultimate aerobic biodegradability in soil by measuring the oxygen demand in a respirometer or the amount of carbon dioxide evolved	soil
14853	Plastics - Determination of the ultimate anaerobic biodegradation of plastic materials in an aqueous system - Method by measurement of biogas production	anaerobic
15985	Plastics-Determination of the ultimate anaerobic biodegradation and disintegration under high-solids anaerobic-digestion conditions - Method by analysis of released biogas	

4. Factors influencing PLA degradation

Biodegradable polymers have already found applications in many fields of the constantly growing market. PLA represents one of the most widespread biopolymer on the market due to its attractive mechanical properties, renewability, biodegradability and relative low cost. It has found applications in medical field, packaging and agriculture. However, nowadays there is a strong demand to extend the range of PLA properties (rigidity, mechanical properties, processability, antimicrobial activity etc.), which comes from requirement of long lasting bioplastics in industry sectors such as electronics and automotive. Therefore, the new PLA based materials (composites, nanocomposites, tailored compositions, etc.) with improved properties are widely investigated. [57]

Generally, the composites consist of two or more chemically and physically distinct phases: matrix and fillers (fibres/additives), separated by distinct interface. The presence of the additive in matrix plays several roles. However, it may accelerate/decelerate or inhibit the degradation mechanisms of PLA. Selected types of additives, which are used to reinforce the PLA matrix and their influence on degradation mechanisms of the PLA are described in the following chapters.

4.1. Natural fibres

To maintain the unique properties of renewability and biodegradability, the natural fibres (NFs) are very often used to reinforce PLA matrix. Moreover, advantages of the NFs can be found in the relatively low price of raw material, low density, high specific strength and stiffness, etc. [57, 58]. Some properties of the selected fibres are shown in Table 2. The attention is focused principally on flax fibres. However, hemp, jute, kenaf and different forms of cellulose extracted from NFs can also be used [4, 58, 59]. The loading of fibres depends on the required properties. It can vary from low filled materials (1–5 wt. %) to high filled system (e.g. 70 wt. %) [60]. Usually, the loading is around 30–50 wt.%.

The NFs are generally hydrophilic materials and thus incompatible with hydrophobic polymer matrix. The NFs hydrophilicity can also cause problems with the reinforcement in PLA, which is sensitive to hydrolysis and higher temperatures. Thus, the pre-treatment, such as drying of PLA and the fibres or NFs surface modification in order to improve adhesion, is necessary. The most

well-known chemical treatment for hydrophobization includes modification with alkali, acetyl, silane, peroxide, etc. [57, 59]

Table 2 - Mechanical properties of fibers. [57]

Fiber	Density (g.cm^3)	Young´s modulus (GPa)	Tensile strength (MPa)	Elongation at break (%)
Flax	1.54	27.5-85	345-2000	1-4
Hemp	1.47	17-70	368-800	1.6
Jute	1.44	10-30	393-773	1.5-1.8
Cotton	1.5-1.6	5.5-12.6	287-597	7-8
Kenaf	1.2	14-53	240-930	1.6
E-glass	2.5	70	2000-3500	2.5

As mentioned above, the NFs are used in order to maintain the biodegradability. Some articles have already described the ability of PLA/flax composites to biodegrade. Wang et al. have modified PLA with flax fibres (40-60 wt. %) and investigated the biodegradability by soil burial test [61]. The addition of the fibres accelerates the process of biodegradability due to prior degradation of fibres. This was confirmed with Alimuzzaman et al. [60]. In this study, the influence of flax content on the biodegradability (compost soil burial test) and water absorption was reported. Both of these properties are increased with the increasing fibres content.

Generally, the content of natural fibres increases the ability of PLA to biodegrade, especially because of high wettability and the preferential biodegradability of the fibres.

4.2. Additives with specific functions

The additives are usually incorporated into polymer system to reduce the cost or modify optical, rheological, physical or other properties. Still, nowadays the growing market creates more specific requirements to biopolymers and the systems with e.g. antimicrobial properties are desired. To reach these functional properties, various agents are incorporated into polymer matrix.

4.2.1. Antimicrobial agents

Demand for materials with specific properties is growing especially in food packaging. There has been an effort to develop innovative solutions both for active packaging and low environmental impact [62]. Therefore, the PLA based nanocomposites are the promising material for this purpose.

Metallic oxides like silver, copper, zinc and gold are often used as the agents to raise a good antibacterial activity. Besides that, the oxides are known due to their prooxidant activity and flame retardant effect in the polymer matrix[62, 63, 64][62, 63, 64] [7, 21, 26]. Out of these metal particles, ZnO takes a predominant place due to nontoxicity, high stability at elevated temperatures and pressures. Moreover, ZnO nanoparticles are well-known bio-safe and multifunctional inorganic additives that can provide antibacterial properties, ultraviolet absorption or photocatalytic effect. Thus, the PLA/ZnO nanocomposites have been produced as an active material for food packaging and textile applications with the unique antibacterial properties. [62, 63, 64, 65]

Recently, the PLA/ZnO system has been widely studied. Pantani et al. prepared PLA/ZnO films by melt-blending and described significant improvement of the antimicrobial activity against E. coli and S. aureus, respectively Gram-negative and Gram-positive bacteria strains, even when the small concentration (1–3 wt. %) of ZnO is incorporated [62]. Further, several publications have been investigated on the influence on PLA degradation processes. Therias et al. studied a photooxidation mechanism of PLA/ZnO films, where the ZnO nanoparticles induce the oxidation and play a significant prodegradant role [65]. A catalytic effect of the ZnO nanoparticles on the rate of the PLA hydrolysis at the temperature below its glass transition temperature was described by Qu et. al. The concentration of ZnO NPs was about 19 % and activation energy for ZnO catalysed PLA hydrolysis was approximately 38% lower than that of pure PLA hydrolysis [66].

4.2.2. Hydrophobity increasing additives

Further expansion of PLA is expected in the automotive and electronic industries. Nevertheless, the requirements for high mechanical properties and durable products with long term performance could be limited by poor mechanical properties and propensity to hydrolysis degradation. [67] Therefore, the resistance to hydrolytic decomposition during the processing and their service life has become the key requirement and has to be satisfactorily guaranteed. It follows that to retard the hydrolysis process either the penetration of water into polymer matrix or the rate of the hydrolysis reaction along with the autocatalysis phenomenon has to be suppressed. The improvement of PLA resistance to abiotic hydrolysis could be reached by means of the incorporation of suitable additives suppressing at least one step of the degradation mechanism. The inhibition of diffusion kinetics can be achieved by the intercalation of nanofillers (e.g. cellulose nanowhiskers), which create the physical barrier in the polymer matrix hindering the penetration of water.[68] Moreover, the rate of hydrolysis can be affected by the addition of appropriate agents which react preferably with water and carboxylic groups [69].

For instance, polycarbodiimides act on the above-mentioned principles and proved to be effective stabilizers PLA against thermal degradation during processing [70]. In particular, carbodiimides are claimed to be efficient stabilizer for polyesters susceptible to hydrolysis. It has been stated that the PLA decomposition in abiotic and biotic degradation processes could be substantially retarded by the addition of carbodiimide-based additive. [71]

AIMS OF DOCTORAL STUDY

The aims of doctoral work defined based on the state of art study and conclusions made out of that are following:

- Preparation and characterization of polylactide based systems with degradation behaviour controlled by specific additives effecting free surface energy.

- Preparation and characterization of biocomposite system based on polylactide/natural fibres. Assessment of natural fibres surface modifications effect on degradation kinetics.

- Tailoring of degradation properties of polylactide by hydride nanostructured fillers.

- Verification of polylactide degradation monitoring possibilities by using dielectric relaxation spectroscopy and comparison with conventional techniques.

EXPERIMENTAL PART

Experimental part of doctoral study is dived into four main part according to the defined aims. The work has been focused generally on preparation of PLA based materials and their modifications. In first part, the properties of PLA were modified by anti-hydrolysis agent, carbodiimide. Further, reinforcement by natural fibres and influence of interfacial adhesion modification on system properties were investigated. The third investigated topic describe possibilities of tailoring of PLA degradation processes by hydride system of silver nanoparticles immobilized on zinc stearate surface. In the last part is research focused on the monitoring of PLA degradability using dielectric relaxation spectroscopy, where obtained results were compared with commonly used method for degradability estimation.

5. Effect of carbodiimide on hydrolytic stability of PLA

PLA can be considered as a replacement for conventional petroleum-based polymers in the electro-technical applications and automotive industry [72, 73, 74, 75]. Nevertheless, this kind of applications requires excellent mechanical properties and durability of the material, which create a limitation for usage of PLA with propensity to thermal and hydrolytic degradation [67, 76, 77]. Particularly, the resistance to hydrolytic decomposition is the key to achieve sufficient PLA properties for long service life applications [78].

Hydrolytic chain scission can be considered as a primary cause of the reduction of molecular weight, which is related with reduction in physical and chemical properties of PLA and, in natural environment, enable subsequent assimilation and mineralisation by microorganisms [77, 79]. Principally, the abiotic hydrolysis was suggested as a major depolymerisation mechanism and the rate-controlling step in of PLA biodegradation during composting [80]. Generally, the hydrolysis process takes place via diffusion-reaction of the aqueous medium, which penetrates through the polymer matrix and simultaneously converts the long polymer chain to low molecular weight water soluble oligomers and the monomer [81]. Moreover, ester bond hydrolysis can be autocatalyzed by carboxyl end groups initially present or formed during the process [21]. The PLA resistance to abiotic hydrolysis can be increased by inhibition of water penetration into the polymer matrix, retardation of hydrolysis

or retardation of the rate of hydrolytic reaction along with the autocatalysis phenomenon.

The inhibition of diffusion kinetics can be achieved by the intercalation of the physical barriers, nanofillers (cellulose nanowhiskers), in the polymer matrix which hindering the penetration of water and delay the onset of hydrolysis [68]. The rate of water diffusion could be also controlled to some extent through the modification of crystallinity of the material by the addition of nucleation agents [82, 83]. Moreover, the reaction kinetics of hydrolysis can be affected by the addition of appropriate agents which react preferably with water and carboxylic groups [69, 84]. Recently, the use of compounds acting on the above-mentioned principle e.g. polycarbodiimides [70] and tris(nony1-phenyl) phosphite [85], proved to be effective to stabilize PLA against thermal degradation during processing. In later phases of its life cycle, in particular, carbodiimides are claimed to be efficient stabilizer for polyesters susceptible to hydrolysis [86]. In the previous work of Stloukal et al. the retardation of the PLA decomposition in abiotic and biotic degradation processes by the addition of carbodiimide-based additive has been investigated [71]. However, further information concerning the stabilization action of carbodiimides (CDI) in various concentrations as well as its subsequent effect on kinetics of abiotic hydrolysis and biodegradation has not been satisfactorily described yet.

In this chapter the influence of bis(2,6-diisopropylphenyl)carbodiimide (BDICDI) incorporated as the anti-hydrolysis agent in PLA polymer matrix in various concentrations on the durability of final material during subsequent lifetime of the products was investigated. The extent of stabilization and subsequent degradation kinetics as well as the mechanism of PLA films in dependence on concentration of BDICDI loaded was tested and monitored by different experimental techniques in the process abiotic hydrolysis and microbial decomposition under compost conditions. The experimental data from abiotic hydrolysis and aerobic composting were analyzed by non-linear regression to fit the first-order kinetic models and to calculate the kinetics parameters, especially material rate constants and the length of lag phase. The duration of suppression of chains scission in BDICDI stabilized material was also evaluated and maintenance of material mechanical properties was demonstrated at the end of this period.

Materials and methods

Materials

Polylactic acid PLA2002D was purchased from NatureWorks® Ingeo™, USA. The antihydrolysis agent ZIKA-AH362 i.e. Bis(2,6-diisopropylphenyl)carbodiimide (BDICDI) was kindly supplied by Ziko Ltd. Seoul, Korea.

Procedure for processing the materials

Preparation of PLA/BDICDI mixture

Prior to being compounded, PLA pellets were dried at 60°C under reduced pressure for more than 24 hours. A co-rotating, twin-screw micro-compounder (DSM Xplore, Geleen, the Netherlands), equipped with two stainless steel screws and a bypass allowing continuous recirculation of the materials, operated at 200°C; the screw speed of 100 RPM was used for the compounding operations. Firstly, the master-batch of PLA with 20% w/w of BDICDI was prepared to allow more homogeneous dispergation of the additive. Secondly, the master-batch of PLA with BDICDI and neat PLA were used to prepare mixtures with 0.125, 0.25. 0.5, 1.0, 1.25, 1.5, 1.75 and 2.0% w/w of BDICDI.

Preparation of films

PLA films of 100 µm thickness were compression moulded. The material was brought up to the processing temperature of 200 ℃ for 1 minute, then moulded for 2 minutes, and immediately cooled down under pressure after transferring the material to a second press kept at 20°C.

Characterization

Gel permeation chromatography

The weight average molecular weight (M_w) and molecular weight distribution of samples and their changes during degradation tests were analysed by gel permeation chromatography (GPC) on an HT-GPC 220 system (Agilent), equipped with a dual detection system ("RI" refractive index and "VIS" viscosity detectors). Samples were dissolved in THF ($\sim$2 mg.ml^{-1}) overnight.

Separation took place on a series of mixed bed columns (1xB, 1xD, 1xE) (300 ×
7.8 mm, Polymer Laboratories). Analyses were carried out at 40°C in THF as
the mobile phase, at a 1.0 mL.min^{-1} flow rate and loading volume of 100 μL.
The GPC system was calibrated with narrow polystyrene standards ranging from
580 to 3 000 000 g.mol^{-1} (Polymer Laboratories Ltd., UK). The molecular
weight averages (M_w, M_n) and molecular-weight dispersity index (MWD =
M_w/M_n) were calculated with the aid of a polystyrene-standards-based
"universal" calibration curve. Values of intrinsic viscosity η were obtained
directly from the viscosity detector. All data processing was carried out using
Cirrus software.

Thermal properties - Differential scanning calorimetry

Thermal properties were investigated by differential scanning calorimetry
(DSC) on a Mettler Toledo DSC1 STAR System. All measurements were
carried out under a nitrogen atmosphere (50 cm^3.min^{-1}). The temperature ramp
was set from 0°C to 200°C (10 K.min^{-1}), followed by annealing at 200°C for 5
min. Subsequently there was a cooling scan from 200°C to 0°C (20 K.min^{-1}),
then an isothermal step at 0°C for 5 minutes. Finally, a second heating scan was
conducted from 0°C to 200°C (10 K.min^{-1}). Melting point temperature (T_m) and
the exothermic response relating to cold crystallization (T_c) were obtained from
the first heating cycle. The region of glass-transition temperature (T_g) was
determined from the second heating scan. The degree of crystallinity χ_c was
calculated according to the following equation [87]:

$$\chi_c = \left(\frac{\Delta H_m - \Delta H_c}{\Delta H_m^0}\right) \times 100 \quad (3)$$

where ΔH_m is the heat of fusion, ΔH_c cold crystallization enthalpy and ΔH^0_m is
the tabulated heat of fusion for theoretically 100% crystalline PLA
homopolymer (93.1 J.g^{-1}) [87].

Fourier Transform Infra-red Spectroscopy

Fourier transform infra-red attenuated total reflectance (FTIR-ATR) spectra were recorded on a Nicolet iS10 instrument equipped with a Zinc/selenide crystal (Thermo Fisher Scientific, Waltham, MA). The collected spectra in the wavenumber range from 500 to 4000 cm^{-1} represented the average of 64 scans at a spectral resolution of 4 cm^{-1}. The spectra for film samples before and during the abiotic hydrolysis process were recorded.

Mechanical properties

The tensile tests of samples before and during abiotic hydrolysis were carried out according to the ČSN EN ISO 527-1-4 standard, using a tensile testing machine – the Testometric M350-5CT - at a crosshead speed of 5 mm.min^{-1}. The dimensions of dog-bone form specimens cut from the compression moulded plates were $60 \times 4.0 \times 0.1$ mm. Prior to testing, the samples were dried at 60°C for 4 h. A minimum of five specimens from each group were tested.

Degradation test

Abiotic hydrolysis

The extent and rate of PLA hydrolysis was followed for 90 days at 58°C. PLA film samples (50 mg) were cut into 0.5×0.5 cm specimens and suspended in 50 mL of sodium phosphate buffer (0.1 mol.L^{-1}, pH 7) amended with a microbial growth-inhibiting substance (NaN$_3$, 2% w/w). The experiment was carried out in three replications for each sample type. 1.5 mL aliquots of the medium were taken out at regular intervals, centrifuged (10 000 g, 10 min.), and the supernatants were analysed for dissolved organic carbon (TOC-L Analyser, Shimadzu). In parallel, at appropriate intervals, the materials were also analysed by GPC.

Biodegradation under composting conditions

Biodegradation tests were performed in 500 mL biometric flasks equipped with septa mounted on the stoppers. Three components were weighed into the flasks: polymer samples (50 mg), mature compost (5 g of dry weight) and perlite (5 g). The sample flasks were incubated at 58°C. Head space gas was sampled at appropriate intervals through the septum with a gas-tight syringe (100 µL), and

then injected manually into a GC instrument – an Agilent 7890 (Agilent technologies, USA), equipped with Porapak Q (1.829 m length, 80/100 MESH) and 5A molecular sieve (1.829 m length, 60/80 MESH) columns connected in series and a thermal conductivity detector (carrier gas helium, flow 53 mL.min^{-1}, column temperature 60°C). From the CO_2 concentration found, the percentage of mineralization with respect to the carbon content of the initial samples was calculated. Endogenous production of CO_2 by the compost in blank incubations was always subtracted to obtain values representing net sample mineralization. Three parallel flasks were run for each sample, along with four blanks.

Degradation kinetics

The data obtained from the degradation experiment were investigated by applying the appropriate kinetic models. The parameters of all individual models were obtained in MS Excel. The fit of the individual models was compared using the coefficient of determination (R^2).

Biodegradation

In order to evaluate the experimental data from the biodegradation test, the model expressing the degradation of organic carbon from a solid sample was adopted [24]. In the previous study by the authors [6] the resulting parameters of the solved model suggested that essentially PLA-materials exhibited only one type of carbon, so herein the hydrolysis component in the model was expressed by merely the hydrolysis rate constant for so called hydrolysable solid carbon.

The analytical solution to the proposed model is expressed by Equation (4) for t > c ($C_{T,t} = 0$ for t ≤ c), where $C_{T,t}$ represents the percentage of total cumulative CO_2 production at time t (days); $C_{h,0}$, are the initial content of hydrolysable solid carbon, respectively; and $C_{aq,0}$ is the initial percentage of water-soluble carbon. The kinetic parameters k_{hr} (day^{-1}) represent respective first-order hydrolysis rate constants for the hydrolysable solid carbon. Further, k_{aq} (day^{-1}) represents the rate constant of mineralization (biodegradation) of water-soluble carbon to carbon dioxide. Finally, parameter c is the duration of the lag phase (days) during the initial phase of biodegradation before the onset of CO_2 production.

$$C_{T.t} = \left\{ C_{aq,0} \cdot \left(1 - e^{-k_{aq}(t-c)}\right) + \left[C_{h,0} \cdot \left(1 - \frac{k_{aq}}{k_{aq}-k_{hr}} e^{-k_{hr}(t-c)} + \frac{k_{hr}}{k_{aq}-k_{hr}} e^{-k_{aq}(t-c)}\right) \right] \right\} \quad (4)$$

The assumed mathematical constraints required to derive a valid model are as follows:

1. $C_{C,0} = C_{aq,0} + C_{h,0}$
2. $C_{C,final} = C_{aq,final} + C_{h,final}$
3. All parameters are positive
4. $C_{h,t}$; $C_{aq,t}$ and $C_{T,t} = 0$ for $t \leq c$

, where $C_{C,0}$ and $C_{C,final}$ are the percentages of total and final initial carbon, respectively.

Hydrolysis

With the purpose of fitting the experimental data of dissolved organic carbon from the abiotic hydrolysis experiments, the mathematical model given above was modified to describe merely the first phase of the degradation process, namely the change of solid organic material into intermediate water-soluble organic carbon forms. Therefore, the rate constant k_{aq}, expressing the mineralization of water-soluble carbon into carbon dioxide, was excluded. The modified model is expressed by Equation (5):

$$C_{aq,t} = C_{aq,0} + C_{r,0} \cdot \left(1 - e^{-k_{hr}(t-c)}\right) \tag{5}$$

Results and discussion

Material characterization

The degradation of PLA is critically affected by the properties of the input material, its composition and processing history. Therefore, investigation was carried out into the properties essential for interpreting data from the degradation experiments (Table 3).

It is well-known [88, 89] that PLA easily undergoes degradation at increased temperatures during processing. Consequently, BDICDI anti-hydrolysis effects could also be expected during thermo-plastic processing. The GPC results listed in Table 3 show a slight decrease in molecular weight for non-stabilized PLA after processing in comparison with the original PLA. As expected, the drop in molecular weight was improved by increasing the concentration of BDICDI, and above 0.5% w/w there were no longer any significant changes indicating degradation during processing.

DSC analysis revealed that BDICDI had no significant effect on the T_m and T_g values in comparison with pure PLA film or with the initial PLA prior to processing. The crystallinity of the films was considerably low and quite resembled neat PLA, probably reflecting the relatively brief time available for crystallization during the preparation of films.

Table 3 - Selected material properties of PLA-based films

Sample	Content of BDICDI (% w/w)	$M_w{}^a$ [g moL^{-1}]	MWD^b	$T_m{}^c$ [°C]	$T_g{}^d$ [°C]	$\chi_c{}^e$ [%]
PLA prior to processing	0	124000	2.22	153.1	58.2	32.6
PLA	0	106000	2.16	152.3	59.5	2.8
PLA + 0.125% BDICDI	0.125	116000	2.16	152.8	59.5	1.9
PLA + 0.25% BDICDI	0.25	121000	2.1	152.5	59.1	1.9
PLA + 0.5% BDICDI	0.5	129000	2.08	152.3	59.6	0.9
PLA + 1% BDICDI	1	121000	2.22	152.3	60.0	2.7
PLA + 1.25% BDICDI	1.25	137000	2.19	152.0	59.0	9.1
PLA + 1.5% BDICDI	1.5	123000	2.21	152.6	58.7	2.8
PLA + 1.75% BDICDI	1.75	122000	2.26	151.3	58.8	7.3
PLA + 2% BDICDI	2	133000	2.28	151.0	58.9	0.4

[a] Weight average molecular weight; [b] molecular-weight dispersity ; [c] melting temperature; [d] glass transition temperature; [e] crystallinity

Abiotic hydrolysis

The sensitivity of PLA to abiotic hydrolysis, especially at elevated temperatures, is considered one of the limiting factors for application in products requiring a longer service life. In order to investigate the stabilization effect of BDICDI applied at various concentrations, the hydrolysis experiment was set up in the aqueous environment at 58°C. The temperature selected was favourable for several reasons. Firstly, it was proven that degradation proceeds at a reasonable rate at this temperature [77], so technically the laboratory study was feasible, also stability at such temperature can expected as a minimal requirement for e.g. in electrotechnic applications. Additionally, the temperature remained under the glass transition temperature (T_g) of the material, consequently the results should be applicable to the temperate interval below T_g. Finally, 58°C is the usual temperature used in laboratory composting tests, hence the results could provide some information on the eventual behaviour of the material during biodegradation under thermophilic conditions. Furthermore, the extent of stabilization and subsequent hydrolysis kinetics were studied by several techniques, including analysis of dissolved organic carbon (TOC), GPC, DSC, FTIR and tensile tests.

Release of water-soluble hydrolysis products

The accumulation of water-soluble, organic carbon products from PLA hydrolysis was observed (Figure 16), and the data fitted with the kinetic model (Eq. (5)). The resulting parameters of the model with the coefficients of determination (R^2) are shown in Table 4. Coefficients of determination (R^2) exceeding 0.96 were obtained for all data sets, indicating the excellent fit of the model.

The results revealed an insignificant stabilization effect of BDICDI at concentrations of up to 0.5% w/w, a moderate stabilization effect at concentrations of 1 and 1.25% w/w, and a very strong stabilization effect at the highest concentrations from 1.5% to 2% w/w, which counteracted the hydrolysis of PLA. This phenomenon was quantified by the resulting length of the lag phase c calculated from the kinetic model (inner graph in Fig. 16). While at the lower concentrations of BDICDI at up to 1.25% w/w the length of lag phase was only slightly extended by increasing the amount of the anti-hydrolysis agent, at higher concentrations of BDICDI a steep rise in the length of lag phase was observed. It was discerned that the hydrolysis rate constants gradually rose with the increasing amount of BDICDI from 0.0128 day^{-1} pertained to BDICDI-

stabilized PLA at the concentration of 0.125%, extending to 0.0240 day^{-1} for PLA+ 1.75% BDICDI. Only PLA + 2% w/w BDICDI really stood out (0.0180 day^{-1}). The calculated rate constants suggest that PLA is protected against hydrolysis and the autocatalytic action of free carboxylic groups for a certain time, depending on the amount of BDICDI. After the dose of BDICDI is depleted, the material is hydrolyzed at a comparable or even slightly higher rate than pure PLA. The values of the rate constants are generally consistent with previous investigations by other authors [90].

In the work [68] authors demonstrated the stabilization effect of cellulose nanowhisker on the hydrolytic degradation behaviour of poly(D,L-lactide). No weight loss was observed for the composite of PLA with 5% nanowhisker, even after 12 weeks. In our case, no release of water soluble product, which is equivalent to weight loss, was observed for more than 100 days application from PLA with lower amount of BDICDI (2% w/w) in comparison with nanowhiskers.
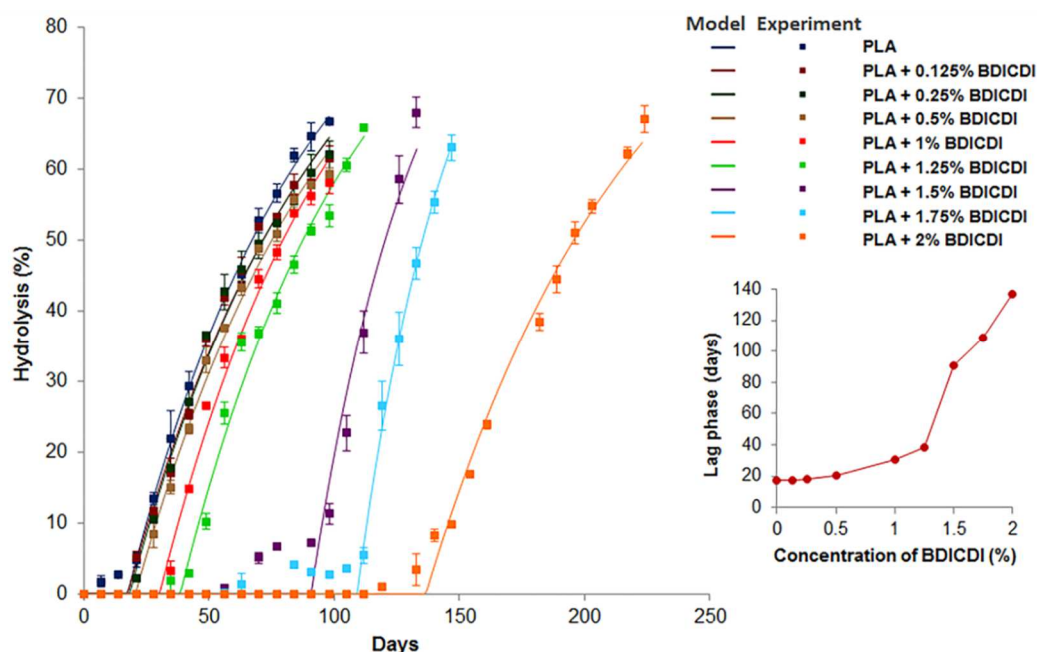
Figure 16 - Abiotic hydrolysis of PLA film samples in 0.1M phosphate buffer (pH = 7) at 58°C The inner graph represents the dependence of lag phases of hydrolysis calculated from the kinetic model on the concentration of BDICDI.

Table 4 - Kinetic model parameters and coefficients of determination (R^2) for abiotic hydrolysis of pure PLA and BDICDI-stabilized PLA films

Sample	$C_{aq.0}$[a] (%)	$C_{r.0}$[b] (%)	k_{hr}[c] (day^{-1})	C[d] (days)	R^2
PLA	0	100	0.0140	17.45	0.9989
PLA + 0.125% BDICDI	0	100	0.0128	17.40	0.9863
PLA + 0.25% BDICDI	0	100	0.0130	18.30	0.9879
PLA + 0.5% BDICDI	0	100	0.0127	20.64	0.9925
PLA + 1% BDICDI	0	100	0.0141	30.23	0.9850
PLA + 1.25% BDICDI	0	100	0.0142	38.46	0.9779
PLA + 1.5% BDICDI	0	100	0.0234	90.71	0.9770
PLA + 1.75% BDICDI	0	100	0.0266	109.09	0.9975
PLA + 2% BDICDI	0	100	0.0118	136.54	0.9633

[a] Percentage of initial intermediate solid carbon; [b] Percentages of initial hydrolysable solid carbon; [c] First-order hydrolysis rate constants; [d] Duration of lag phase during the initial phase of hydrolysis prior to water-soluble carbon production.

Changes in molecular weight distribution

In order to explain in more detail the time frame of the stabilization and the changes in the material at a molecular level, especially during the initial phase of the hydrolysis process, GPC measurements were carried out (Figure 17) during the hydrolysis experiment.

The data obtained clearly confirmed previous findings that the chain scission during hydrolysis was significantly retarded by adding BDICDI in an amount above 1.5% w/w. The stabilization effect of BDICDI is characterized by only slight reduction in M_w within a certain time (the "plateau period"), which increased alongside heightened concentration of the anti-hydrolysis agent. Afterwards, the rate of M_w decrease approximately equates to that of pure PLA.

The stabilization effect was quantified by the estimation of the time necessary to bring about 20% reduction in M_w in comparison with materials before hydrolysis (see the inner graph in Figure 17). Such a drop in M_w roughly corresponded with the "plateau period" for highly stabilized samples. The drop in M_w even exceeding 20% after around 2 days of incubation signified the immediate onset of the hydrolytic scission of ester bonds for BDICDI at concentrations below 0.5% w/w. For higher concentrations, the stabilization effect gradually increased alongside heightened BDICDI concentration. The 20% decrease in M_w from the original value was delayed by 8, 23, 69, 87 and 95 days for BDICDI-stabilized PLA at concentrations of 1, 1.25, 1.5, 1.75 and 2% w/w, respectively. This type of carbodiimide additives showed to be more effective in comparison with the carbodiimide based additive applied in our

previous study [71], when the M_w of PLA with 2 % w/w of stabilizer remained approximately unchanged for only about 40 days. The significantly better stabilization effect was also achieved in comparison with study [91], where the deceleration of PLA hydrolysis by addition of Talc was demonstrated.

The insignificant stabilization effect of BDICDI at its low concentrations might be due to depletion of the same taking place as early as during thermal processing in the reaction of BDICDI with the moisture and carboxylic groups. It suggests that a certain amount of BDICDI above a minimal concentration limit should be necessary, depending on the time and conditions of thermal processing, so as to ensure the effective stabilization of PLA against hydrolysis during the expected lifetime of a product. In accordance with the amount of BDICDI applied above this minimal concentration, the duration of stabilization can be effectively tuned.
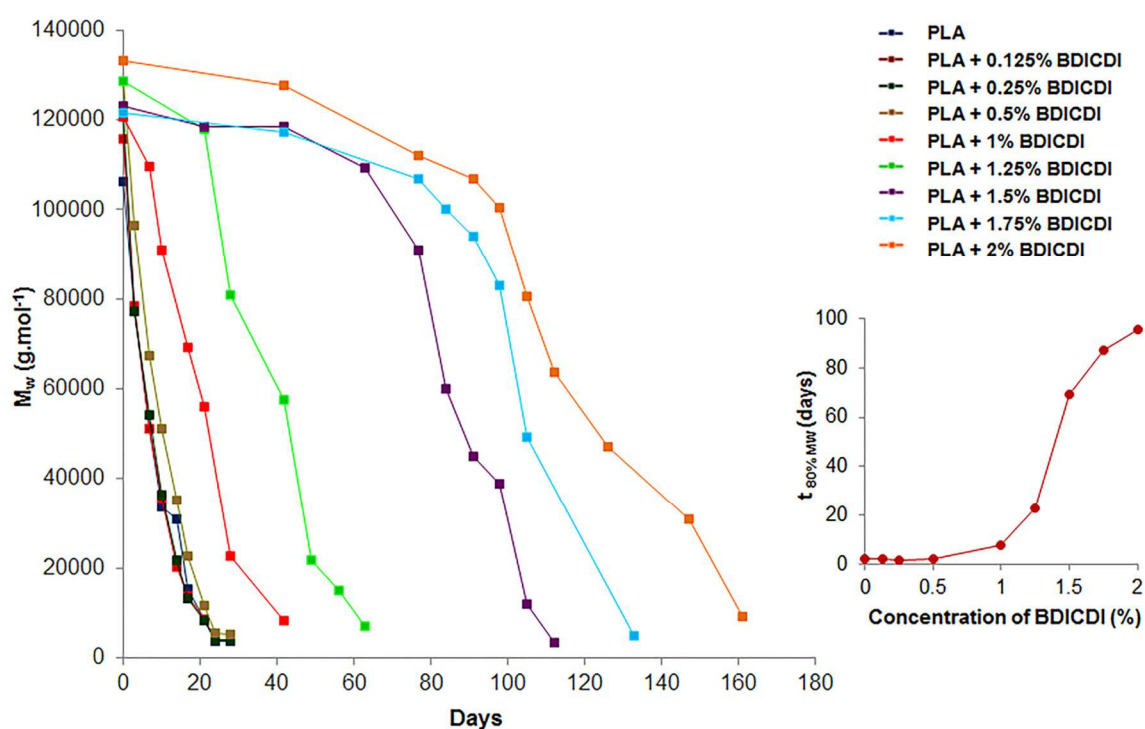
Figure 17 - Molecular weight evolution of PLA with a differing content of BDICDI.
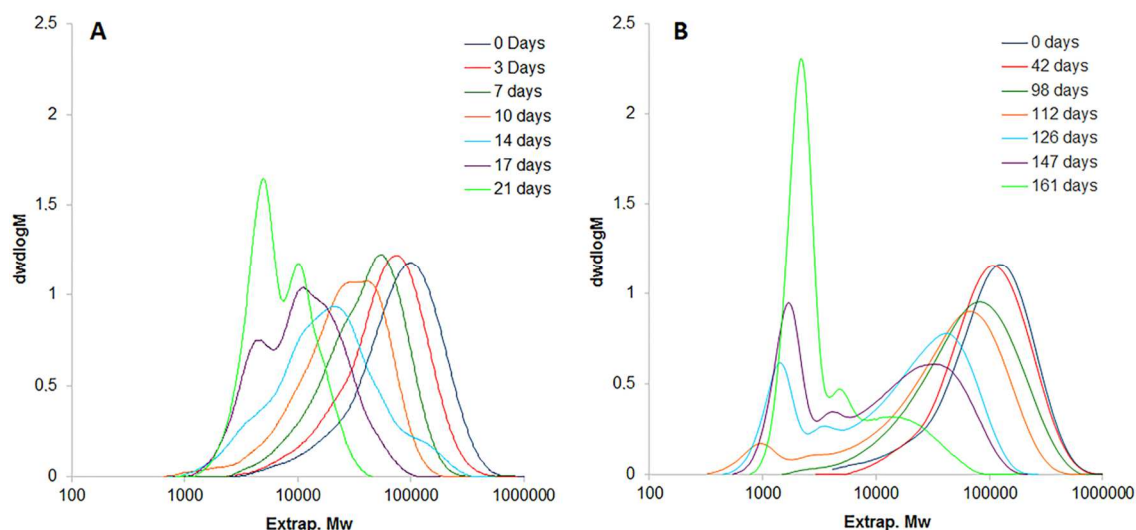
Figure 18 - Molecular weight distribution curves for pure PLA (A) and PLA with 2% of BDICDI (B) during abiotic hydrolysis.

In order to evaluate the hydrolysis behaviour of pure BDICDI and that containing PLA at a molecular level, the changes in molecular weight distribution (MWD) for pure PLA and PLA with 2% w/w of BDICDI were observed during the hydrolysis experiment and compared (Figure 18). Prior to hydrolysis, both materials - either non-stabilized or stabilized, possessed a narrow, unimodal and moderately symmetrical distribution with a polydispersity (PDI) index of about 2. In the course of the hydrolysis experiment, the MWD of non-stabilized PLA gradually broadened out (PDI = 2.94 after 14 days, and 1.36 after 28 days), and later the overall unimodal shape of the distribution changed to bimodal, with a distinct peak in substances with an M_w of several thousand, which was probably just over the water solubility limit for PLA oligomers [77].

A different situation arose in the case of PLA with BDICDI content. Firstly, for almost 100 days, the molecular weight distribution broadened out only slightly (the PDI changed from 2.28 to 2.77). After this period, rather rapid MWD changes could be observed, characterized by an overall shift in the distribution to a lower M_w, and building up a peak of low M_w substances. At the close of the hydrolysis experiment, the higher molecular weight fraction gradually disappeared and the PDI decreased to about 2.18. The described trends were detected for all stabilized samples with an intensity that depended on their BDICDI concentrations.

It is known that bimodal distribution is connected with hydrolysis of semi-crystalline PLA, herein exhibiting a different degradation rate for crystalline and amorphous regions within the samples [21, 76]. Although the crystallinity of all

the tested samples was initially considerably low, it increased during the hydrolysis experiment probably due to reorganization of loose polymer chains (see capture 3.1.3 and Tab. 3). This behaviour was significantly more intense in BDICDI stabilized materials, most likely as a consequence of the prolonged time available for recrystallization.

Thermal properties of the materials

The changes in thermal properties of the selected samples were observed with DSC in order to enable better interpretation of the stabilization effect of BDICDI and subsequent hydrolysis mechanisms (Table 5). A slight decline in T_m and T_g was revealed for pure PLA and weakly stabilized PLA with 0.5% w/w BDICDI even after as little as three weeks of hydrolysis. The reduction in melting temperature indicated formation of a low-molecular-weight fragment, caused by chain scission of ester bonds entrapped in the polymer matrix. Consequently, the plasticizing effect of newly formed oligomers with sufficient mobility also decreased the glass transition temperature, potentially resulting in further acceleration of the hydrolysis processes. The obvious delay in reducing thermal properties alongside increase in concentration underlines the stabilizing effect of BDICDI in PLA.

The significant increment in the crystalline phase in all initially highly amorphous samples might also be caused by low-molecular-weight products of hydrolysis, which partially release the polymer chains and thus enhance mobility of the same [21]. Consequently, recrystallization of the polymer chains to produce a crystalline lattice is promoted. The effect is more obvious for rapidly hydrolyzing samples, with the degree of crystallization reaching 34% within 21 days.

Table 5 - Thermal properties of selected materials prior to and during the hydrolysis process.

Sample	Initial			21 Days			42 days			98 days			140 days		
	T_m^a [°C]	T_g^b [°C]	χ_c^c [%]	T_m^a [°C]	T_g^b [°C]	χ_c^c [%]	T_m^a [°C]	T_g^b [°C]	χ_c^c [%]	T_m^a [°C]	T_g^b [°C]	χ_c^c [%]	T_m^a [°C]	T_g^b [°C]	χ_c^c [%]
PLA	152.3	59.5	2.8	148.8	49.9	32.0	-	-	-	-	-	-	-	-	-
PLA + 0.5% BDICDI	152.3	59.6	0.9	149.2	49.1	34.0	-	-	-	-	-	-	-	-	-
PLA + 1% BDICDI	152.3	60.0	2.7	154.1	56.8	34.0	144.3	49.2	33.9	-	-	-	-	-	-
PLA + 1.5% BDICDI	152.6	58.7	2.8	152.5	59.2	24.4	153.3	59.0	26.6	154.7	54.2	33.5	-	-	-
PLA + 2% BDICDI	151.0	58.9	0.4	151.2	58.3	23.3	151.0	58.5	25.9	150.4	57.0	29.1	156.6	53.0	29.5

[a] Melting temperature; [b] glass transition temperature; [c] crystallinity

Infrared spectroscopy

In order to support evidence for the stabilizing effect of BDICDI, which occurs through scavenging free carboxylic groups and water molecules, recordings were made of the FTIR-ATR spectra of the sample with 2% BDICDI prior to and during the hydrolysis experiment; these are presented as an example (Figure 19). The reaction of aromatic BDICDI with carboxylic acids leads predominantly to N-acyl urea (Figure 20 A), witnessed by the secondary (C=O stretch at about 1640 cm^{-1} and N-H bend at about 1550 cm^{-1}) and tertiary amide bands (C=O stretch at about 1640 cm^{-1} and C-N bend at about 1320 cm^{-1}), as well as with water leading to urea derivatives (Figure 20 B) characterized by a secondary amide band. The presence of these reaction products was visible from infrared peaks at about 1560 and 1640 cm^{-1} (the red circle) as soon as after 42 days of hydrolysis (Figure 19). After 98 days, which roughly corresponded to the duration of the stabilizing effect in PLA with 2% of BDICDI, and by which time the majority of the anti-hydrolysis agent should have transformed into reaction products, the appearance of newly formed peaks became obvious. Finally, the amides peak represented by the N-H bend continued to grow and become dominant, with a small peak (C=O stretch band) appearing as its shoulder (the blue circle). The tertiary amide peak at 1320 cm^{-1} also proved distinctive and grew significantly (the yellow circle). Comparable peaks were recorded for all stabilized samples, their intensity depending on the given BDICDI concentrations.

Showing a relatively intensive secondary amide peak, it follows that the majority of BDICDI product was formed in reaction with water, although the product resulting from a reaction with the carboxylic groups represented by the tertiary peak was also clearly present. Thus, both of the stabilization mechanisms considered herein have be taken into account so as to explain the stabilization mechanism of BDICDI in PLA.
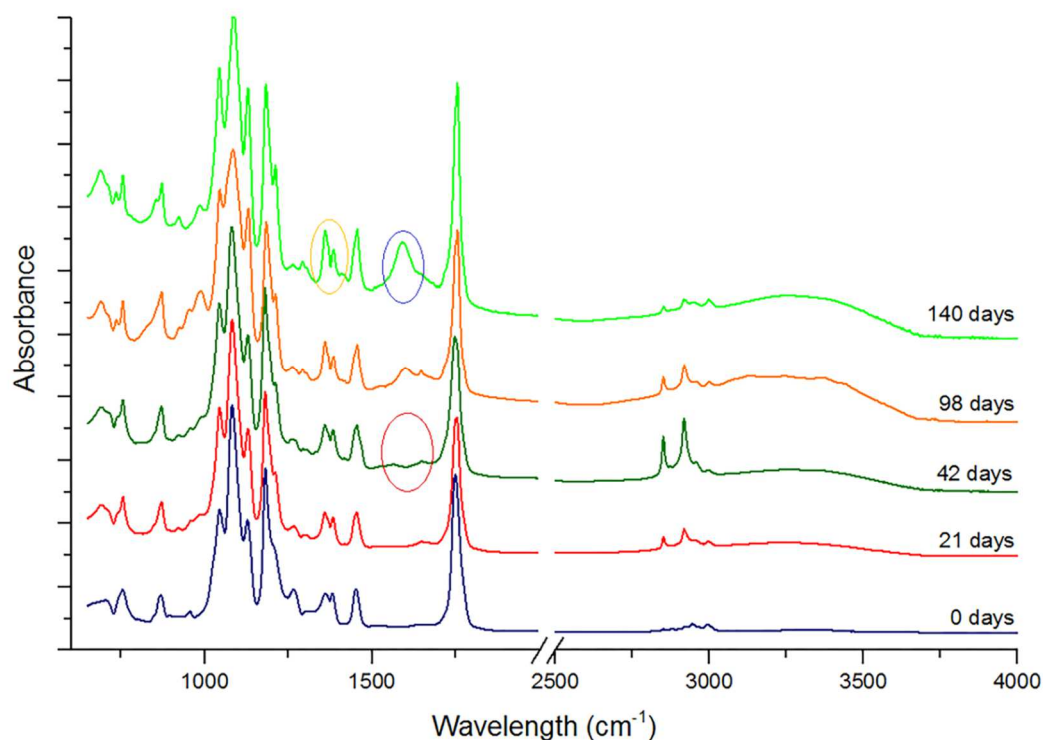

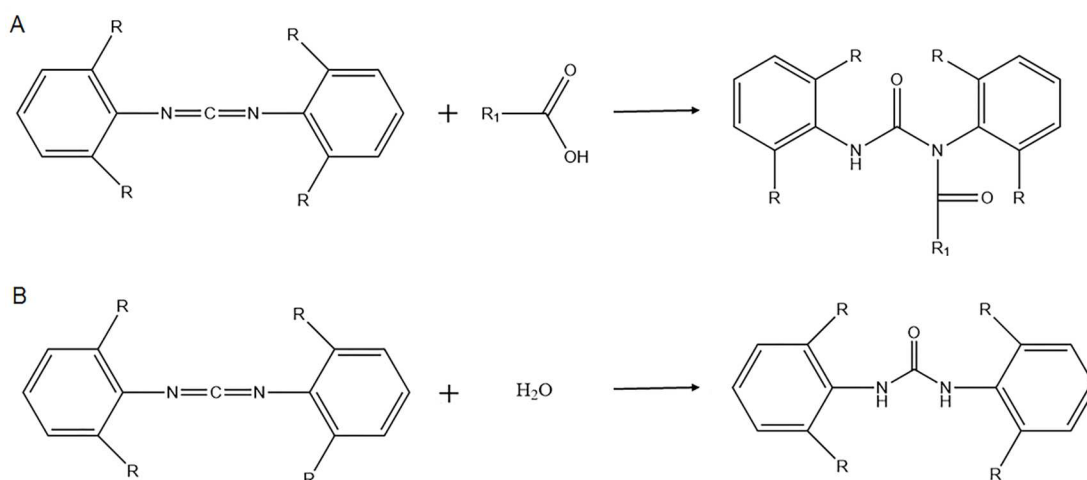*Figure 19 - FTIR-ATR spectra of PLA film stabilized with 2% of BDICDI during abiotic hydrolysis.*

Figure 20 - Reaction of aromatic carbodiimide with carboxylic group (A) and water (B).

51

Mechanical properties

Mechanical properties were tested in order to verify the effect of BDICDI at higher concentrations on maintaining the long-term performance of PLA. The samples were examined before and after exposure to abiotic hydrolysis at appropriate times. The time of sampling was logically chosen on the basis of evolution of molecular-weight analysis (Table 6). Insignificantly stabilized samples with concentrations of BDICDI of up to 1% w/w were subjected to testing after a short period of hydrolysis, despite an already considerable drop in M_w By contrast, the times of sampling the materials stabilized with higher BDICDI concentrations approximately corresponded to the end of the individual plateau phases in Figure 17, characterized by only a slight reduction in M_w.

Table 6 - Changes in the mechanical properties of materials after exposure to abiotic hydrolysis at the time of sampling.

|	Time (days)	M_w[b] (g.mol^{-1})	Δ Tensile strength[c] (%)	Δ Elongation at break[d] (%)	Δ Young modulus[e] (%)
PLA	7	51027	-74.3	-71.5	-3.8
PLA + 0.5% BDICDI	10	51257	-76.8	-63.1	14.6
PLA + 1% BDICDI	21	55980	-89.8	-82.0	-1.2
PLA + 1.25% BDICDI	28	80993	3.1	13.3	7.5
PLA + 1.5% BDICDI	63	109478	-7.5	-11.6	-0.6
PLA + 1.75% BDICDI	77	106979	-10.5	-19.6	28.9
PLA + 2% BDICDI	98	100350	1.5	-19.2	-1.2

[a] Time of sampling of material; [b] weight-average molecular weight of material at the time of sampling; [c] percentage change in tensile strength before and after hydrolysis; [d] percentage change in elongation at break before and after hydrolysis; [d] percentage change in Young modulus before and after hydrolysis.

The resultant tensile strengths, elongations at break and tensile modulus of the samples prior to and after hydrolysis are depicted in Figures 21 - 23. Before hydrolysis the pure and BDICDI-stabilized PLA materials exhibited similar tensile strengths of approximately 57 MPa, elongation at break of about 5.5%, and tensile modulus from 2 GPa to 2.5 GPa, the latter slightly rising with increasing concentration of BDICDI. After hydrolysis a dramatic decline in tensile strength and elongation at break was detected for pure PLA and PLA with low concentrations of BDICDI (PLA with 0, 0.5 and 1% w/w, after 7, 10 and 21 days of exposure, respectively) (Table 6). An almost total drop in tensile strength exceeding 70% and similar trends in elongation at break indicated

significant deterioration in the materials during the particular observation periods. For the record, the tensile modulus of materials remained almost unchanged.

On the contrary, preservation of mechanical properties became evident for PLA with higher concentrations of BDICDI. The percentage differences in tensile strength and elongation at break for the materials between the initial and later stages of the stabilization period clearly documented substantial stability in mechanical properties (Table 6).

The above finding is in accordance with the evolution of molecular weights during hydrolysis as derived by GPC analysis. For PLA stabilized with up to 1% w/w of BDICDI, inclusive-rapid-chain scission resulted in loss of mechanical properties even during short periods of hydrolysis, whereas at higher BDICDI concentrations suppression of hydrolytic degradation led to preservation of performance by the materials over time, clearly depending on the relevant BDICDI concentration.
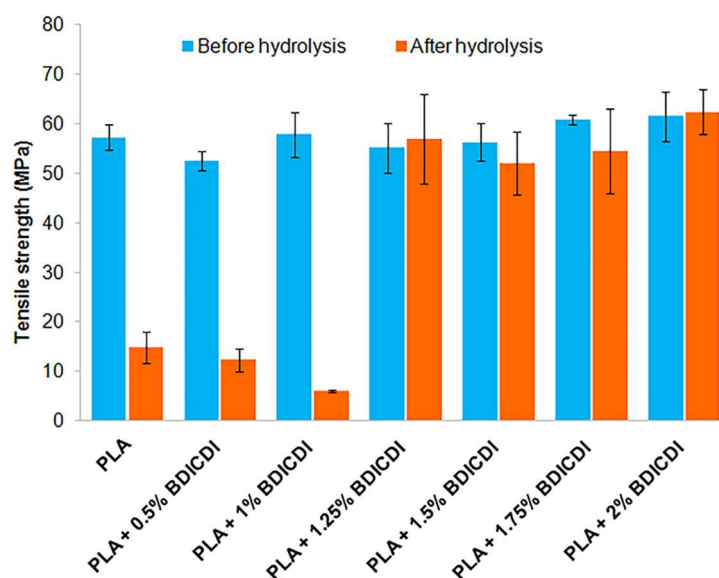
Figure 21 - Tensile strength of samples before and after exposure to abiotic hydrolysis at 7, 10, 21, 28, 63, 77 and 98 days with respect to PLA containing 0, 0.5, 1, 1.25, 1.5, 1.75 and 2% w/w of BDICDI, respectively.
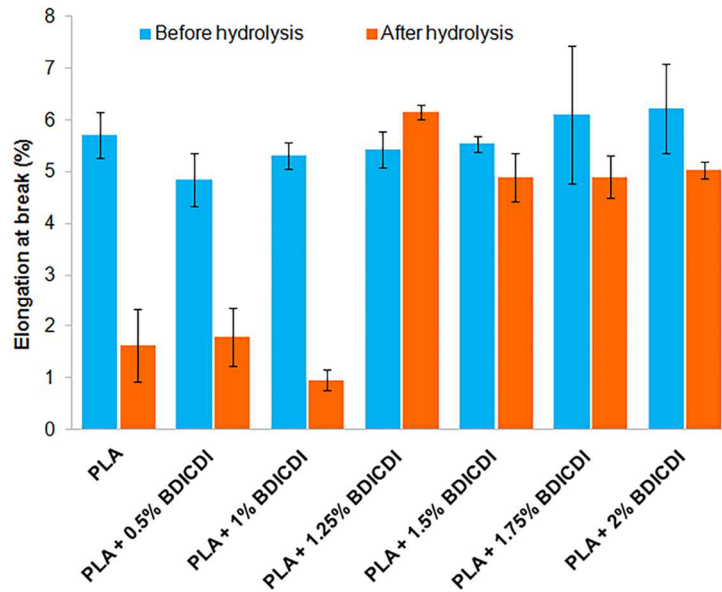
Figure 22 - Elongation at break of samples before and after exposure to abiotic hydrolysis at 7, 10, 21, 28, 63, 77 and 98 days for PLA containing 0, 0.5, 1, 1.25, 1.5, 1.75 and 2% w/w of BDICDI, respectively.
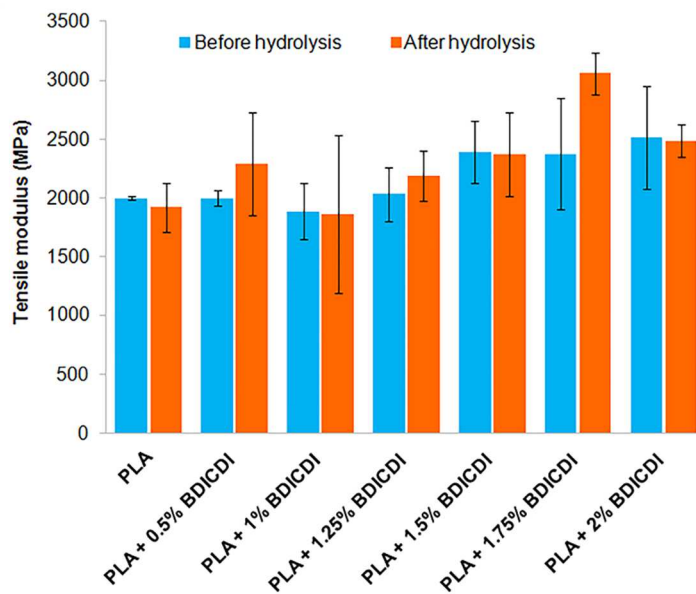

Figure 23 - Tensile modulus of samples before and after exposure to abiotic hydrolysis at 7, 10, 21, 28, 63, 77 and 98 days for PLA containing 0, 0.5, 1, 1.25, 1.5, 1.75 and 2% w/w of BDICDI, respectively.

Biodegradation

The materials investigated were also subjected to an aerobic biodegradation test simulating decomposition under composting conditions, which represents the potential process for eventual disposal at the end of their service life (Figure 24). The data describing PLA biodegradation were evaluated by applying Equation 4, which represents a model for the biodegradation of organic carbon. The parameters of the equation, along with the correlation coefficient R, are listed in Table 7. The model is generally in accordance with the plotted experimental data, and the resultant coefficients of determination proved significant at confidence levels less than 0.01.

The results obtained showed similar trends as revealed in abiotic hydrolysis experiments; these being either a non-existent or negligible stabilization effect at concentrations of 0.5 and 1% w/w BDICDI and strong effects at 1.5% and 2% w/w BDICDI, which increased in conjunction with the concentration of the anti-hydrolysis agent. The stabilization effect could be quantified by the length of lag phase c calculated from the kinetics model, which expressed the initial phase of biodegradation prior to the onset of CO_2 production. While the least delay in the onset of carbon mineralization was almost identical for pure PLA and PLA + 0.5% BDICDI (16 and 15.6 days respectively), for PLA with 1% of BDICDI it increased to 24.5 days. For PLA stabilized with 1.5 and 2% w/w BDICDI, the onset of decomposition was delayed to almost 70 and 100 days, respectively.

Previous works [80] have suggested that abiotic hydrolysis could represent the rate-limiting step of PLA biodegradation under composting conditions. In order for this assumption to be correct the lengths of lag phase c determined from both experiments - abiotic hydrolysis and biodegradation - should be relatively comparable for individual samples. However, after comparing the corresponding parameters, it became evident that while pure PLA with almost identical lengths of lag phase complied with this hypothesis, the stabilized samples - especially those with higher BDICDI concentrations - exhibited earlier onset of CO_2 in comparison with the corresponding curve for abiotic hydrolysis (see Fig. 16).
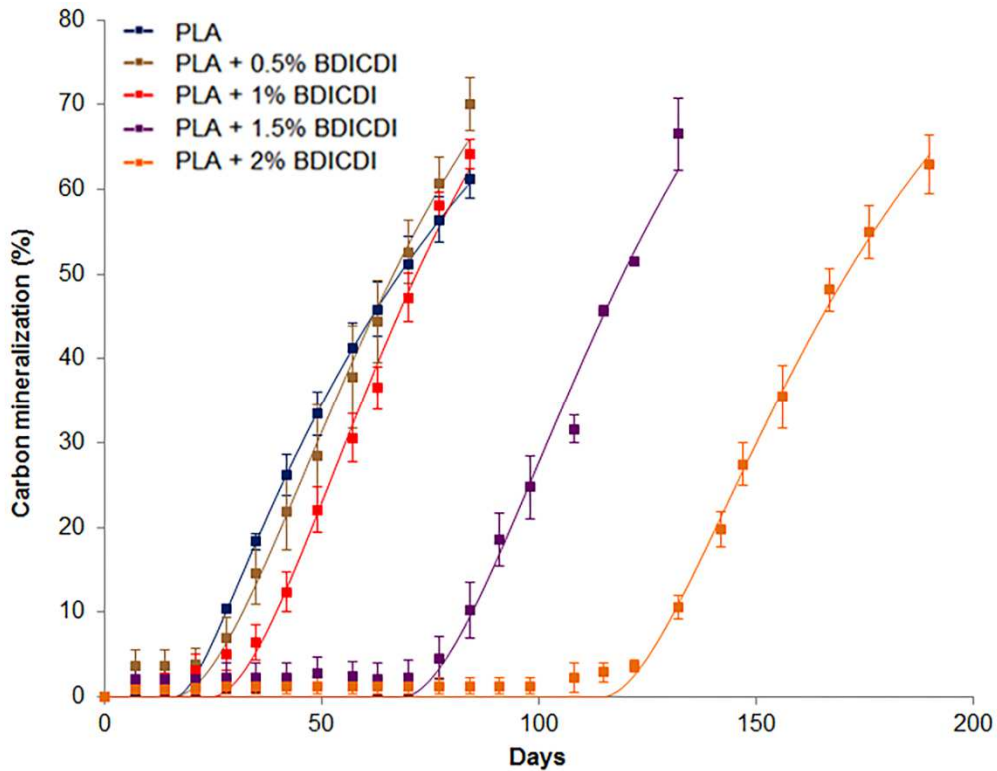
Figure 24 - Biodegradation experiment under composting conditions for pure PLA and BDICDI-stabilized PLA films; error bars correspond to twice standard deviation (n = 3).

This indicates a certain level of acceleration for depolymerization processes above the level set by abiotic hydrolysis during incubation under biotic composting conditions. In highly stabilized samples, which are well protected against abiotic hydrolysis, the cleavage of ester bonds by extracellular enzymes of microorganisms might have become manifest concurrently with abiotic hydrolysis. This assumption is also supported by the slightly higher hydrolysis rate constants for BDICDI-stabilized samples in comparison with pure PLA. Another explanation could be the low stability of the BDICDI additive in such a biotic environment.

Table 7 - Kinetic model parameters and coefficients of determination (R^2) for the biodegradation of pure PLA and BDICDI-stabilized PLA films

Sample	$C_{aq,0}$[a] (%)	$C_{h,0}$[b] (%)	k_{aq}[c] (day^{-1})	k_h[d] (day^{-1})	C[e] (days)	R^2
PLA	0	100	0.1866	0.0150	16.0	0.9999
PLA + 0.5% BDICDI	0	100	0.0330	0.0330	15.7	0.9961
PLA + 1% BDICDI	0	100	0.0358	0.0352	24.5	0.9953
PLA + 1.5% BDICDI	0	100	0.0320	0.0318	69.2	0.9922
PLA + 2% BDICDI	0	100	0.0589	0.0183	100	0.9977

[a] Percentage of initial intermediate solid carbon; [b] percentages of initial hydrolysable solid carbon; [d] rate constant for mineralizing water-soluble carbon into carbon dioxide; [f] first-order hydrolysis rate constants; [i] duration of lag phase during the initial phase of biodegradation before the onset of CO_2 production; [j] percentage of total cumulative CO_2 production at time t = 90 days.

Conclusion

Investigation was made on the stabilization effects of various concentrations of the anti-hydrolysis agent (BDICDI) in PLA films, prepared by melt blending, and these were compared with the initial pure polymer during an abiotic hydrolysis experiment and aerobic composting.

Bis(2,6-diisopropylphenyl)carbodiimide (BDICDI) was shown to be an efficient stabilizer of PLA-suppressing chain scissions of ester bonds during abiotic hydrolysis, especially at concentrations above 1.5% w/w. Beyond this concentration limit the stabilization effect furthered in conjunction with greater concentrations of BDICDI. The period of stabilization can be characterized by only a slight reduction in M_w, not more than 20% from the original values at around 69, 87, and 96 days, in PLA film stabilized with 1.5, 1.75 and 2% w/w of BDICDI at 58ºC. After the dose of stabilizer is depleted, probably via reaction with water molecules and carboxylic groups, the material is hydrolyzed at a comparable or even slightly higher rate than pure PLA. At low BDICDI concentrations (of up to 1% w/w), the stabilization effect was insignificant, potentially caused by depletion of BDICDI as early on as during melt processing at relatively high temperatures. Suppression of hydrolytic degradation within the suggested period also triggered preservation of thermal and mechanical properties, thereby meeting requirements for products intended for long-term performance. In the composting environment, the stabilization effect of BDICDI was comparable, albeit with a slightly faster onset of mineralization for samples stabilized with higher concentrations of BDICDI. The reasons for such modest acceleration in depolymerization processes might due to extracellular enzymes produced by microorganisms or more rapid degradation of the additive under biotic conditions. It can be concluded that a certain amount of BDICDI above the minimal concentration limit, dependent on the duration and conditions of thermal processing, shall be necessary for effectively stabilizing PLA against hydrolysis during the lifetime of a product. By applying the appropriate amount of BDICDI, the approximate duration of stabilization could be set to suit the desired requirements of the final product. This principle demonstrates the potential that exists to design a material with time-programmable properties. The strong stabilization effect shown at relatively low BDICDI concentrations, and the subsequent rapid onset of hydrolysis after BDICDI depletion, strongly support the hypothesis for autocatalytic mechanisms relating to hydrolytic degradation.

6. Natural fibre reinforced polyester urethane copolymer

Over the past few decades, polymer composites have been used heavily in various business sectors, such as civil engineering, the construction industry, transportation, aerospace, electronics and the biomedical area. [92, 93] Their low weight, excellent mechanical behaviour and ability to tailor properties to meet wide-ranging performance requirements, along with the possibility to considerably decrease costs, are the most beneficial properties of this type of polymeric material. [94]

Owing to the recycling problem concerning petroleum-based polymers, great effort has been made to replace them with biodegradable polymers, which exhibit a so-called sustainable life cycle. As regards polymer composites consisting at least of two different materials - a polymer matrix (continuous phase) and a reinforcing agent (dispersed phase) - it is supposed that both phases of the composites would turn out to be biodegradable within a reasonable time. [94, 95] Polylactide (PLA) as the biodegradable aliphatic linear thermoplastic polyester is recognized as being a favoured polymer matrix. [96, 97] Its properties of biocompability, biodegradability and reasonable mechanical behaviour mark it out as a disposable and biodegradable plastic substituent, having been so applied in tissue engineering, drug delivery and food packaging.[21, 98, 99, 100]

As a biodegradable reinforcing phase, natural fibres are commonly used due to their combination of good mechanical properties, low weight and price. However, their relatively high hydrophilicity make them poorly compatible with hydrophobic polymer matrices and pre-treatment is necessary. [101, 102] The most common methods known for hydrophobization of flax fibres are alkali etching [103], acetylation [104], silanization [105] and peroxide treatment.14 Furthermore, maleic-anhydride-based compatibilizing agents have also been launched commercially as well as efficient additives for promoting adhesion between flax fibres and a hydrophobic matrix.[106]

Due to the actual high cost of PLA, which partially results from the complex purification process during its synthesis, endeavour has been made to investigate other methods to synthesize biodegradable polymers based on renewable resources. One of them is the so-called chain-linking of lactic-acid-based prepolymers of low molecular weight with di-isocyanates, resulting in high molecular weight polyester-urethane (PEU). [107] The resultant copolyesters

might prove suitable for use in practical applications resembling those for standard commercial PLA. [108]

Although several papers have dealt with the preparation of PLA-based PEU [109, 110], there is a lack of work looking at their utilization in blends and composites. Therefore, this study explores the preparation and characterization of novel biocomposites based on PEU and flax fibres. Due to limited compatibility between flax fibres and polymeric matrices, caused by complex physical and chemical structures [95, 111], the work present herein focuses on modifying interfacial compatibility between the flax fibres and PEU matrix.

Moreover, examination and discussion is given on the thermal and mechanical properties of biocomposites, resulting from the flax fibre pre-treatment applied or the modification of the PLA-PEG chain linked copolyester, as well as selecting compatibilizing agents.

Materials

Materials for PEU synthesis

L-lactic acid (LA), 80% water solution; PEG, (Mn ~ 380 – 420 g.mol^{-1}, in text labelled as PEG400) were products of Merck, Hohensbrunn, Germany. Tin(II) 2-ethylhexanoate (Sn(Oct)$_2$), ~95%; hexamethylene diisocyanate (HMDI), 98%, were purchased from Sigma Aldrich, Steinheim, Germany. Solvents: chloroform, acetone, methanol and ethanol (all analytical-grade) came from IPL Petr Lukes, Uhersky Brod, the Czech Republic. Chloroform (HPLC-grade) was sourced from Chromspec, Brno, the Czech Republic. All chemicals were used as obtained without further purification.

Materials for composite preparation

The flax fibres were provided by Havivank Bv (the Netherlands). The properties guaranteed by the supplier were as follows: density of 1.45 g.cm^{-3} and tensile strength of 600 MPa. On the basis of electron microscopy observation, the lengths of the fibres were between 150 and 320 µm, and diameters varied between 10 and 30 µm. Acetic acid, Sodium hydroxide, oleic acid (OA) and di-tert-butyl peroxide (DTBP) were supplied by Sigma Aldrich, Steinheim, Germany. The commercial additive 3-(aminopropyl) trimethoxy silane (ATMS) was obtained from Sigma Aldrich (Germany).

Experimentally synthesized materials named as additive 1 and additive 2 were prepared at the University of Pannonia, Veszprém, Hungary, and their composition and properties are summarized in Table 8. These compounds were chosen on the basis of previously reported publications, since they and their derivatives worked well as compatibilizing agents between the hydrophilic and hydrophobic phases.[111, 112, 113, 114]

Table 8 - Characteristics of synthesized compatibilizing additives

	Experimental additive 1	Experimental additive 1
Type	polyalkenyl-poly-maleic-anhydride	Polyalkenyl-poly-maleic-anhydride-ester
Olefin component	styrene	C_{15}-C_{25}
Alcohol component	-	dodecanol
Appearance	white-yellow	white-yellow
Acid number [mg KOH.g^{-1}]	125.2	14.8
M_w [g.mol^{-1}]	1620	3435
M_n [g.mol^{-1}]	1355	2420
α	1.20	1.42
ASTM colour	0.5	0.5

Sample preparation

Copolymer preparation

A diisocyanate chain-linked copolymer of PLA and PEG (PEU) was prepared as described in one of our previous works.20 Namely, 100 mL of L-LA was added into a 250 mL two-neck distillation flask equipped with a Teflon stirrer. The distillation flask was then connected to a condenser and placed in an oil bath. Firstly, dehydration of L-LA solution at 160°C took place, under a reduced pressure of 20 kPa for 4 hours. Secondly, 0.5 wt. % Sn(Oct)$_2$ and 7.5 wt. % PEG were added and the reaction procedure continued for 6 hours at 10 kPa. Afterwards, the pressure was reduced to 3 kPa for another 10 hours. The resultant hot product with high viscosity was poured out onto aluminium foil and cooled. The whole procedure was repeated till a sufficient amount of material had been collected. Finally, the desired numbers of batches were cut and mixed using a cutting mill (Retsch SM 100) to particles of approximately 3 mm in diameter. The granular PLA-PEG prepolymer was stored in a desiccator.

For PLA-PEG chain-linking, 30 g of PLA-PEG prepolymer was added into a 250 mL two-neck flask equipped with a mechanical stirrer. The prepolymer was slowly heated to a predetermined temperature (160°C), under N$_2$ atmosphere. Once the mixture had completely melted, HMDI was added and reaction continued for 20 minutes. The PEU obtained was cooled down, dissolved in chloroform, precipitated into a water/methanol mixture (1:1), filtered and dried under vacuum at 30°C for 24 hours.

Composite preparation

A two-roll mill (Laboratory two-roll mill, Lab Tech LRM-S-110/T3E) was used for composite preparation. The copolymer, PEU, as well as flax fibres were dried at 80°C for 3 hours before mixing. The processing temperatures were 95°C (first roll, n=8 rpm) and 125°C (second roll, n=19 rpm). The mixing time was 10 minutes. The fibres and additives were added into the molten polymer during the mixing procedure. The compositions of the composites are summarized in Table 9.

Table 9 - Composition of PEU/flax fibre composites

Component	Unit	Composite label and amount of component						
		A	B	C	D	E	F	G
Natural fibre	[wt.%]	20	20	20	20	20	20	20
Copolymer		80	79.5	80	80	79	79	79.7
ATMS			0.5					
Acid treatment[a]				YES				
Alkali treatment[b]					YES			
Experimental additive - 1						1		
Experimental additive - 2							1	
Oleic acid + DTBP								0.2+ 0.1

[a] - *The flax was treated for 30 min. in 10% acetic acid and then dried in hot air (80°C) for 4 hours*
[b] -*The flax was treated for 30 min. in 10% NaOH and then dried in hot air (80°C) for 4 hours*

Characterization

Molecular weight determination

Change in molecular weight following the blend preparation was examined on a GPC device equipped with a dual detection system (refractive index and viscometric detector). Analysis was conducted using the Agilent HT-GPC 220 system. Samples, PEU and its composites (A, B, C, E, F and G) were dissolved in THF (~3 mg.ml^{-1}) overnight and filtered (syringe filter, 45 μm). Separation and detection took place on a series of PL gel-mixed bed columns (1x Mixed-B, 300×7.8 mm, 10 μm particles + 1x Mixed-D, 300×7.8 mm, 5 μm particles) at 30°C in THF. The flow rate equalled 1.0 ml.min^{-1} and injection volume was 100 μL. The GPC system was calibrated with narrow polystyrene standards ranging from 580 to 1 000 000 g.mol^{-1} (Polymer Laboratories Ltd., UK). The weight average molar mass Mw, number average molar mass Mn and molar-mass dispersity (MWD = Mw/Mn) were determined from their peaks corresponding to the polymer. All data processing was carried out using Cirrus software.

FTIR analysis

In order to identify the physico-chemical structure of composites, FTIR spectroscopy analysis was carried out. The experiments were conducted on a TENSOR 27 type FTIR-ATR spectrometer equipped with an attenuated total reflectance (ATR) accessory (Ge crystal) at room temperature. The uniform number of 32 scans with resolution of 3 cm^{-1} was maintained in all cases.

Tensile testing

To determine the tensile and three-point flexural properties (mainly stress and extension) (CSN EN ISO 527-1-4:1999, CSN EN ISO 14125:1999), an M350-5 CT Materials Testing Machine was used. Tensile and flexural tests were carried out at the testing speed of 50 mm.min^{-1} and at 10 mm.min^{-1} crosshead speed. Charpy impact strength measurements of the produced composites were provided by a ZWICK 5113 to measurements according to the CSN EN ISO 179-2:2000 standard.

Scanning electron microscopy (SEM)

Scanning electron microscopy (TESCAN VEGA II LMU, the Czech Republic, equipped with a thermo-emission cathode) was applied to characterize the structural arrangement. The samples were obtained from impact-fracture-

surface specimens. All specimens were coated with a thin layer of Au/Pd. The microscope was operated in high vacuum mode at an acceleration voltage of 5 kV.

Differential scanning calorimetry (DSC)

The thermal properties of the samples were measured by differential scanning calorimetry (DSC1 STAR, Mettler Toledo) under a nitrogen atmosphere and constant heat rate of 10°C/min, using a following heating programme: running a heating cycle from -10°C to 150°C. Samples with a weight of ~ 10 mg were placed in sealed aluminium pans.

Thermogravimetric analysis (TGA)

The thermal stability of the neat and treated PEU copolymer as well as the prepared composites was determined by thermogravimetric analysis (TGA Q500, TA INSTRUMENTS) under a helium atmosphere (gas flow of 30 ml.min^{-1}). Samples with a weight of approximately 15 mg were heated from 25°C to 500°C at a heat rate of 10°C.min^{-1}. The decomposition temperature of samples was determined as an onset degradation temperature on the TGA curve.

Results

Molecular weight is an important characteristic describing in one way the effectiveness of polymer synthesis or processing. The molecular weight properties of untreated and treated copolymers and composites are summarized in Table 10. It can be seen that the applied modification to the both the polymer matrix as well as the fibres altered the final molecular weights. The initial M_w of PEU decreased from 85.5 to 57.6 kg.mol^{-1} after processing the same with the fibres in a two-roll mill, revealing the high sensitivity of the sample to hydrothermal degradation.[115] However, the value of M_n was not changed, highlighting the dominant degradation of long polymer chains. The drop in molecular weight was determined also for composites with treated fibres (C and D). Generally, the decrease in M_n and M_w was 35% and 50%, respectively. The reason for composite degradation during thermal processing can be explained by the presence of thermally unstable ester bonds in the copolymer structure, the high shear forces during mixing and the presence of ambient humidity. The fact that degradation was more significant in composites, which contained a

compatibilizer or treated fibres suggests that all of the applied modifications to enhanced chain scission during processing.

Table 10 - Molecular weight properties of PEU copolymer before and after composite processing.

Sample	Additive	M_n [Kg.mol^{-1}]	M_w [Kg.mol^{-1}]	MWD
Neat copolymer[a]	No	18.4	85.5	4.7
A	No[b]	18.9	57.6	3.1
B	ATMS	12.0	39.6	3.3
C	Acid treatment	12.5	44.5	3.6
D	Alkali treatment[c]	-	-	-
E	Experimental additive - 1	12.0	45.2	3.8
F	Experimental additive - 2	9.9	44.1	4.5
G	Oleic acid + DTBP	11.9	42.6	3.6

a – pure copolymer after synthesis
b – pure copolymer with non-modified flax fibres after mixing
c – material degraded extensively during processing/not measured

The chemical composition of neat PEU and its composites was characterized by infrared spectroscopy. Figure 25 shows the FTIR – atr spectra of neat copolymer and all the biocomposites investigated. The spectrum of the neat PLA-PEG chain-linked copolymer contains signals typical for PLA, PEG and amide bonds, resulting from a reaction of end groups with di-isocyanate. The spectrum has already been described in a previous work by the authors [108]. Therefore, just the most important signals show following the presence of an amide I bond arising from the reaction of NCO with unreacted COOH groups: region 3400 cm^{-1} (absorbed water), 3300 nm (N-H) and 1520 cm^{-1} (N-H amide II) bonds, and the broadening of –C=O to 1640 cm^{-1}.

The spectrum of flax has been described previously and is also given here: 3335 cm^{-1} (free OH), 2900 cm^{-1} (C-H), 2850 cm^{-1} (CH$_2$), 1645 cm^{-1} (adsorbed water) 1155 cm^{-1} (C-C) ring breathing, 1105 cm^{-1} (C-O-C) glycosidic, 1050 cm^{-1} and 1025 cm^{-1} (C-OH) [116].
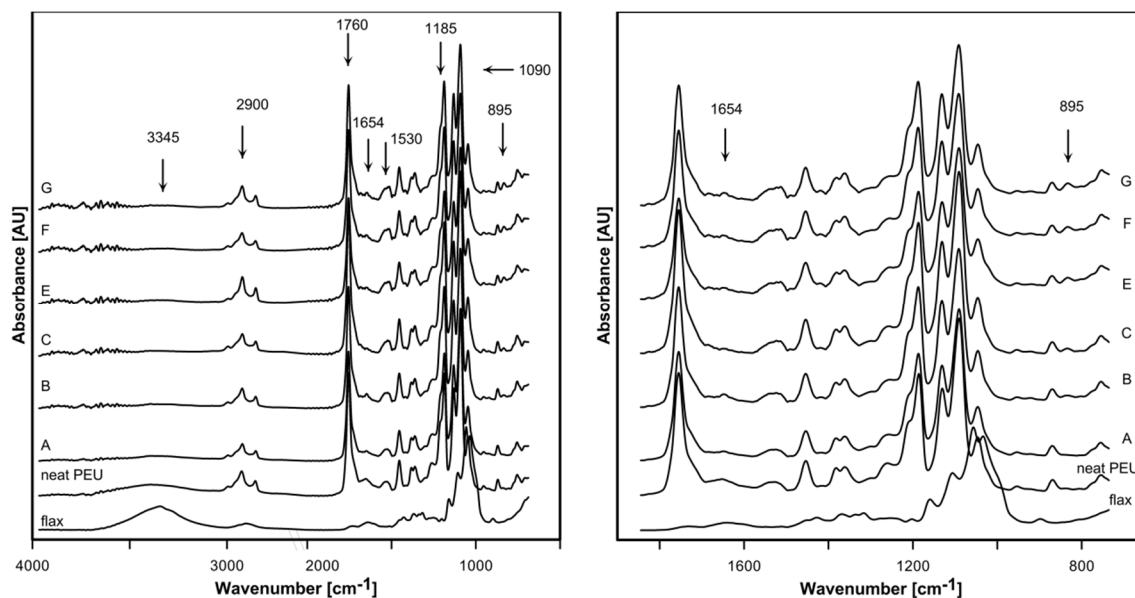
Figure 25 – FTIR ATR spectra of prepared biocomposites and neat components.

In the case of biocomposites, the signals of amine at 3300 cm^{-1} from the copolymer and OH groups from flax overlapped and decreased in intensity due to such mixing. A new peak, appearing at 835 cm^{-1}, was observed only in composites (B – G) and suggests the presence of –NH$_2$ groups created during thermal degradation.

The mechanical properties of composites reflect the level of an interfacial compatibility between the polymer matrix and fibres. Table 11 shows the values for the mechanical properties of biocomposites with modified and unmodified fibres/matrix. The nominal values of the individual, determined mechanical properties of the treated composites were compared with original untreated composite A, and the relative changes are shown in Figure 26.

Table 11 - Summary of mechanical properties of prepared composites. Average values for a minimum of six measurements are presented. Standard deviation was up to 10 % in all cases.

	A	B	C	E	F	G
Tensile strength at maximum, [MPa]	11.3	15.3	13.3	15.1	14.9	13.4
Elongation at break, [%]	3.3	2.2	2.6	2.8	2.2	2.1
E-modulus (tensile),[MPa]	750	780	880	853	940	987
Charpy impact strength, [kJ.mm^{-2}]	2.5	3.8	2.7	3.6	4.2	3.4
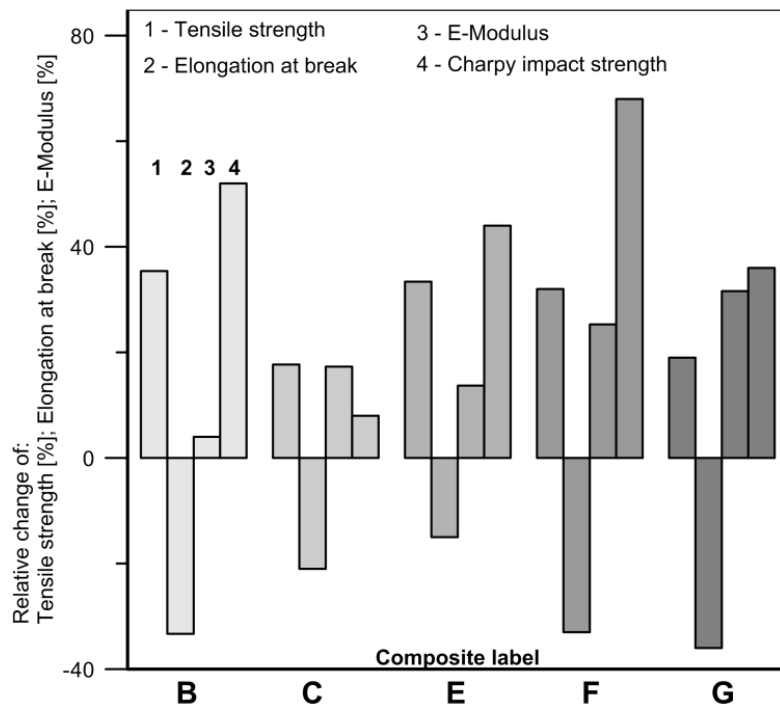
Figure 26 – Relative changes in mechanical properties of treated composites in relation to original untreated composite A. Average values of a minimum of six measurements are presented. Standard deviation was up to 10 % in all cases

The biocomposite without any additives or fibre treatment (A) exhibited the lowest tensile strength (11.3 MPa) and E-modulus (750 MPa). Table 11 and Figure 26 show that all the modification applied to fibres with the compatibilizing agents contributed to the higher interfacial adhesion between the treated fibres and PEU. The better stress transition between the fibres and polymer actually improved the tensile properties (E-modulus and tensile strength at maximum) of the composites subsequently. Composites B (acid treatment) and G (Oleic acid + DTBP) showed mild enhancement in tensile properties when their tensile strength at maximum was increased by more than approximately 17% in comparison with composite A. Moreover, E-modulus values for composites C and G rose by about 17% and 32%, respectively. More interesting results were observed for samples with commercial and both experimental additives (B, E, F), which exhibited the highest values, ~15 MPa of tensile strength at maximum. This is approximately equal to 35% improvement. The enhancement in tensile strength thus observed is significantly higher than in a previously published work, where commercial PLA/flax fibre composites reported only ~10% with a comparable concentration of flax [102]. The enhancement of E-modulus was also observed for composites B, E and F. While sample B proved only to display a slight increase (780 MPa) in comparison with untreated composite A (750 MPa), composites E and F showed significantly higher values (853, 940 MPa). In all cases, the improved tensile strength at maximum and E-modulus were accompanied by reduction of elongation at break (between 15% – 32%), which results through the presence of inexpensive flax fibres with the matrix.

Charpy impact strength is directly related to energy consumed during the sample cracking under experimental conditions. It is clear that introducing the flax fibres would create obstructions for a crack path; hence more energy is needed [117]. This effect is even more pronounced if fibre/matrix interaction increases. As all the modified biocomposites exhibited a higher value for impact strength in comparison with original untreated composite A, indication is given that flax/PEU copolymer interaction was successfully improved. The highest Charpy impact strength value of 4.2 kJ/mm^2 was determined for composite F, demonstrating the great efficiency of compatibilizing additive 2.

Furthermore, interfacial compatibility between flax fibres and copolyester was investigated by scanning electron microscopy. Figure 27 shows the fracture surface of composite without any modification (sample A, top image). There are gaps between the flax fibres and the PLA which could either occur through

debonding during mechanical testing or as a result of poor approximation during composite production. A great quantity of holes, caused by the residue of the fibres, is visible on the surface of the fracture, in addition to which it can be seen that the surfaces of fibres are clean. All these observations can also be found in the literature, suggesting poor adhesion between the fibres and the matrix [102]. Composites C and F were selected for comparison purposes on compatibility between the modified polyester or modified flax fibres. Both composites C and F, compared with untreated composit A, show improved interfacial compatibility (the occurrence of fibre pull-outs was rare). However, composite F exhibits better coating of fibres with polyester as well as showing a more compact structure.

The thermal properties of the copolyester and composites reflect the values for molecular weight properties. DSC thermograms are shown in Figure 4 and nominal values for thermal properties are summarized in Table 12. The original copolyester possesses a semi-crystalline character with a low crystalline portion (specific heat of fusion, $\Sigma\Delta H_m = 1.4$ J/g), with a glass transition temperature (T_g) of 33°C and single melting peak at 129.7°C. The thermal properties of PEU composites with untreated and treated flax fibres were variously modified depending on the treatment utilized. In composite A (without treatment) cold crystallization occurred at 89.8°C and the melting peak exhibits multiple crystalline phenomenon due to the occurrence of crystallites of a new kind, but the final value of $\Sigma\Delta H_m$ is comparable with original unfilled PEU. Applying treatment to flax fibres or adding a compatibilizing agent to the composites, when compared with untreated composite A, caused a decrease in glass transition temperature of around 8.9°C -9.5°C, which corresponds with the drop in molecular weight. However, this excludes composite F, which could indicate the high compatibilizing efficiency of additive 2. Silane, acid and alkali treatment of flax fibres slightly changed the semi-crystalline character of composites. Silane treatment especially increased the value for $\Sigma\Delta H_m$ by about 2.5 times (composite B), whereas acid treatment almost eradicated the crystalline structure of composite C, in addition to which alkali treated fibres fully degraded composite D. A totally different influence was effected by compatibilizing additives 1 and 2, which changed the character of composites E and F, making them amorphous in nature. The semi-crystalline character of composite G was comparable to that of composite B.
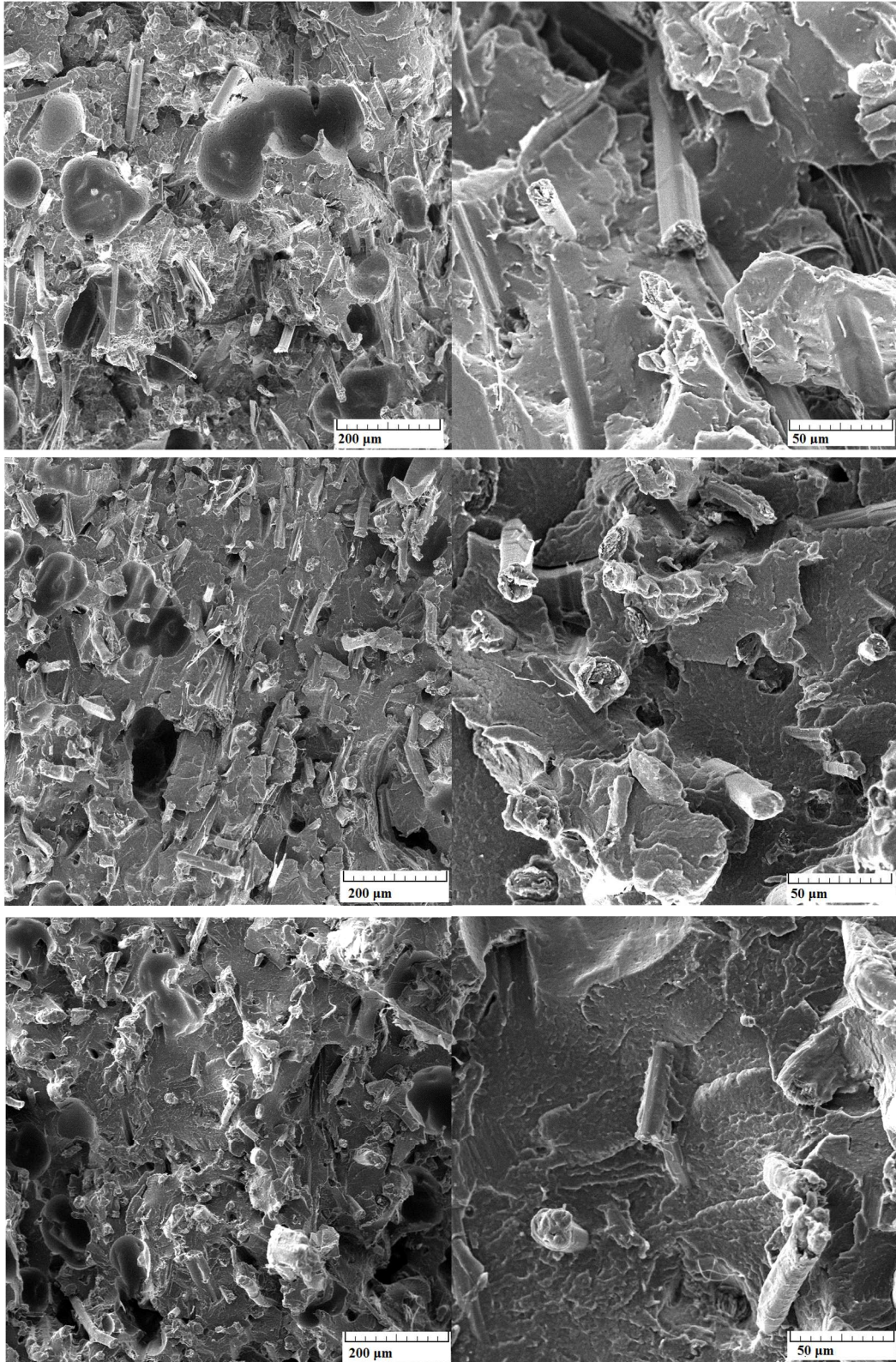
Figure 27 – Selected SEM micrographs of fractured biocomposites under various magnifications. Top – (A), middle – (C), bottom – (F)

Table 12 - Thermal properties of prepared composites.

Sample	1st heating cycle					
	T_c	ΔH_c	T_m	ΔH_m	$\Sigma \Delta H$	T_g
	(°C)	(J/g)	(°C)	(J/g)	(J/g)	(°C)
PEU	-	-	129.7	1.4	1.4	32.1
Composite A	89.8	0.8	105.1/112.8/122.1	2.3	1.5	30.2
Composite B	-	-	95.9/111.1	5.3	5.3	20.7
Composite C	-	-	128.7	0.5	0.5	21.3
Composite D	nd	nd	nd	nd	nd	nd
Composite E	-	-	-	-	0	21.7
Composite F	-	-	-	-	0	33.2
Composite G	82.7	1.3	95.9/111.1	6.7	5.4	21.1

nd – not determined
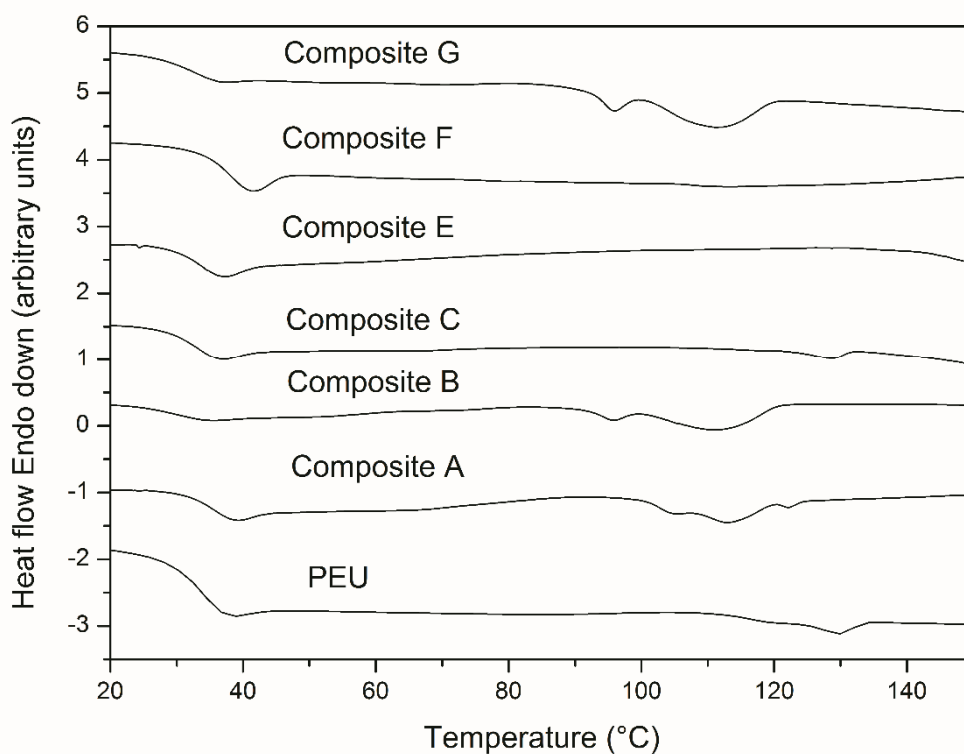
Figure 28 – DSC thermograms of PEU and PEU/flax fibre composites

The presence of three melting peaks in composite A can be attributed to the presence of crystals possessing different lamellar thicknesses or possibly different crystalline forms. The decline in the melting region is indicated on less perfect crystals than on neat copolymer. A similar change in crystallites and the melting behaviour of polylactic acid/flax fibre composites was observed in a work by Battegazzore et al. [105] As Table 12 shows, after treatment had been applied to flax fibres or composites, the crystalline character of the final composite was significantly changed. Only Composite C shows a single melting peak comparable with neat copolymer. Composites A, B and G exhibit a multi-melting characteristic, and composites E and F are amorphous. The explanation for the amorphous nature of samples E and F lies in the presence of an anhydride ring; this acts as an obstruction that inhibits chain-folding. It is also possible that the compatibilizer reacts with the copolymer, which might lead to the creation of structures unable to crystallize under experimental conditions.

Thermal stability was measured by thermogravimetric analyses, and TGA thermograms are depicted in Figure 29 while analysed values are summarized in Table 13. As can be seen, neat copolymer exhibited single step decomposition at 250°C during heating with onset degradation temperature. The onset degradation of unmodified composite A was around 10°C higher than for neat copolymer, which highlights the beneficial effect of flax fibres on the thermal stability of a biocomposite. This is in disagreement with most papers published on PLA/flax (or other cellulose fibres), where a small decrease in thermal stability was observed. [105, 118, 119] This discrepancy can be explained by the dominant effect of heat absorption by the flax fibres rather than their catalytic effect on decomposition.

The mass loss commencing at around 130°C in all blends was attributed to the evaporation of absorbed moisture [120]. Due to the significantly higher second decomposition temperature of Composite C ($T_o = 340°C$) it can be concluded that acid treatment increased the thermal stability of flax fibres, whereas other modifications did not have a significant impact on the decomposition temperature of flax fibres in the composite. The significantly increased residues of composites at 500°C, in comparison with neat copolymer, were attributed to ash and mineral components from flax, since it was known that about 10% of such residues usually remained after burning flax [105].
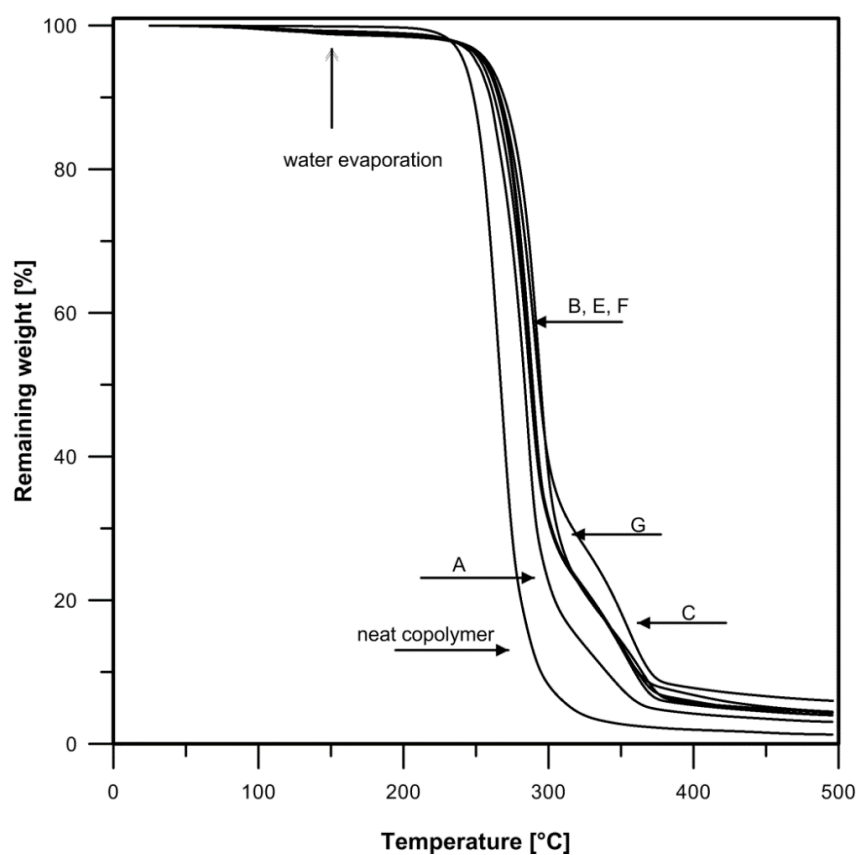
Figure 29 – TGA curve of prepared biocomposites and neat copolymer

Table 13 - Summary of thermogravimetric analysis results – T_{o1} – onset temperature 1, T_{o2} – onset temperature 2 and weight percentage of residues at 500°C.

	T_{o1} [°C]	Remaining weight[a] [%]	T_{o2} [°C]	Remaining weight[a] [%]	Residue weight [%]
Neat copolymer	250	88.7	-	-	1.29
A	260	97.0	-	-	3.1
B	268	78.9	326	17.2	3.9
C	271	83.2	341	12.5	4.3
E	270	77.9	323	17.6	4.5
F	266	78.9	326	17.1	4.0
G	270	72.3	324	21.7	6.0

[a] *– Remaining weight at onset temperature*

Conclusions

The aim of the work was to find an optimal compatibilization method for a thermoplastically prepared biocomposite system, based on natural flax fibres and a novel polyester-urethane copolymer matrix. Two types of experimentally prepared additives, a commercial additive and oleic acid and di-tert-butyl peroxide were used as compatibilizing agents. In addition, the effect of alkali or acid treatment on the fibres was investigated. The resultant biocomposites were characterized by gel permeation chromatography, infrared spectroscopy, differential scanning calorimetry, thermogravimetric analysis, and scanning electron microscopy. Mechanical properties were determined by tensile and impact resistance tests.

Results show that the molar mass of the polymer matrix was considerably decreased due to thermal degradation of material during biocomposite preparation. It was also confirmed by infrared spectroscopy. Electron microscopy revealed better adhesion between the fibres and matrix after each type of modification, which corresponds to the mechanical properties of such biocomposite enhancement. Differential scanning calorimetry analysis highlighted the amorphous or semi-crystalline nature of composites. The presence of natural fibres led to overall thermal stability of biocomposites improvement.

From the viewpoint of the studied polymer matrix – a natural filler compatibilization process, involving application of an experimental additive based on maleic anhydride and a commercial additive - 3-(aminopropyl) trimethoxy silane, was found to be the most effective methodology. Nevertheless, almost all of the fibre treatment methods researched significantly improved the properties of biocomposites, in comparison with the system utilizing untreated flax fibres. The only exception observed was for the alkali treatment of fibres, which led to strongly negative interaction with the polyester-urethane matrix.

7. Effect of hybrid zinc stearate-silver system on degradation behaviour of PLA

PLA is widely investigated as promising polymer for applications in food packaging, medical applications and especially in hygienic materials. However, such applications require good mechanical as well as specific properties, such as antimicrobial activity and thus, the modifications of initially brittle PLA are necessary.

The mechanical properties of PLA are of great interest. The improvement of the mechanical properties can be achieved, either by chain orientation, by blending with other biodegradable polymers or by introducing plasticizer systems into it [121]. Common plasticizers are e.g. glycerol, triacetin, and low molecular weight citrates, partial fatty acid esters [122]. A large number of investigations have also been reported on blending PLA with various polymers such as plasticizers, for example, thermoplastic starch [123], poly(ethylene oxide) [124, 125], poly(ethyleneglycol) [125], poly(ε-caprolactone) [126], cellulose acetate [127], to improve the flexibility of PLA.

Antimicrobial modifications of polymers are used to prevent or inhibit a growth of microorganisms on its surface. Nowadays, a commonly used method for modification of polymers is the addition of an antimicrobial agent/additive directly into the polymer matrix. Currently, silver-based (Ag) additives have received significant attention due to the low toxicity of the active Ag ion to human cells as well as for being a long lasting biocide with high thermal stability and low volatility [128, 129]. Microwave (MW) synthesis is one of the well-known effective methods of the preparation of Ag-NPs [130, 131]. Immobilization of Ag-NPs by MW synthesis on various organic substrates has been studied by Bazant et al. [129]. The authors successfully immobilized nanosilver, nanostructured ZnO and hybrid nanostructured Ag/ZnO on a wood flour (WF) surface by MW synthesis. Subsequently, the modified WF was compounded into a PVC matrix (5 wt. % loading) and the antimicrobial activity was tested while the most efficient system was the hybrid nanostructured Ag/ZnO. Iqbal et al. described the surface modification by MW synthesis of Ag-Nps on surface of inorganic substances [128]. Ag-Nps were successfully bonded on hydroxyapatite and caused antimicrobial activity of the prepared system.

Pantani et al. [62] prepared PLA/ZnO based nanocomposites with good antimicrobial activity. However, they reported that parameters of mechanical

properties, such as elongation at yield and break, should be improved by addition of a plasticizer into the nanocomposite film.

Therefore, the objective of this part of work was to prepare PLA based composites with additive, which fulfil both functions: fragility suppression and exhibit the antimicrobial activity. Therefore, the Ag nanoparticles have been immobilized by MW synthesis on the surface of zinc stearate (ZnSt) (a well-known plasticizer) and the resulting hybrid system (ZnSt-Ag) was incorporated in PLA polymer matrix in various concentrations. The changes in thermal and mechanical properties as well as morphology of composites in dependence on concentration of ZnSt-Ag were investigated. Moreover, the influence of the ZnSt-Ag system on PLA degradation behaviour was observed during the abiotic hydrolysis, which represents a major depolymerisation mechanism of PLA.

Materials and methods

Materials

Polylactide was obtained from NatureWorks (Ingeo™ 4060D). Its weight average molar mass Mw was 158000 g.mol^{-1} and polydispersity 3.5 as determined by GPC (Agilent HT-GPC 220). Density of PLA was 1.24 kg.m^{-3}. Zinc stearate (ZnSt) was supplied by Sigma Aldrich (USA). Silver nitrate (AgNO$_3$), Hexamethylenetetramine (HMTA) and ethanol were purchased from PENTA, Czech Republic.

Preparation of hybrid ZnSt-Ag particles

Hybrid ZnSt-Ag particles were prepared under reflux in the microwave open vessel system MWG1K-10 (RADAN, Czech Republic; 1.5 kW, 2.45 GHz) operating in continuous mode (zero idle time) with external cooler. First, 200 mL of AgNO$_3$ (0.85 g) solution in water and 450 mL of ZnSt (11.02 g) dispersion in ethanol were transferred into 1000 mL reaction bottle.

The reaction mixture was heated in MW oven for 2 min. After that, 100 mL of HMTA (7.00 g) solution in water was added and the MW heating continued for 10 min under continuous stirring (250 rpm). The reaction product was collected by suction microfiltration and left to dry in a laboratory oven (50 °C) up to the constant weight. The prepared ZnSt-Ag system contained 4.09 wt. % of Ag (determined by energy dispersive x-ray fluorescence spectrometer, ARL Quant´X EDXRF Analyzer, Thermo Scientific, Germany).

Preparation of PLA/ZnSt-Ag mixture

Before compounding, PLA pellets were dried at 45 °C under reduced pressure for at least 24 hours. Prepared hybrid particles were incorporated into the PLA matrix by co-rotating twin screw micro-compounder MiniLab II HAAKE Rheomex CTW5 (Thermo Scientific, Germany, 5 mL chamber volume). System temperature was 160 °C, speed 100 rpm and time of mixing 5 min, concentration of the filler was 1; 3; 5 and 10 wt. %.

PLA films 500 µm thick were compression molded. The material was brought to the processing temperature of 160 ℃ during 1 min, then molded for 2 min. and immediately cooled down under pressure after transferring the material to a second press kept at 20 °C.

Characterization

Gel permeation chromatography

The weight average molecular weight (Mw) and its changes during degradation tests were analysed by gel permeation chromatography (GPC). Analysis was conducted using Agilent HT-GPC 220 chromatographic system. Samples were dissolved in THF (~1.5 mg/mL) overnight. Separation and detection took place on 1xPL gel-mixed-B and 2x PLPL gel-mixed-D (300×7.8 mm) columns connected in series with an RI and viscometric response detectors, respectively. Analyses were carried out at 40°C with a THF flow rate of 1.0 ml/min and a 100 μL injection loop. The GPC system was calibrated with narrow polystyrene standards ranging from 580 to 1 000 000 g.mol^{-1} (Polymer Laboratories Ltd., United Kingdom). The weight average molar mass M_w, number average molar mass M_n and molar-mass dispersity (MWD = M_w/M_n) of the tested samples were determined from their peaks corresponding to the polymer fraction based on universal calibration curve (polystyrene standard). All data processing was carried out using Cirrus software.

Thermal properties - Differential scanning calorimetry

Thermal characteristics were obtained by differential scanning calorimetry (DSC) on the Mettler Toledo DSC1 STAR System. All measurements were carried out under a nitrogen atmosphere (50 cm^3.min^{-1}). The temperature ramp was set from 0°C to 210°C (10 K.min^{-1}), followed by annealing at 210°C for 5 min and afterwards by cooling scan of 210–0°C (10 K.min^{-1}), then an isothermal step at 0°C for 5 min, and finally the second heating scan at 0–210°C (10 K.min^{-1}). Melting point temperature (T_m) was obtained from the first heating cycle. The glass-transition temperature (T_g) was determined from the second heating scan.

Mechanical properties

The tensile tests of composites were carried out according to ČSN EN ISO 527-1-4 standard by using tensile testing machine Testometric M350-5CT at a crosshead speed of 5 mm.min^{-1}. The dimensions of dog-bone form specimens cut from the compression molded plates were $60 \times 4.0 \times 0.5$ mm. Prior to the testing samples were dried over-night at 45 °C. At least seven specimens from each group were tested.

Atomic absorption spectroscopy (AAS)

The exact concentration of the ZnSt-Ag particles in PLA matrix was determined by atomic absorption spectroscope Agilent DUO 240FS/240Z/UltrAA (Agilent Technologies) equipped with a hollow cathode lamp (Ag: I = 4 mA and wavelength = 328.1 nm, Zn: I = 5 mA and wavelength = 213.9 nm) and with background correction by a deuterium lamp. The mixture of gasses, acetylene and air, was used in the flame at 2.0 and 13.5 L min^{-1} flow rates, respectively. Concentration was calculated according to calibration which was measured with standards with specified concentrations (Ag:1000 mg/L, Agilent Technologies, Zn:1000 mg/L, Fluka Analytical).

Scanning electron microscopy (SEM)

Structure of the prepared samples was observed by scanning electron microscopy (VEGA IILMU, TESCAN). Specimens were coated with a thin Au/Pd layer. The microscope was operated in vacuum mode at an acceleration voltage of 10 kV.

Antimicrobial activity

Antimicrobial testing was performed on films containing ZnO and CuO nanoparticles according to international standard ISO 22196:2007. The activity was tested against bacteria strains, Escherichia coli (Gram-negative) and Staphylococcus aureus (Gram-positive). Colony forming units (CFU) were determined and the antimicrobial activity (R) was defined as differences between logarithm values of growth of untreated and treated samples:

$$R = U_t - A_t \tag{6}$$

where U_t is the average of the common logarithm of the number of viable bacteria, in cells/cm^2, recovered from the untreated test specimens after 24 h, A_t the average of the common logarithm of the number of viable bacteria, in cells/cm^2, recovered from the treated test specimens after 24 h and R is the antibacterial activity.

The colony forming units reduction (CR) is expressed by the reduction of the number of the formed colonies per cm^2 in percentage:

$$CR = \left(1 - \frac{N_S}{N_B}\right) \cdot 100 \qquad (7)$$

where N_B is the number of viable colonies per cm^2 after 24 h recovered from the material without additive (blank) and N_S is the number of viable colonies per cm^2 after 24 h recovered from samples with antimicrobial agents.

Abiotic degradation

Abiotic hydrolysis was determined at 37 °C. The samples (50 mg) were cut to 0.3 x 0.5 cm specimens and suspended in 10 ml of sodium phosphate buffer (0.1 mol.L^{-1}, pH 7.00) with a microbial growth inhibitor (NaN$_3$, 2 wt. %). The medium (10 mL) was taken in regular intervals and the supernatant liquids were analysed for dissolved organic carbon (TOC-L analyser, Shimadzu). The samples were also analysed at appropriate intervals by GPC.

Results

Initial properties, composition and processing history are essential parameters for further investigations of the prepared composites. Therefore, the molecular weight and other characteristics of the neat PLA and PLA with ZnSt-Ag composites were investigated (Table 14) as well as the morphology of the prepared ZnSt-Ag system and composites.

SEM micrographs of the ZnSt-Ag additive and PLA 10 % ZnSt-Ag composite are shown in Figure 30. Immobilized Ag particles with size below 100 nm are visible in case of pure additive (Figure 30a) as well as in composite (Figure 30b). Size and shape of MW prepared Ag-NPs correspond to results published by Bazant et al., where Ag-NPs were immobilized on a wood flour [129]. Furthermore, SEM analysis revealed that immobilized Ag-NPs had good cohesion to ZnSt substrate even after thermoplastic processing.
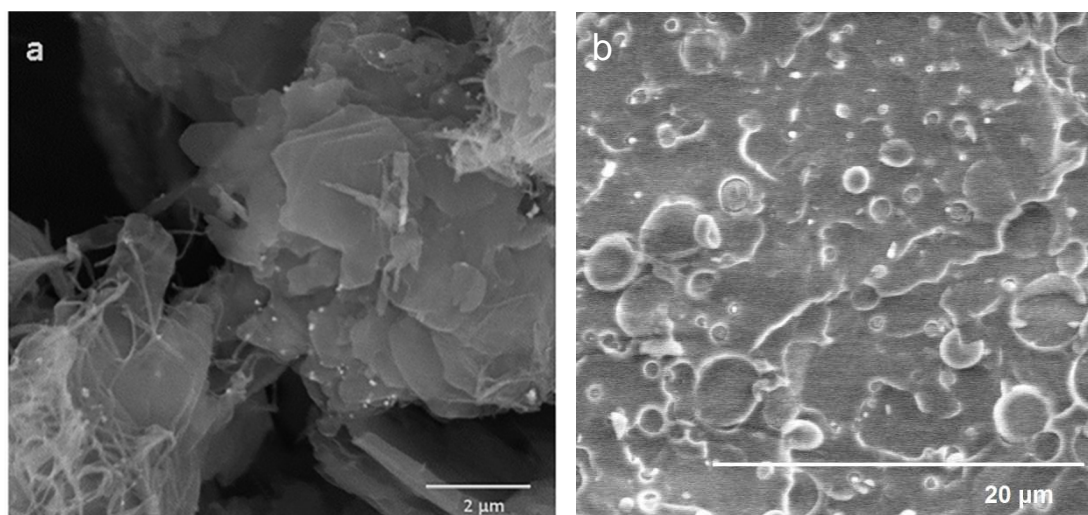
Figure 30 - Scanning electron micrographs of prepared ZnSt-Ag system (a) and PLA 10 wt. % ZnSt-Ag (b).

The silver concentration estimated by AAS is listed in Table 14. As expected, the highest concentration, 0.22 wt. %, of silver NPs was determined in the sample with the highest filler loading (10 wt. % of ZnSt-Ag). The composites with 1, 3 and 5 wt. % of the ZnSt-Ag contained 0.02, 0.07 and 0.13 wt % of Ag NPs, respectively.

As mentioned in previous chapters, PLA is sensitive to increased temperatures and during the processing subjects to thermal degradation. The GPC results confirm this phenomenon. The stearates based additives are known for their thermal stabilization effects in PVC. Wang et al. proposed the stabilization effect of $CaSt_2$, $ZnSt_2$ and their mixture $CaSt_2/ZnSt_2$ on PVC, which was, moreover, improved with synergistic effect between $CaSt_2/ZnSt_2$ and pentaerythritol and organic tin [132]. However, no stabilization effect of the prepared ZnSt-Ag system was observed during the thermal degradation and the M_w decreased from 158 000 to 1000 000 after processing with 1 wt. % of ZnSt-Ag. This behaviour was also described by Rosa et al., where the cobalt stearate and magnesium stearate made the blends with polypropylene more susceptible to thermal degradation [133]. Nevertheless, with the increasing ZnSt-Ag concentration, the molecular weight started to increase slightly as well (Table 14). The PLA during the thermal degradation is subjected to random chain scission generating oligomers [134]. Thus, the resulting M_w increase occurred probably due to subsequent recombination of the generated oligomers [135].

Table 14 - Material properties of PLA/ZnSt-Ag composites.

Sample	Content of Ag (wt.%)*	M_w^a [g.mol^{-1}]	MWD^b	T_g^c [°C]	T_m^d [°C]	ΔHm^e [J.g^{-1}]
PLA	-	158000	3.5	55.81	-	-
PLA + 1 wt.% ZnSt-Ag	0.02	103000	3.1	50.85	-	-
PLA + 3 wt.% ZnSt-Ag	0.07	118000	3.11	51.29	116.40	0.75
PLA + 5 wt.% ZnSt-Ag	0.13	132000	3.02	51.85	116.83	2.1
PLA + 10 wt.% ZnSt-Ag	0.22	157000	3.62	52.6	117.52	5.37

* analysed by AAS, [a] Weight average molecular weight; [b] Molecular-weight dispersity; [c] Glass transition temperature; [d] Melting temperature, [e] Enthalpy of melting
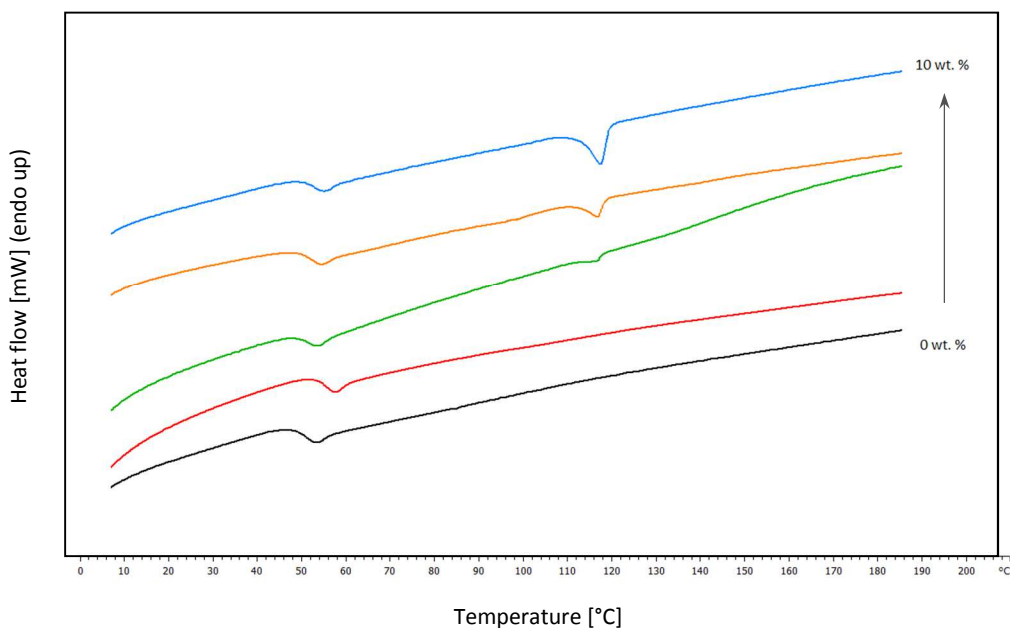
Figure 31 - DSC thermograms of PLA and PLA/ZnSt-Ag composites

Thermal behaviour was analysed by DSC method. It revealed that the thermal properties of neat PLA and composites reflected the values of molecular weight properties. The neat PLA possessed the amorphous character with a glass transition temperature (T_g) of almost 56 °C. The ZnSt-Ag reduced the T_g of the composites to ~50 °C. Nevertheless, the temperature had tendency to grow with the increased ZnSt-Ag concentration, which was in agreement with GC results. Furthermore, it was evident from DSC curves (Figure 31), that from the concentration of 3 wt. %, the material possessed a melt temperature $T_m \approx 117$ °C. The values of T_m and enthalpy were attributed to thermal properties of ZnSt (tabulated value of T_m is 120–130 °C [136]), which were negligible at the lower concentrations.

In order to verify the plasticization effect of ZnSt on PLA matrix, the mechanical properties were tested. As shown in Figure 32a, the addition of ZnSt-Ag into PLA leads to significant decrease (almost 50 %) of the rigidity (Young´s modulus). Opposite effect was described by Rosa et al., where the addition of stearates into PP caused a growing effect of Young´s modulus [133]. Tensile strength values (43–48 MPa) of the prepared composites exhibited only slight decrease in comparison with neat PLA (52 MPa) (Figure 32b). This could be associated to low interphase interaction between PLA and ZnSt-Ag, reduction of molecular weight and to formation of low molecular products [137]. However, interesting values revealed results of elongation at break

(Figure 32c). With loading less than 10 wt. % ZnSt-Ag, the elongation (13 %) was lower even than the elongation of neat PLA (23 %), which suggested the reduction of Mw due to degradation, and also, there was no plasticizer effect, when the concentration of ZnSt-Ag was 1, 3 or 5 %. The determined elongation of neat PLA was generally higher than the values presented by e.g. Yu et al. [138] and Pantani et al. [62]. It could be due to amorphous structure of neat PLA. However, significant improvement of elongation was noted when the loading of ZnSt-Ag was 10 wt. %. Compared to several publications [62] and [138], where the values do not exceed 10 %, in this case, the elongation reached almost 40 %, which could be ascribed to the plasticizer effect of ZnSt-Ag.
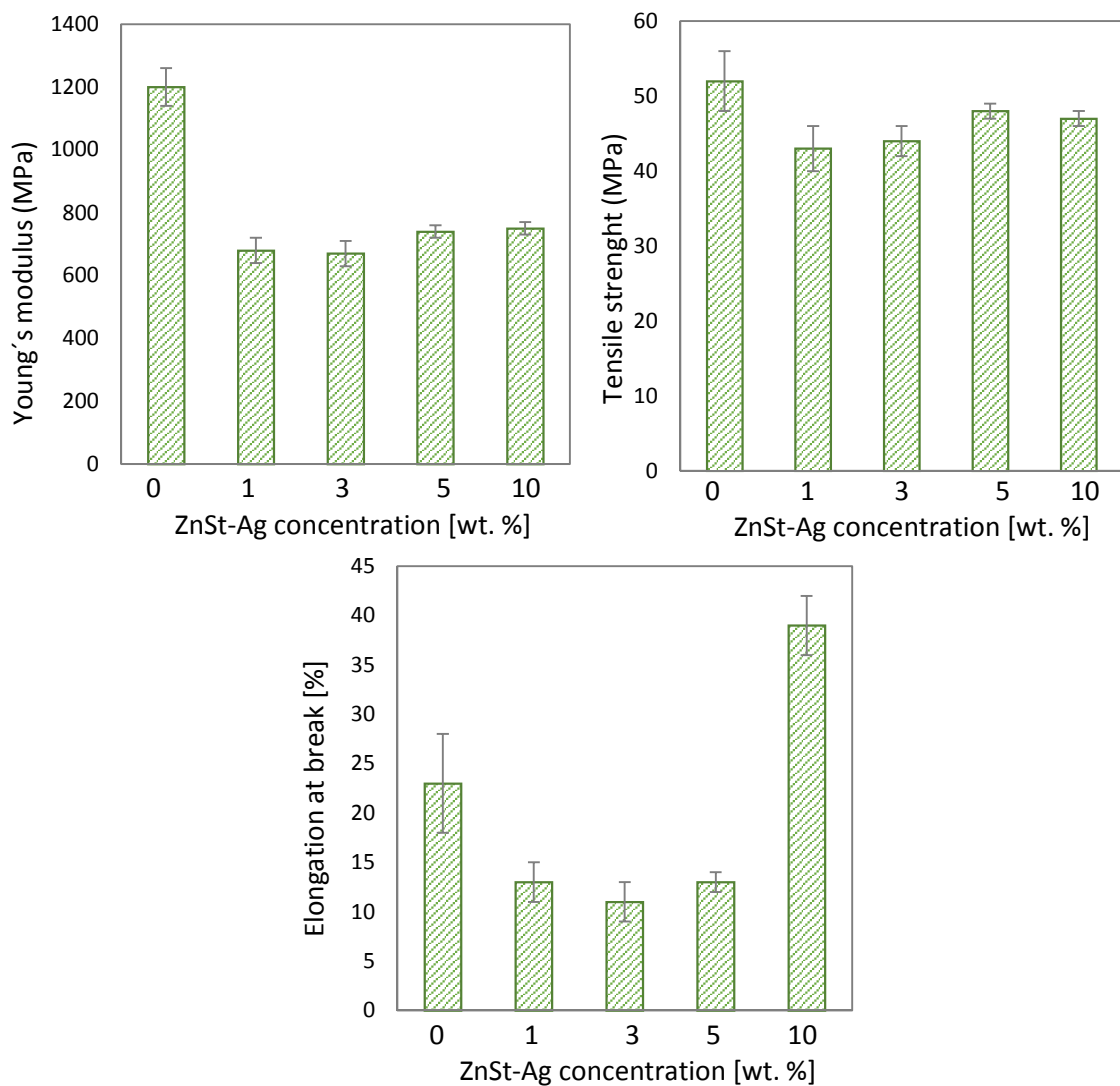
Figure 32 – Mechanical properties of PLA and PLA/ZnSt-Ag composites:a) Young´s modulus [MPa], b) Tensile strength [MPa], c) Elongation at break [%].

Table 15 - Antimicrobial activity of prepared composites determined according to ISO 22196.

Sample	*Staphylococcus aureus* CCM 4516				*Escherichia coli* CCM 4517		
	N (cfu/cm^2)	CR (%)	R = U$_t$ - A$_t$	N (cfu/cm^2)	CR (%)	R = U$_t$ - A$_t$
PLA	$2,4.10^5$		U$_t$ = 5,4	$1,2.10^6$		U$_t$ = 6,1
PLA + 1 wt.% ZnSt-Ag	$1,5.10^5$	38	0,21	$9,2.10^5$	23	0,13
PLA + 3 wt.% ZnSt-Ag	$1,6.10^5$	33	0,17	$3,6.10^5$	70	0,53
PLA + 5 wt.% ZnSt-Ag	$6,5.10^4$	73	0,56	$6,0.10^5$	50	0,32
PLA + 10 wt.% ZnSt-Ag	$1,1.10^1$	100	4,32	< 1	100	> 6,1

The antimicrobial activity of PLA based composite films against *E. coli* (Gram-negative) and *S. aureus* (Gram-positive) bacterial strains are listed in Table 15. Number of colony forming units per cm^2 of sample (N) was determined and the antibacterial activity (R) and the percentage of colony forming units reduction (CR) were estimated. As expected, the distinctive antimicrobial activity exhibited films with the highest Ag loading (0.22 wt. %). The activity was stronger against *E.coli* than *S. aur*eus. It is in agreement with the results published by Shankar et al., who reports the significant antimicrobial activity of PBAT based composites with almost the same concentration (0.25 wt. %) of Ag NPs, where the activity was also higher against Gram-negative bacteria [139]. According to CR results, it is still significant that the reduction of growth of microbial cells was observed in the case of the rest of samples with 1, 3 and 5 wt. % of ZnSt-Ag, where the reduction of colony forming units per cm^2 was from approximately 25 to 70 %.

It is a well-known fact that the Gram-negative bacteria strains are more sensitive to Ag NPs action than the Gram-positive strains. Several mechanisms of Ag NPs have been reported; however, a clear mechanism has not been established yet. As the most widely accepted mechanism was proposed the interaction of the Ag$^+$ with negatively charged phosphorous of sulfur-containing biomacromolecular compounds (proteins and nucleic acids), which cause

structural changes and deformation of metabolic processes leading to cell death [140].

The sensitivity of PLA to abiotic hydrolysis is considered as one of the limiting factors for its long service applications. The effect of the ZnSt-Ag on the rate of hydrolysis was investigated by several techniques including total carbon analysis (TOC) and GPC. The hydrolysis analysis was supported by AAS measurements, where the release of the ZnSt-Ag system into the phosphate buffer was investigated.

The data describing dissolved organic carbon accumulation as a result of the samples hydrolysis are plotted in Figure 33. The results revealed almost negligible effect of the additive on the onset of the degradation, which was for all the samples 14 days. After that period, a sharp increase in the degradation rate of the neat PLA was observed. However, the extent of hydrolysis was supressed with a respect of the concentration of ZnSt-Ag. While the neat PLA was hydrolysed after 21 days in 10 %, the composites hydrolysis reached 4, 2.5, 2.3 and 1.5 % according to the increasing concentration of ZnSt-Ag in PLA. The sudden rise of degradation kinetics could be attributed to the release of low molecular substances, which were formed due to hydrolysis in polymer bulk. It could be possible that the substances gradually cumulated in the polymer bulk and after saturation, they diffused into the surrounding environment. The suppression of PLA hydrolysis by Zn based additives was described by Benali et al. [17]. They noted that the neat PLA exhibited better ability to water uptake than the system with 3 wt. % of surface treated ZnO. Thus, it could be considered, that the reduction of the hydrolysis extent might be caused by barrier effect of ZnSt, which probably decelerated the diffusion of water into the matrix and consequently the diffusion of low molecular substance from the PLA matrix.

As mentioned, the reduction M_w was observed during the processing initiating by thermal degradation. A further decrease of M_w along degradation time was observed during the hydrolysis. The curves (Figure 34) exhibited similar phenomenon as in the case of TOC analysis. The major M_w decrease was observed within 14 and 21 days in the neat PLA.
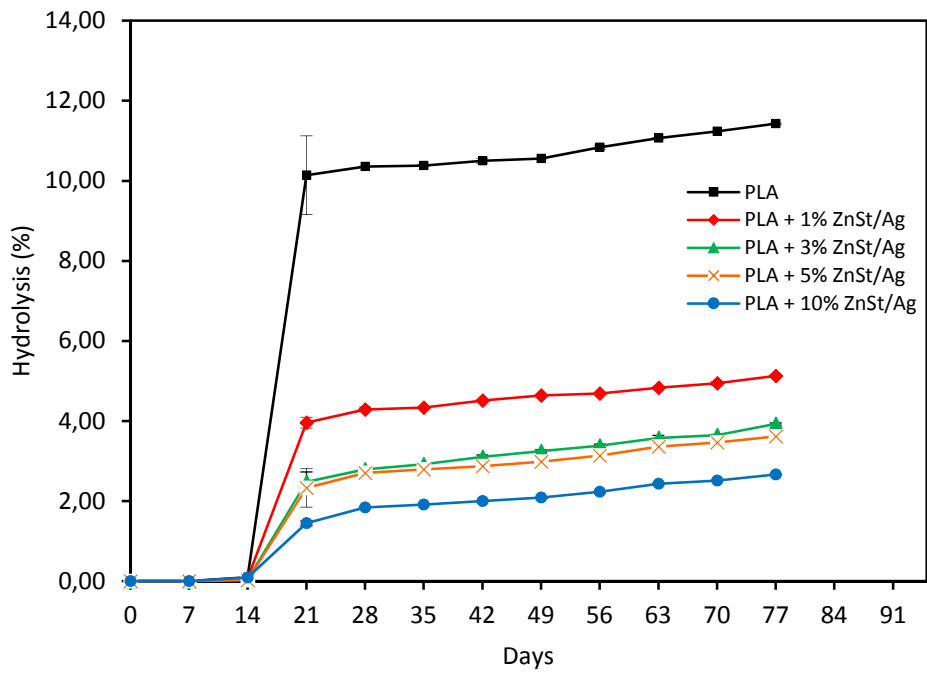
Figure 33 - Abiotic hydrolysis of PLA samples in 0.1M phosphate buffer (pH = 7) at 37 °C. Error bars correspond to twice the standard deviation.
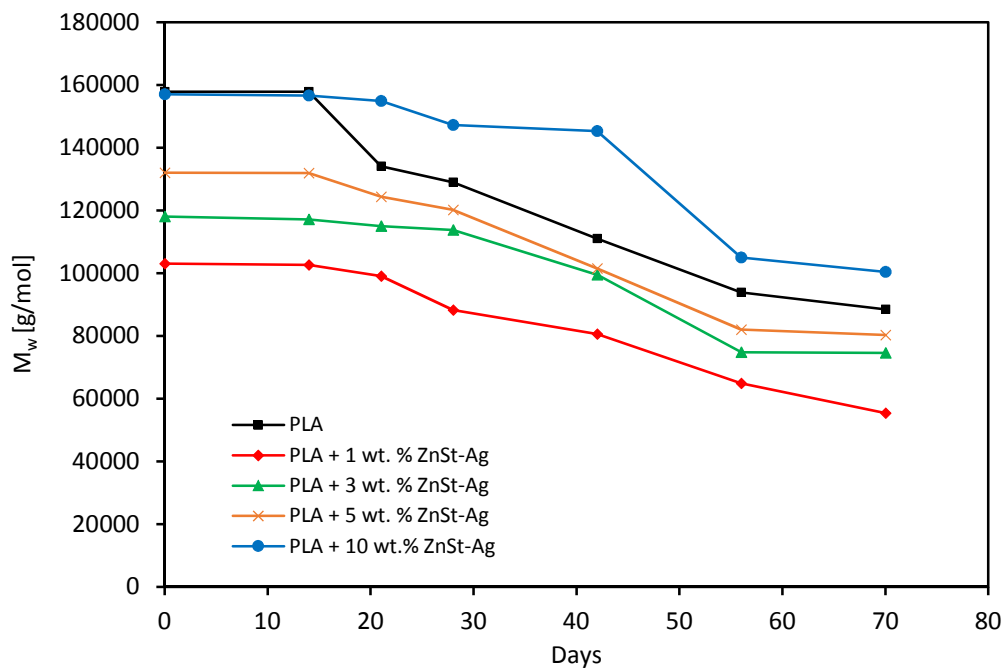
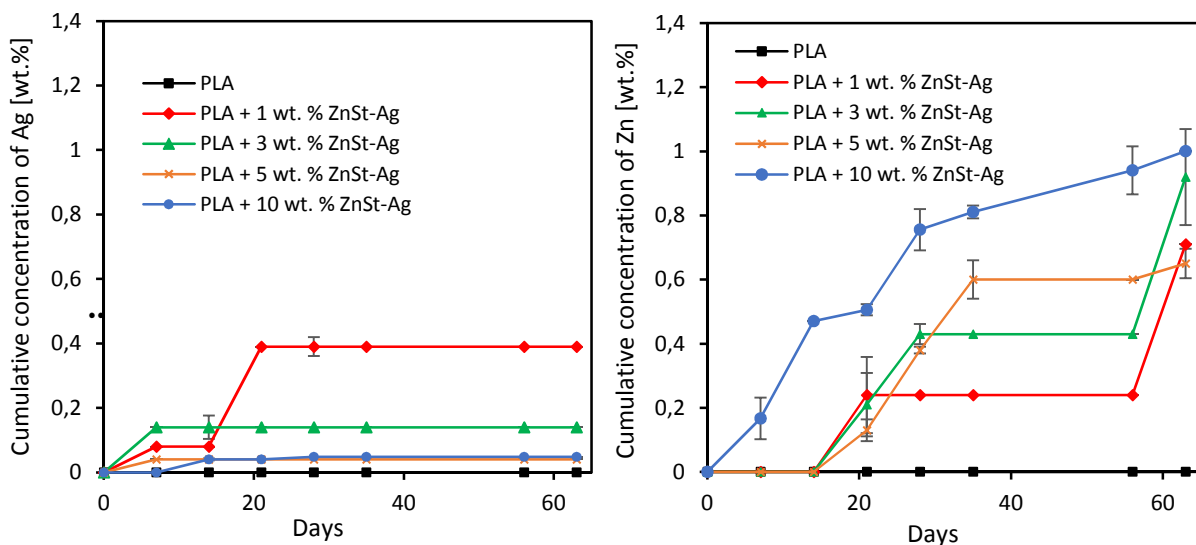*Figure 34 - Molecular weight evolution of neat PLA and PLA-based composites during abiotic hydrolysis.*

Figure 35 – Cumulative concentration of evolved Ag (a) and Zn (b) in phosphate buffer determined during the hydrolysis of PLA/ZnSt-Ag composites.

It could be expected that the additive was released from the PLA matrix into the liquid medium (phosphate buffer) due to hydrolysis induced erosion. To verify this hypothesis, analysis of the phosphate buffer, where the samples hydrolysis took place, was performed by atomic absorption spectroscopy. The concentration evolution curves for both elements are depicted in Figure 35 (a – Ag; b – Zn). The concentration (wt. %) of the elements was recalculated with the respect of initiate weight of the Ag and Zn elements in the samples (did not included the whole weight of the sample). During 63 days of hydrolysis, only slight release of Ag and Zn was observed. A modest rise in concentration of Ag was observed after 14 days, when the hydrolysis onset takes place. It is in agreement with TOC results. This could be ascribed to a small amount of Ag particles, which was "washed out" from the PLA matrix. Subsequently, up to 63rd day, the silver release did not proceed and its ultimate concentration did not exceed 0.2 wt. %. The slight ZnSt (Figure 35b) was observed after 21 days except the sample with the highest loading, when the concentration of Zn was already apparent after 7 days. The concentration was slightly increasing during the whole period of hydrolysis. However, after 63 days, the cumulative concentration of Zn was less than 0.8 wt. %. In both cases, the release of ZnSt-Ag was negligible.

Conclusions

The hybrid system of ZnSt and Ag nanoparticles were prepared by MW synthesis and incorporated by thermoplastic processing into PLA matrix. The influence of the ZnSt-Ag system on PLA properties and degradation mechanism were studied and compared with the initial neat polymer.

The ZnSt-Ag concentration was 1, 3, 5 and 10 wt. %. The exact amount of Ag nanoparticles in composites was determined by atomic absorption spectroscopy where the Ag concentration of highest filling system (10 wt. % ZnSt-Ag) was 0.22 wt. %. As was expected, thermal degradation of PLA occurred during processing with no stabilization effect of ZnSt-Ag. It was characterized by reduction of M_w. However, initiation of recombination process was observed during processing when the filler content was above 3 wt. % and the M_w started to increase. The analysis of thermal properties revealed slight decrease of T_g from 56 °C (neat PLA) to approximately 50 °C and in the case of samples with 3, 5 and 10 wt. % of ZnSt-Ag, the value of melt temperature 117 °C was observed, which was ascribed to filler contribution. Antimicrobial activity was evident, when even the lower concentration of the ZnSt-Ag was added. The bacterial colonies were reduced to approximately 30 %. However, the significant activity exhibited the system with 10 wt. % of the filler. Furthermore, the significant improvement of mechanical properties, especially in elongation at break, was achieved with addition of 10 wt. % of ZnSt-Ag. The initial elongation of neat PLA was approximately 23 %, and after incorporation of the filler, the value increased to almost 40 % of elongation. The ZnSt-Ag played significant role in suppression of abiotic hydrolysis of PLA. The hydrolysis of neat PLA was 10 % after 21 days. After addition of 1, 3, 5 and 10 wt. % of ZnSt-Ag the hydrolysis rate decreased to 4, 2.5, 2.3 and 1.5 %, respectively. The role in the reduction could play the barrier effect of ZnSt-Ag, which limited water diffusion into PLA matrix and the subsequent diffusion of water-soluble oligomers and monomers into the surrounding environment.

It can be concluded that the additive with specific functions, such as antimicrobial activity and plasticizer effect, was prepared. Moreover, after incorporation into PLA matrix, the inhibition effect of abiotic hydrolysis was observed. This kind of modification could be the solution for the request of PLA based materials for prolonged lifetime applications.

8. Dielectric relaxation spectroscopy of hydrolysed PLA

Polymers, which are subjected to chain scission during the degradation, possess changes in properties and structure. According to these changes, the degradation rate can be estimated. Dielectric relaxation spectroscopy (DRS) is well-known for being a very useful tool to study the internal structure changes and thus, it can be used as one of the estimation techniques for degradation determination.

DRS is based on the interaction of an external electric field with the electric dipole moment and charges of the medium. It is a method, which is sensitive to movements of the elements of the polymer chain, which possess dipole moments with certain relaxation mechanisms [141]. Polymers exhibit two main relaxation processes: β relaxation is characterized for local motions of main chains and side chains movements; α processes, which are related with Brown motion (glass transition) [142].

Polylactide possesses the dipole moment parallel to the chain and in amorphous form, it exhibits three relaxation maxima α_n (normal mode relaxation), α_s (segmental motions associated with T_g) and β (local motions) in order of decreasing temperature [141, 143]. The dielectric relaxation measurement is a widespread method to investigate molecular mobility and thus the polymers structure and properties. Ren et al. investigated the changes in thermal and dielectric behaviour of PLA blends composed of semi-crystlline and amorphous structure [143]. Further investigations by DRS were conducted by Pluta et al. In this study, the influence of montmorillonite filler on dielectric properties was observed [141]. The degradation of PLA is closely connected with changes in polymers structure. Thus, the DRS can be considered an effective tool to study the degradation processes. For example, Badia et al. analysed by DRS the thermo-mechanical degradation, where changes in microstructure and segmental dynamics were investigated [54].

In this chapter, the characterisation of changes in dielectric properties of amorphous PLA initiated by abiotic hydrolysis was investigated and correlated with GPC analysis.

Material

Polylactide was obtained from NatureWorks (Ingeo™ 4060D). Its weight average molar mass Mw was 158000 g.mol^{-1} and polydispersity 3.5 as determined by GPC (Agilent HT-GPC 220). Density of PLA was 1.24 kg.m^{-3}.

Methods

Sample preparation

Before compression moulding into plate with 1 mm thickness, the PLA pellets were dried at 45 °C under reduced pressure for at least 24 hours. During the compression moulding, the material was brought to the processing temperature of 160 ℃ during 2 min., then molded for 3 min and immediately cooled down under pressure after transferring the material to a second press kept at 20 °C. Rounded samples with diameter of 9 mm were subsequently cut from the plate.

Abiotic degradation – Hydrolysis

Abiotic hydrolysis was determined at 37 °C. The samples (50 mg) were cut to 0.3 x 0.5 cm specimens and suspended in 10 ml of sodium phosphate buffer (0.1 mol.L^{-1}, pH 7.00) with a microbial growth inhibitor (NaN$_3$, 2 wt. %). The medium (10 mL) was taken in regular intervals and the supernatant liquids were analysed for dissolved organic carbon (TOC-L analyser, Shimadzu).

Dielectric relaxation spectroscopy

Samples before and after hydrolysis were dried over night at 30 °C under reduced pressure and analysed by dielectric measurements using a Broadband Dielectric Impedance Analyzer Concept 40 (Novocontrol, Germany) in the frequency range from 10^{-1} to 10^7 Hz and at temperatures from 0 to 100 °C. The amplitude of the applied AC voltage was 1 V. To examine the dielectric properties of the material, the complex impedance was determined using a standard sample cell BDS 1200 employing RC model of the sample. Based on these values and the knowledge of the sample dimensions, the complex permittivity was determined.

Several variables were investigated in the study of dielectric properties during the PLA degradation. The complex permeability, ε^*, the real ε' and imaginary ε'' parts of dielectric permittivity were studied, according to the equation:

$$\varepsilon^* = \varepsilon^{'} - i\varepsilon^{''} \tag{8}$$

The thermal activation of the dielectric processes was characterized in Arrhenius plots using the maximum frequency of the relaxations at each temperature.

Results

Figure 36 shows frequency dependencies of the imaginary part $\varepsilon^{''}$ of the dielectric permittivity for samples of amorphous PLA and PLA after 7 days hydrolysis (PLAH). Concerning the evolution of curves of the PLA, the maximum was clearly observed above 50 °C, actually above T_g (~55 °C), which moved to higher frequencies with the increasing temperature. It was ascribed to the αs relaxation [54, 141]. Below 50 °C no relaxation peaks occured. Pluta et al. described the decrease in α_s maximum above 80 °C due to crystallization of PLA [141]. The results described here did not exhibit this type of behaviour. Subsequently, at low frequencies, direct conductivity effects appear (směrnice - 1), which led to increase in $\varepsilon^{''}$. Regarding to the evolution of PLAH curves, the maximum of the relaxation motions moved to higher frequency.

For better illustration of the changes during hydrolysis, the $\varepsilon^{''}$ spectra of all samples at 80 °C were compared (Figure 37). It was evident that, with the increasing PLA degradation time, the relaxation took place at the higher frequencies. Even after 2 days of hydrolysis, when the PLA degradation was 0.25 %, the slight shift was observed. The changes could be ascribe to the increasing mobility of polymer segments due to better availability of shorter chains, which were created due to chain scission. This dependence was also observed by Badia et al. during the thermal-mechanical degradation of PLA [54].
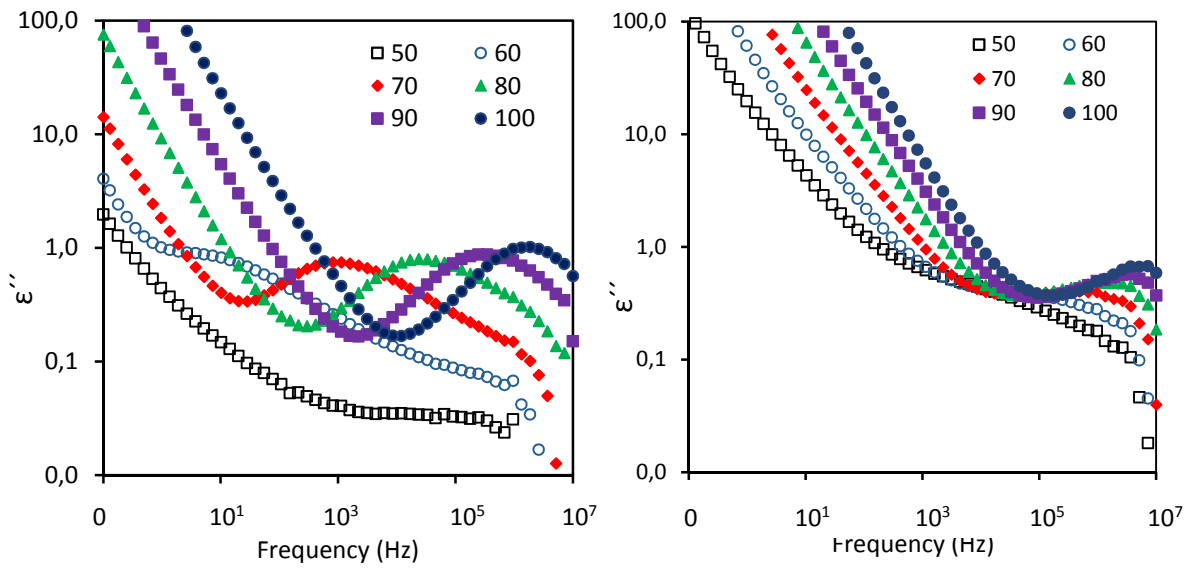
Figure 36 – Dielectric spectra of PLA (left) and PLA after 7 days of hydrolysis (right) at temperatures above the T_g.
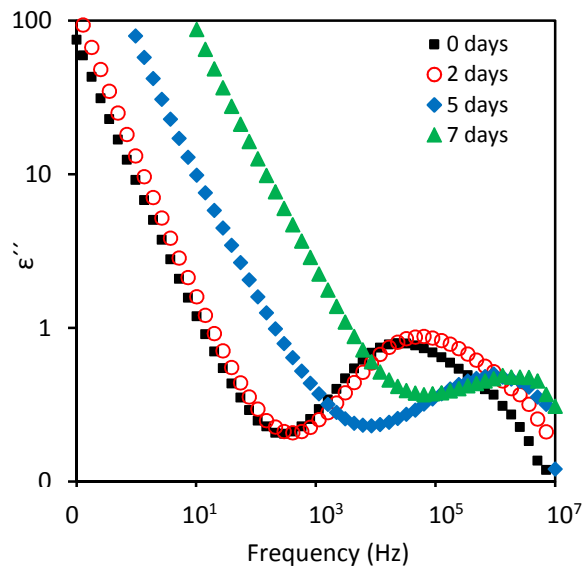
Figure 37 – Comparison of ε´´ spectra vs. frequency at 80 °C of PLAand hydrolysed PLA for 2, 5 and 7 days.

Figure 38 shows the Arrhenius plots (temperature dependence of the relaxation time) for the α_s relaxation. Generally, the linear Arrhenius behaviour exhibits β relaxations [Santangelo] and it can be fit by Arrhenius model [144]:

$$\tau = \tau_0 exp\left(\frac{E_a}{T}\right) \tag{9}$$

where τ is the relaxation time (s), that is $(2\pi f)^{-1}$, τ_0 is a time reference scale and E_a is the apparent activation energy.

However, the thermal activation of segmental relaxation times did not exhibit Arrhenius behaviour (Equation 9). The plots were fitted to the Vogel-Fulcher-Tammann (VFT) equation as observed commonly for α_s relaxations [141]:

$$\tau = \tau_0 exp\left(\frac{B}{T-T_0}\right) \tag{10}$$

where B and T_0 are parameters. T_0 generally appears 40–60 K below the T_g.

Based on Arrhenius plots, the "fragility" of polymers can be classified. It means, if the curves deviate strongly from Arrhenius behaviour and can be fit by VFT, the material is fragile. On the other hand, if the curves have almost linear character, they can be classified as "strong" material. [144] Therefore, it could be claimed that the results in Figure 38 revealed the increasing fragility of PLA during the hydrolysis, which is connected with the decrease of MW due to PLA abiotic degradation after 2, 5 and 7 days, which was 0.25, 0.27 and 8 %, respectively.
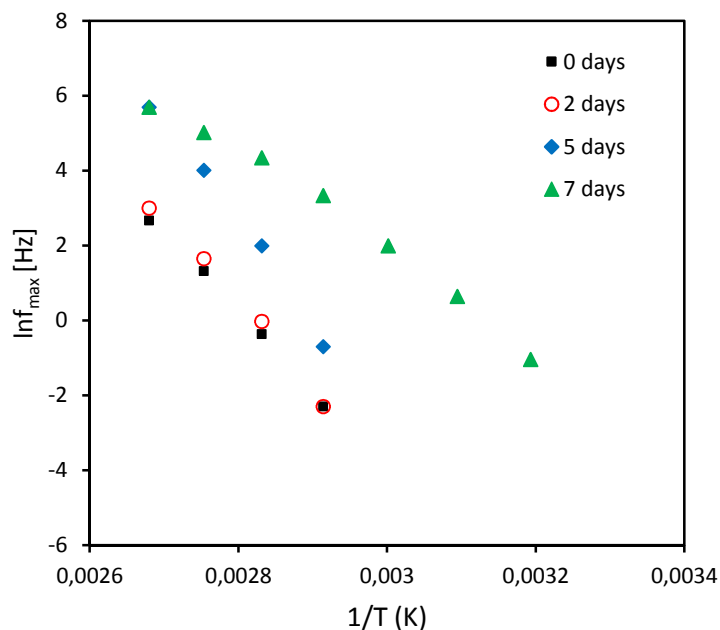
Figure 38 – Arrhenius plots of α_s relaxationsof PLA and hydrolysed PLA for 2, 5 and 7 days.

Conclusions

The dielectric relaxation spectroscopy was used to investigate the PLA abiotic hydrolysis. The hydrolysis of samples was measured after 2, 5 and 7 days and took place in 0.25, 0.27 and 8 %, respectively.

The dielectric measurements in a wide frequency and temperature range revealed one relaxation time α_s, which is connected with segmental movements above the T_g. It was observed that due to degradation, the relaxation peaks were shifted to higher frequencies. It could be ascribed to the increasing mobility of polymer segments due to better availability of shorter chains, which were created due to chain scission. For better observation of the changes caused by degradation, the Arrhenius plots were investigated. It was evident that with the increasing degradation the PLA fragility increased.

SUMMARY OF WORK

This thesis presents in the theoretical part an overview of the current state of art on biodegradable polymers, degradability testing and modification of biopolymers properties. Besides the general classification of biodegradable polymers, various degradation mechanisms and methodology of biotic and abiotic rate evaluation were described. Further, the possibilities in modifications of the polymer degradability via specific additives and fillers were stated.

It has been shown that the pure biodegradable polymers often possess insufficient material properties needed for their applications. Thus, tailoring of the degradation mechanisms through modifications with specific compounds or the addition of the specific fillers were suggested as the methods to improving the properties. On the basis of this, the experimental part of work was divided into the four topics.

The first part was devoted to investigation of the stabilization effects of various concentrations of the anti-hydrolysis agent (BDICDI) in PLA films during an abiotic hydrolysis experiment and aerobic composting. The strong stabilization effect shown at relatively low BDICDI concentrations, and the subsequent rapid onset of hydrolysis after BDICDI depletion, strongly support the hypothesis for autocatalytic mechanisms relating to hydrolytic degradation. By applying the appropriate amount of BDICDI, the approximate duration of stabilization could be set to suit the desired requirements of the final product. The results of this study have been published in a scientific journal.

Secondly, the optimal compatibilization method for a thermoplastically prepared biocomposite system, based on natural flax fibres and a novel polyester-urethane copolymer matrix was investigated. Two types of experimentally prepared additives, a commercial additive and oleic acid and di-tert-butyl peroxide were used as compatibilizing agents. In addition, the effect of alkali or acid treatment on the fibres was investigated. An experimental additive based on maleic anhydride and a commercial additive - 3-(aminopropyl) trimethoxy silane, was found to be the most effective methodology to a natural filler compatibilization process. Furthermore, almost all of the fibre treatment methods researched significantly improved the properties of biocomposites, in comparison with the system utilizing untreated flax fibres. The results of this study have been published in a scientific journal.

The third part was focused on the investigation of the influence of the ZnSt-Ag hybrid filler on PLA properties and degradation mechanism. The addition of

ZnSt-Ag exhibited the antimicrobial activity and plasticizer effect in PLA matrix. Moreover, the inhibition effect of abiotic hydrolysis was observed. The results of this study will be used for manuscript preparation.

In the last part, the dielectric relaxation spectroscopy was used to investigate the PLA abiotic hydrolysis. The relaxation peaks, which were ascribed to α_s, were shifted to higher frequencies due to hydrolysis. According to Arrhenius plots, the increasing fragility with the increasing range of the degradation was observed. The results of this study will be used for manuscript preparation.

The outputs of this work could represent a promising knowledge for further research in the field of biodegradable polyesters lifetime tailoring and studies of structural changes during the degradation processes.

CONTRIBUTIONS TO SCIENCE AND PRACTICE

This doctoral thesis bring novel approaches to modification of the environmentally degradadable polymers lifetime. It is current topic due to intensive both research, practical and commertial interest.

The main contribution to science can be found in testing and description of newly designed systems consisting of polylactide based matrix and

- specific anti-hydrolysis additive Bis(2,6-diisopropylphenyl)carbodiimid

- chemically modified flax fibres with modified interfacial compatibility between the fibres and polymers

- hybrid filler based on zinc stearate and silver nanoparticles prepared by microwave synthesis.

Futhermore, novel technique for polylactide degradation procedure using, the dielectric relaxation spectroscopy was tested. The outputs of this work have been presented in the international scientific journals and conferences.

LIST OF FIGURES

LIST OF TABLES

LIST OF ABBRAVIATIONS AND SYMBOLS

ADP	Adenosine diphosphate
AFM	Atomic force microscopy
Ag	Silver
$AgNO_3$	Silver nitrate
A_t	Average of common logarithm of number of viable bacteria recovered after 24 hours
ATMS	3-(aminopropyl) trimethoxy silane
ATP	Adenosine triphosphate
BDICDI	bis(2,6-diisopropylphenyl)carbodiimide
BOD	Biochemical oxygen demand
c	Duration of the lag phase (days)
$C_{aq,0}$	Initial percentage of water-soluble carbon (%)
CaSt	Calcium stearate
CDI	Carbodiimides
CFU	Colony forming units
$C_{h,0}$	Initial content of hydrolysable solid carbon (%)
CR	Colony forming units reduction
$C_{T,t}$	Percentage of total cumulative CO_2 production at time t (%)
DO	Dissolved oxygen
DSC	Differential scanning calorimetry
DRS	Dielectric relaxation spectroscopy
DTBP	Di-tert-butyl peroxide
E_a	Apparent activation energy
FTIR	Fourier transform infrared spectroscopy
GC	Gas chromatography
GPC	Gel permeation chromatography
HMDI	Hexamethylene diisocyanate
HPLC	High performance liquid chromatography
ΔH_c	Cold crystallization enthalpy (J.g^{-1})
ΔH_m	Enthalpy of melting (J.g^{-1})
ΔH_m^0	Enthalpy of melting (J.g^{-1}) of 100 % crystalline polymer
k_{aq}	Rate constant of mineralization (biodegradation) of water-soluble carbon to carbon dioxide (day^{-1})
k_{hr}	Perspective first-order hydrolysis rate constants for the hydrolysable solid carbon (day^{-1})
M_n	Number average molecular weight (g.mol^{-1})
MW	Molecular weight
M_w	Weight average molecular weight (g.mol^{-1})
MWD	Molecular-weight dispersity
NaN_3	Sodium nitrate

N_B	Number of viable colonies per cm^2 after 24 h recovered from the material without additive (blank)
NFs	Natural fibres
NMR	Nuclear magnetic resonance
NPs	Nanoparticles
N_S	Number of viable colonies per cm2 after 24 h recovered from samples with antimicrobial agents
OA	Oleic acid
PA4	Palyamide 4
PCL	Poly(ε-caprolactone)
PDLA	Poly(D-lactic acid)
PDLLA	Poly(D,L-lactic acid)
PE	Polyethylene
PEU	Polyester-urethane
PGA	Poly(glycolic acid)
PHAs	Poly(β-hydroxyalkanoate)s
PHB	Poly(β-hydroxybutyrate)
PHV	Poly(-hydroxyvalerate)
PLA	Poly(lactic acid)/polycatide
PLLA	Poly(L-lactic acid)
R	Antimicrobial activity
SEM	Scanning electron microscopy
Sn(Oct)$_2$	Tin(II) 2-ethylhexanoate
T_c	Cold crystallization temperature (°C)
T_g	Glass-transition temperature (°C)
T_m	Melting point temperature (°C)
TGA	Thermogravimetric analysis
THF	Tetrahydrofuran
TOC	Total organic carbon analysis
U_t	Average of common logarithm of number of viable bacteria
VFT	Vogel-Fulcher-Tammann equation
Zn	Zinc
ZnO	Zinc oxide
ZnSt	Zinc stearate
E	Photons energy (eV)
h	Planck constant (J.s)
$\varepsilon*$	Complex permitivity
ε'	Dielectric permitivity - real part
ε''	Dielectric permitivity - imaginary part
λ	Wavelength (nm)
v	Frequency (s^{-1})
χ_c	Degree of crystallinity
τ	Relaxation time

τ_0 Time reference scale

REFERENCES

1. LUCAS, Nathalie et al. Polymer biodegradation: Mechanisms and estimation techniques – A review. *Chemosphere*. 2008, vol. 73, no. 4, s. 429-442. ISSN 0045-6535.

2. ALLEN, N. S. and J. F. McKELLAR. *Photodegradation and stabilization of commercial polyolefins*. The Royal Society of Chemistry. 533 s. ISBN - 0306-0012.

3. OJEDA, Telmo F. M. et al. Abiotic and biotic degradation of oxo-biodegradable polyethylenes. *Polymer Degradation and Stability*. 2009, vol. 94, no. 6, s. 965-970. ISSN 0141-3910.

4. ALBERTSSON, A-Ch and S. J. HUANG. *Degradable Polymers, Recycling, and Plastics Waste Management*. Taylor & Francis, 1995. 336 s. ISBN - 9780824796686.

5. AMMALA, Anne et al. An overview of degradable and biodegradable polyolefins. *Progress in Polymer Science*. 2011, vol. 36, no. 8, s. 1015-1049. ISSN 0079-6700.

6. CHANDRA, R. and Renu RUSTGI. Biodegradable polymers. *Progress in Polymer Science*. 1998, vol. 23, no. 7, s. 1273-1335. ISSN 0079-6700.

7. NAIR, Lakshmi S. and Cato T. LAURENCIN. Biodegradable polymers as biomaterials. *Progress in Polymer Science*. 2007, vol. 32, no. 8–9, s. 762-798. ISSN 0079-6700.

8. ASHTER, Syed A. *Introduction to bioplastics engineering*. Syed Ali ASHTER. Oxford: William Andrew Publishing. 2016. 5 - Types of Biodegradable Polymers. 81-151 s. ISBN 9780323393966.

9. SUKAN, Artun, Ipsita ROY and Tajalli KESHAVARZ. Dual production of biopolymers from bacteria. *Carbohydrate Polymers*. 2015, vol. 126, s. 47-51. ISSN 0144-8617.

10. ARNOSTI, C. Fluorescent derivatization of polysaccharides and carbohydrate-containing biopolymers for measurement of enzyme activities in complex media. *Journal of Chromatography B*. 2003, vol. 793, no. 1, s. 181-191. ISSN 1570-0232.

11. MOHANTY, A. K., M. MISRA and G. HINRICHSEN. Biofibres, biodegradable polymers and biocomposites: An overview. *Macromolecular*

Materials and Engineering. 2000, vol. 276-277, no. 1, s. 1-24. ISSN 1439-2054. Dostupné

12. HEMJINDA, Sarunya., et al. United nations industrial development organization.,International centre for science and technology. *Environmentally degradable polymeric materials and plastics [also] EDP : guidelines to standards and testing practices*.Trieste: International Centre for Science and High Technology, United Nations Industrial Development Organization, 2007ID: 438831843.

13. SHIMAO, Masayuki. Biodegradation of plastics. *Current Opinion in Biotechnology*. 2001, vol. 12, no. 3, s. 242-247. ISSN 0958-1669.

14. MIDDLETON, John C. and Arthur J. TIPTON. Synthetic biodegradable polymers as orthopedic devices. *Biomaterials*. 2000, vol. 21, no. 23, s. 2335-2346. ISSN 0142-9612.

15. TIAN, Huayu et al. Biodegradable synthetic polymers: Preparation, functionalization and biomedical application. *Progress in Polymer Science*. 2012, vol. 37, no. 2, s. 237-280. ISSN 0079-6700.

16. MURTHY, N., S. WILSON and J. C. SY. *Polymer science: A comprehensive reference*. Krzysztof MATYJASZEWSKI a Martin MÖLLER. Amsterdam: Elsevier. 20129. 28 - Biodegradation of Polymers. 547-560 s. ISBN 9780080878621.

17. BENALI, Samira et al. Key factors for tuning hydrolytic degradation of polylactide/zinc oxide nanocomposites. *Nanocomposites*. 2015, vol. 1, no. 1, s. 51-61.

18. SAWPAN, M. A., K. L. PICKERING and A. FERNYHOUGH. *Hemp fibre reinforced poly(lactic acid) composites*. 2007. 337-340 s.

19. PRAPRUDDIVONGS, Chana and Narongrit SOMBATSOMPOP. Biodegradation and Anti-bacterial Properties of PLA and Wood/PLA Composites Incorporated with Zeomic Anti-bacterial Agent. *Multi-Functional Materials and Structures Iv*. 2013, vol. 747, s. 111-114. ISSN 1022-6680; 978-3-03785-771-7.

20. ALBERTSSON, Ann-Christine and Indra K. VARMA. *Degradable aliphatic polyesters*[online].Berlin, Heidelberg: Springer Berlin Heidelberg. 2002Aliphatic Polyesters: Synthesis, Properties and Applications. 1-40 s. ISBN 978-3-540-45734-3. F: Albertsson2002.

21. KUCHARCZYK, Pavel et al. Novel aspects of the degradation process of PLA based bulky samples under conditions of high partial pressure of water vapour. *Polymer Degradation and Stability*. 2013, vol. 98, no. 1, s. 150-157. ISSN 0141-3910.

22. JEON, Hyun Jeong and Mal Nam KIM. Biodegradation of poly(l-lactide) (PLA) exposed to UV irradiation by a mesophilic bacterium. *International Biodeterioration & Biodegradation*. 2013, vol. 85, no. 0, s. 289-293. ISSN 0964-8305.

23. TSOU, Chi-Hui et al. Synthesis and properties of biodegradable polycaprolactone/polyurethanes by using 2,6-pyridinedimethanol as a chain extender. *Polymer Degradation and Stability*. 2013, vol. 98, no. 2, s. 643-650. ISSN 0141-3910.

24. QU, Wen-Qiang et al. Synthesis and characterization of a new biodegradable polyurethanes with good mechanical properties. *Chinese Chemical Letters*. 2016, vol. 27, no. 1, s. 135-138. ISSN 1001-8417.

25. DOMANSKA, Agata and Anna BOCZKOWSKA. Biodegradable polyurethanes from crystalline prepolymers. *Polymer Degradation and Stability*. 2014, vol. 108, s. 175-181. ISSN 0141-3910.

26. TATAI, Lisa et al. Thermoplastic biodegradable polyurethanes: The effect of chain extender structure on properties and in-vitro degradation. *Biomaterials*. 2007, vol. 28, no. 36, s. 5407-5417. ISSN 0142-9612.

27. CELIKBAG, Yusuf et al. The effect of ethanol on hydroxyl and carbonyl groups in biopolyol produced by hydrothermal liquefaction of loblolly pine: 31P-NMR and 19F-NMR analysis. *Bioresource Technology*. 2016, vol. 214, s. 37-44. ISSN 0960-8524.

28. SOLANKI, Archana, Jayen MEHTA and Sonal THAKORE. Structure–property relationships and biocompatibility of carbohydrate crosslinked polyurethanes. *Carbohydrate Polymers*. 2014, vol. 110, s. 338-344. ISSN 0144-8617.

29. MAJÓ, M. Antonia et al. Synthesis and characterization of polyamides obtained from tartaric acid and l-lysine. *European Polymer Journal*. 2004, vol. 40, no. 12, s. 2699-2708. ISSN 0014-3057.

30. CAOUTHAR, A. et al. Synthesis and characterization of new polyamides derived from di(4-cyanophenyl)isosorbide. *European Polymer Journal*. 2007, vol. 43, no. 1, s. 220-230. ISSN 0014-3057.

31. KAWASAKI, Norioki et al. Synthesis, thermal and mechanical properties and biodegradation of branched polyamide 4. *Polymer*. 2005, vol. 46, no. 23, s. 9987-9993. ISSN 0032-3861.

32. YAMANO, Naoko et al. Polyamide 4 with long-chain fatty acid groups – Suppressing the biodegradability of biodegradable polymers. *Polymer Degradation and Stability*. 2014, vol. 108, s. 116-122. ISSN 0141-3910.

33. HASHIMOTO, Kazuhiko, Tsuyoshi HAMANO and Masahiko OKADA. Degradation of several polyamides in soils. *Journal of Applied Polymer Science*. 1994, vol. 54, no. 10, s. 1579-1583. ISSN 1097-4628.

34. JAIN, Jay Prakash et al. Role of polyanhydrides as localized drug carriers. *Journal of Controlled Release*. 2005, vol. 103, no. 3, s. 541-563. ISSN 0168-3659.

35. SIVAN, Alex. New perspectives in plastic biodegradation. *Current Opinion in Biotechnology*. 2011, vol. 22, no. 3, s. 422-426. ISSN 0958-1669.

36. ABRUSCI, C. et al. Biodegradation of photo-degraded mulching films based on polyethylenes and stearates of calcium and iron as pro-oxidant additives. *International Biodeterioration & Biodegradation*. 2011, vol. 65, no. 3, s. 451-459. ISSN 0964-8305.

37. BRIASSOULIS, Demetres et al. Degradation in soil behavior of artificially aged polyethylene films with pro-oxidants. *Journal of Applied Polymer Science*. 2015, vol. 132, no. 30.ISSN 1097-4628.

38. YASHCHUK, O., F. S. PORTILLO and E. B. HERMIDA. Degradation of Polyethylene Film Samples Containing Oxo-Degradable Additives. *Procedia Materials Science*. 2012, vol. 1, s. 439-445. ISSN 2211-8128.

39. MEHMOOD, Ch Tahir et al. Biodegradation of low density polyethylene (LDPE) modified with dye sensitized titania and starch blend using Stenotrophomonas pavanii. *International Biodeterioration & Biodegradation*. ISSN 0964-8305.

40. SHAH, Aamer Ali et al. Biological degradation of plastics: A comprehensive review. *Biotechnology Advances*. 2008, vol. 26, no. 3, s. 246-265. ISSN 0734-9750.

41. SHANSHOOL, Jabir, M. F. Abdul JABBAR and Izzat N. SLAIMAN. The influence of mechanical effects on degradation of polyisobutylenes as drag

reducing agents. *Petroleum & Coal*. 2011, vol. 53, no. 3, s. 218-222. ISSN 1337-7027.

42. KIM, C. A. et al. Mechanical degradation of dilute polymer solutions under turbulent flow. *Polymer*. 2000, vol. 41, no. 21, s. 7611-7615. ISSN 0032-3861.

43. YOUSIF, Emad and Raghad HADDAD. Photodegradation and photostabilization of polymers, especially polystyrene: review. *SpringerPlus* [online]. 2013, vol. 2, s. 398. ISSN 2193-1801.

44. NECKE, D. C. et al. *Developmental photochemistry. norrish type II reaction*. American Chemical Society, 1971. 1838 s. ISBN - 0022-3263.

45. KARPUKHIN, O. N. and E. M., SLOBODETSKAYA. *Kinetics of the photochemical oxidation of polyolefins*. 173 s. ISBN - 0036-021X.

46. MIYAZAKI, Kensuke et al. Study on biodegradation mechanism of novel oxo-biodegradable polypropylenes in an aqueous medium. *Polymer Degradation and Stability*. 2012, vol. 97, no. 11, s. 2177-2184. ISSN 0141-3910.

47. SANTONJA-BLASCO, L., A. RIBES-GREUS aND R. G. ALAMO. Comparative thermal, biological and photodegradation kinetics of polylactide and effect on crystallization rates. *Polymer Degradation and Stability*. 2013, vol. 98, no. 3, s. 771-784. ISSN 0141-3910.

48. COMPTON, R. G., C. H. BAMFORD aND C. F. H. TIPPERT . *Degradation of Polymers*. Elsevier Science, 1975. ISBN 9780080868080.

49. KOUTNY, Marek, Jacques LEMAIRE and Anne-Marie DELORT. Biodegradation of polyethylene films with prooxidant additives. *Chemosphere*. 2006, vol. 64, no. 8, s. 1243-1252. ISSN 0045-6535.

50. GÖPFERICH, Achim. Polymer Scaffolding and Hard Tissue Engineering Mechanisms of polymer degradation and erosion. *Biomaterials*. 1996, vol. 17, no. 2, s. 103-114. ISSN 0142-9612.

51. FAN, Lusheng et al. Endocytosis and its regulation in plants. *Trends in Plant Science*. 2015, vol. 20, no. 6, s. 388-397. ISSN 1360-1385.

52. BASTIOLI, C. and Technology L. RAPRA. *Handbook of Biodegradable Polymers*. Rapra Technology, 2005. ISBN 9781859573891.

53. MÜLLER, Rolf-Joachim. *Biopolymers online*.Wiley-VCH Verlag GmbH & Co. KGaA. , 2005Biodegradability of Polymers: Regulations and Methods for Testing. ISBN 9783527600038.

54. BADIA, J. D. et al. Dielectric spectroscopy of recycled polylactide. *Polymer Degradation and Stability*. 2014, vol. 107, s. 21-27. ISSN 0141-3910.

55. TCHMUTIN, Igor et al. Study on biodegradability of protein filled polymer composites using dielectric measurements. *Polymer Degradation and Stability*. 2004, vol. 86, no. 3, s. 411-417. ISSN 0141-3910.

56. FUNABASHI, Masahiro, Fumi NINOMIYA and Masao KUNIOKA. Biodegradability Evaluation of Polymers by ISO 14855-2. *International Journal of Molecular Sciences*. 2009, vol. 10, no. 8, s. 3635-3654. ISSN 1422-0067.

57. MURARIU, Marius and Philippe DUBOIS. PLA composites: From production to properties. *Advanced Drug Delivery Reviews*. ISSN 0169-409X.

58. PICKERING, K. L. and M. G. ARUAN EFENDY. Preparation and mechanical properties of novel bio-composite made of dynamically sheet formed discontinuous harakeke and hemp fibre mat reinforced PLA composites for structural applications. *Industrial Crops and Products*. 2016, vol. 84, s. 139-150. ISSN 0926-6690.

59. AZWA, Z. N. et al. A review on the degradability of polymeric composites based on natural fibres. *Materials & Design*. 2013, vol. 47, s. 424-442. ISSN 0261-3069.

60. ALIMUZZAMAN, Shah, R. H. GONG and Mahmudul AKONDA. Biodegradability of nonwoven flax fiber reinforced polylactic acid biocomposites. *Polymer Composites*. 2014, vol. 35, no. 11, s. 2094-2102. ISSN 1548-0569.

61. Rui Wang, Chun-Hong Wang and Zhao-Hui Jiang. Biodegradability of Flax Noil Fibers Reinforced with Poly(Lactic Acid) Composites. *Journal of Fiber Bioengineering and Informatics*. 2010, vol. 3, no. 2, s. 75.

62. PANTANI, Roberto et al. PLA-ZnO nanocomposite films: Water vapor barrier properties and specific end-use characteristics. *European Polymer Journal*. 2013, vol. 49, no. 11, s. 3471-3482. ISSN 0014-3057.

63. CHENNAKESAVULU, K. et al. Synthesis, characterization and photo catalytic studies of the composites by tantalum oxide and zinc oxide nanorods.

Journal of Molecular Structure. 2015, vol. 1091, no. 0, s. 49-56. ISSN 0022-2860.

64. GONZÁLEZ, Alfonso et al. Fire retardancy behavior of PLA based nanocomposites. *Polymer Degradation and Stability*. 2012, vol. 97, no. 3, s. 248-256. ISSN 0141-3910.

65. Sandrine Therias, Jean-Francois Larché, Pierre-Olivier Bussiére, Jean-Luc Gardette, Marius Murariu, Philippe Dubois. *Photochemical behavior of polylactide/ZnO nanocomposite films*. American Chemical Society, 2012. 3283 s. ISBN - 1525-7797.

66. QU, Meng et al. Zinc oxide nanoparticles catalyze rapid hydrolysis of poly(lactic acid) at low temperatures. *Journal of Applied Polymer Science*. 2014, vol. 131, no. 11. ISSN 1097-4628.

67. NOTTA-CUVIER, Delphine et al. Tailoring Polylactide Properties for Automotive Applications: Effects of Co-Addition of Halloysite Nanotubes and Selected Plasticizer. *Macromolecular Materials and Engineering*. 2015, vol. 300, no. 7, s. 684-698. ISSN 1439-2054.

68. LUIZ DE PAULA, Everton, Valdir MANO and Fabiano Vargas PEREIRA. Influence of cellulose nanowhiskers on the hydrolytic degradation behavior of poly(d,l-lactide). *Polymer Degradation and Stability*. 2011, vol. 96, no. 9, s. 1631-1638. ISSN 0141-3910.

69. PRETSCH, Thorsten and Werner W. MÜLLER. Shape memory poly(ester urethane) with improved hydrolytic stability. *Polymer Degradation and Stability*. 2010, vol. 95, no. 5, s. 880-888. ISSN 0141-3910.

70. YANG, Lixin, Xuesi CHEN and Xiabin JING. Stabilization of poly(lactic acid) by polycarbodiimide. *Polymer Degradation and Stability*. 2008, vol. 93, no. 10, s. 1923-1929. ISSN 0141-3910.

71. STLOUKAL, Petr et al. The influence of a hydrolysis-inhibiting additive on the degradation and biodegradation of PLA and its nanocomposites. *Polymer Testing*. 2015, vol. 41, no. 0, s. 124-132. ISSN 0142-9418.

72. MOHANTY, A. K., M. MISRA and L. T. DRZAL. Sustainable Bio-Composites from Renewable Resources: Opportunities and Challenges in the Green Materials World. *Journal of Polymers and the Environment*. 2002, vol. 10, no. 1, s. 19-26. ISSN 1572-8900.

73. FUKUSHIMA, Kazuki and Yoshiharu KIMURA. Stereocomplexed polylactides (Neo-PLA) as high-performance bio-based polymers: their formation, properties, and application. *Polymer International*. 2006, vol. 55, no. 6, s. 626-642. ISSN 1097-0126.

74. POLJANŠEK, I. et al. Biodegradable polymers from renewable resources: Effect of proteinic impurity on polycondensation products of 2-hydroxypropanoic acid. *Materials and Technology*. 2011, vol. 45, no. 3, s. 265-268. ISSN 1580-2949.

75. MAI, Fang et al. Preparation and properties of self-reinforced poly(lactic acid) composites based on oriented tapes. *Composites Part A: Applied Science and Manufacturing*. 2015, vol. 76, s. 145-153. ISSN 1359-835X.

76. KUCHARCZYK, P. et al. Correlation of Morphology and Viscoelastic Properties of Partially Biodegradable Polymer Blends Based on Polyamide 6 and Polylactide Copolyester. *Polymer-Plastics Technology and Engineering*. 2012, vol. 51, no. 14, s. 1432-1442.

77. STLOUKAL, Petr et al. Kinetics and mechanism of the biodegradation of PLA/clay nanocomposites during thermophilic phase of composting process. *Waste Management*. 2015, vol. 42, s. 31-40. ISSN 0956-053X.

78. GIL-CASTELL, O. et al. Hydrothermal ageing of polylactide/sisal biocomposites. Studies of water absorption behaviour and Physico-Chemical performance. *Polymer Degradation and Stability*. 2014, vol. 108, s. 212-222. ISSN 0141-3910.

79. GORRASI, Giuliana and Roberto PANTANI. Effect of PLA grades and morphologies on hydrolytic degradation at composting temperature: Assessment of structural modification and kinetic parameters. *Polymer Degradation and Stability*. 2013, vol. 98, no. 5, s. 1006-1014. ISSN 0141-3910.

80. HUSÁROVÁ, Lucie et al. Identification of important abiotic and biotic factors in the biodegradation of poly(l-lactic acid). *International Journal of Biological Macromolecules*. 2014, vol. 71, s. 155-162. ISSN 0141-8130.

81. VERT, Michel. Aliphatic Polyesters: Great Degradable Polymers That Cannot Do Everything. *Biomacromolecules*. 2005, vol. 6, no. 2, s. 538-546. ISSN 1525-7797.

82. PANTANI, Roberto and Andrea SORRENTINO. Influence of crystallinity on the biodegradation rate of injection-moulded poly(lactic acid) samples in

controlled composting conditions. *Polymer Degradation and Stability*. 2013, vol. 98, no. 5, s. 1089-1096. ISSN 0141-3910.

83. ZHOU, Q. and M. XANTHOS. Nanoclay and crystallinity effects on the hydrolytic degradation of polylactides. *Polymer Degradation and Stability*. 2008, vol. 93, no. 8, s. 1450-1459. ISSN 0141-3910.

84. NAJAFI, N. et al. Control of thermal degradation of polylactide (PLA)-clay nanocomposites using chain extenders. *Polymer Degradation and Stability*. 2012, vol. 97, no. 4, s. 554-565. ISSN 0141-3910.

85. CICERO, John A. et al. Phosphite stabilization effects on two-step melt-spun fibers of polylactide. *Polymer Degradation and Stability*. 2002, vol. 78, no. 1, s. 95-105. ISSN 0141-3910.

86. ULRICH, H. *Chemistry and Technology of Carbodiimides*. Wiley, 2008. ISBN 9780470516676.

87. LIM, L. T, R. AURAS and M. RUBINO. Processing technologies for poly(lactic acid). *Progress in Polymer Science*. 2008, vol. 33, no. 8, s. 820-852. ISSN 0079-6700.

88. TAUBNER, V. and R. SHISHOO. Influence of processing parameters on the degradation of poly(L-lactide) during extrusion. *Journal of Applied Polymer Science*. 2001, vol. 79, no. 12, s. 2128-2135. ISSN 1097-4628.

89. SIGNORI, Francesca, Maria-Beatrice COLTELLI and Simona BRONCO. Thermal degradation of poly(lactic acid) (PLA) and poly(butylene adipate-co-terephthalate) (PBAT) and their blends upon melt processing. *Polymer Degradation and Stability*. 2009, vol. 94, no. 1, s. 74-82. ISSN 0141-3910.

90. LEEJARKPAI, Thanawadee et al. Biodegradable kinetics of plastics under controlled composting conditions. *Waste Management*. 2011, vol. 31, no. 6, s. 1153-1161. ISSN 0956-053X.

91. JO, Mi-Yeong et al. Hydrolysis and thermal degradation of poly(L-lactide) in the presence of talc and modified talc. *Journal of Applied Polymer Science*. 2013, vol. 129, no. 3, s. 1019-1025. ISSN 1097-4628.

92. FARUK, Omar et al. Biocomposites reinforced with natural fibers: 2000–2010. *Progress in Polymer Science*. 2012, vol. 37, no. 11, s. 1552-1596. ISSN 0079-6700.

93. STRONG, A. B. *Fundamentals of Composites Manufacturing - Materials, Methods, and Applications*. 2. Brent Strong. Michigan: Society of Manufacturing Engineers (SME), 2008. ISBN 978-0872638549.

94. SAHEB, D. Nabi and JP JOG. Natural fiber polymer composites: a review. *Advances in Polymer Technology*. 1999, vol. 18, no. 4, s. 351-363.

95. ZINI, Elisa and Mariastella SCANDOLA. Green composites: an overview. *Polymer Composites*. 2011, vol. 32, no. 12, s. 1905-1915.

96. GREGOROVA, Adriana et al. Effect of Compatibilizing Agent on the Properties of Highly Crystalline Composites Based on Poly(lactic acid) and Wood Flour and/or Mica. *Journal of Polymers and the Environment*. 2011, vol. 19, no. 2, s. 372-381. ISSN 1572-8900.

97. YU, Long, Katherine DEAN and Lin LI. Polymer blends and composites from renewable resources. *Progress in Polymer Science*. 2006, vol. 31, no. 6, s. 576-602.

98. DICKER, Michael P. M. et al. Green composites: A review of material attributes and complementary applications. *Composites Part A: Applied Science and Manufacturing*. 2014, vol. 56, s. 280-289. ISSN 1359-835X.

99. MUKHERJEE, Tapasi and Nhol KAO. PLA Based Biopolymer Reinforced with Natural Fibre: A Review. *Journal of Polymers and the Environment*. 2011, vol. 19, no. 3, s. 714-725. ISSN 1572-8900.

100. STLOUKAL, Petr et al. Assessment of the interrelation between photooxidation and biodegradation of selected polyesters after artificial weathering. *Chemosphere*. 2012, vol. 88, no. 10, s. 1214-1219. ISSN 0045-6535.

101. ZHU, Jinchun et al. Recent Development of Flax Fibres and Their Reinforced Composites Based on Different Polymeric Matrices. *Materials*. 2013, vol. 6, no. 11, s. 5171-5198.

102. OKSMAN, K., M. SKRIFVARS and J. F. SELIN. Natural fibres as reinforcement in polylactic acid (PLA) composites. *Composites Science and Technology*. 2003, vol. 63, no. 9, s. 1317-1324. ISSN 0266-3538.

103. AYDIN, Merlin et al. Effects of Alkali Treatment on the Properties of Short Flax Fibers/Poly(Lactic Acid) Eco-Composites. *Journal of Polymers and the Environment*. 2011, vol. 19, no. 1, s. 11-17. ISSN 1572-8900.

104. BLEDZKI, A. K. et al. The effects of acetylation on properties of flax fibre and its polypropylene composites. *Express Polymer Letters*. 2008, vol. 2, no. 6, s. 413-422.

105. BATTEGAZZORE, Daniele, Jenny ALONGI and Alberto FRACHE. Poly(lactic acid)-Based Composites Containing Natural Fillers: Thermal, Mechanical and Barrier Properties. *Journal of Polymers and the Environment*. 2014, vol. 22, no. 1, s. 88-98. ISSN 1572-8900.

106. HORNSBY, P. R., E. HINRICHSEN and K. TARVERDI. Preparation and properties of polypropylene composites reinforced with wheat and flax straw fibres: Part I Fibre characterization. *Journal of Materials Science*. 1997, vol. 32, no. 2, s. 443-449. ISSN 1573-4803.

107. NARAYANAN, N., Roychoudhury P.K. and A. Srivastava. L (+) lactic acid fermentation and its product polymerization. *Journal of Biotechnology*. 2004, vol. 7, no. 2, s. 167-179.

108. PAVELKOVA, Alena et al. Novel poly(lactic acid)–poly(ethylene oxide) chain-linked copolymer and its application in nano-encapsulation. *Polymers for Advanced Technologies*. 2014, vol. 25, no. 6, s. 595-604. ISSN 1099-1581.

109. KYLMÄ, J. et al. Chain extending of lactic acid oligomers. Effect of 2,2′-bis(2-oxazoline) on 1,6-hexamethylene diisocyanate linking reaction. *Polymer*. 2001, vol. 42, no. 8, s. 3333-3343. ISSN 0032-3861.

110. RAJ, Gijo et al. *Role of polysaccharides on mechanical and adhesion properties of flax fibres in flax/PLA biocomposite*. 2011. 11 s.

111. MISKOLCZI, Norbert et al. Plastic waste minimization: Compatibilization of polypropylene/polyamide 6 blends by polyalkenyl-poly-maleic-anhydride-based agents. *Journal of Applied Polymer Science*. 2013, vol. 129, no. 5, s. 3028-3037. ISSN 1097-4628.

112. KUCHARCZYK, P. et al. Properties enhancement of partially biodegradable polyamide/polylactide blends through compatibilization with novel polyalkenyl-poly-maleic-anhydride-amide/imide-based additives. *Journal of Reinforced Plastics and Composites*. 2012, vol. 31, s. 189-202.

113. MISKOLCZI, N. et al. Production of Acrylonitrile Butadiene Styrene/High-Density Polyethylene Composites from Waste Sources by Using Coupling Agents. *Mechanics of Composite Materials*. 2014, vol. 50, no. 3, s. 377-386. ISSN 1573-8922.

114. VARGA, Cs et al. Effects of industrial scale production on the chemical composition of novel coupling agents and its relationship to the mechanical properties of chopped glass fibre mat reinforced thermoset composites. *Materials & Design*. 2011, vol. 32, no. 1, s. 12-20. ISSN 0261-3069.

115. CAIRNCROSS, Richard A. et al. Moisture sorption, transport, and hydrolytic degradation in polylactide. *Applied Biochemistry and Biotechnology*. 2006, vol. 131, no. 1, s. 774-785. ISSN 1559-0291.

116. TITOK, V. et al. Thermogravimetric Analysis of the Flax Bast Fibre Bundle. *Journal of Natural Fibers*. 2006, vol. 3, no. 1, s. 35-41. ISSN 1544-0478.

117. ALIMUZZAMAN, Shah, R. Hugh GONG and Mahmudul AKONDA. Nonwoven polylactic acid and flax biocomposites. *Polymer Composites*. 2013, vol. 34, no. 10, s. 1611-1619. ISSN 1548-0569.

118. AVELLA, Maurizio et al. A new class of biodegradable materials: Poly-3-hydroxy-butyrate/steam exploded straw fiber composites. I. Thermal and impact behavior. *Journal of Applied Polymer Science*. 1993, vol. 49, no. 12, s. 2091-2103. ISSN 1097-4628.

119. DIMZOVSKI, B., et al. *Journal of Polymer Engeneering*. 2008, vol. 28, s. 369-384.

120. ZHENG, D. et al. Thermal Properties of Flax Fiber Scoured by Different Methods. *THERMAL SCIENCE*. 2015, vol. 19, no. 3, s. 939-945.

121. JACOBSEN, S. and H. G. FRITZ. Plasticizing effect of different plasticizers on the mechanical properties of polylactide. *Polymer Engineering & Science*. 1999, vol. 39, no. 7, s. 1303-1310. ISSN 1548-2634.

122. MEKONNEN, Tizazu et al. Progress in bio-based plastics and plasticizing modifications. *Journal of Materials Chemistry A*. 2013, vol. 1, no. 43, s. 13379-13398. ISSN 2050-7488.

123. MARTIN, O. and L. AVÉROUS. Poly(lactic acid): plasticization and properties of biodegradable multiphase systems. *Polymer*. 2001, vol. 42, no. 14, s. 6209-6219. ISSN 0032-3861.

124. MAGLIO, Giovanni et al. Immiscible Poly(L-lactide)/Poly(ε-caprolactone) Blends: Influence of the Addition of a Poly(L-lactide)-Poly(oxyethylene) Block Copolymer on Thermal Behavior and Morphology. *Macromolecular Chemistry and Physics*. 2004, vol. 205, no. 7, s. 946-950. ISSN 1521-3935.

125. MAGLIO, Giovanni, Anna MIGLIOZZI and Rosario PALUMBO. Thermal properties of di- and triblock copolymers of poly(l-lactide) with poly(oxyethylene) or poly(ε-caprolactone). *Polymer*. 2003, vol. 44, no. 2, s. 369-375. ISSN 0032-3861.

126. MAGLIO, Giovanni et al. Compatibilized poly(ε-caprolactone)/poly(L-lactide) blends for biomedical uses. *Macromolecular Rapid Communications*. 1999, vol. 20, no. 4, s. 236-238. ISSN 1521-3927.

127. OGATA, Nobuo et al. Structure and physical properties of cellulose acetate/poly(L-lactide) blends. *Journal of Applied Polymer Science*. 2002, vol. 85, no. 6, s. 1219-1226. ISSN 1097-4628.

128. IQBAL, Nida et al. Rapid microwave assisted synthesis and characterization of nanosized silver-doped hydroxyapatite with antibacterial properties. *Materials Letters*. 2012, vol. 89, no. 0, s. 118-122. ISSN 0167-577X.

129. BAZANT, Pavel et al. Wood flour modified by hierarchical Ag/ZnO as potential filler for wood–plastic composites with enhanced surface antibacterial performance. *Industrial Crops and Products*. 2014, vol. 62, no. 0, s. 179-187. ISSN 0926-6690.

130. BREITWIESER, Doris et al. In situ preparation of silver nanocomposites on cellulosic fibers – Microwave vs. conventional heating. *Carbohydrate Polymers*. 2013, vol. 94, no. 1, s. 677-686. ISSN 0144-8617.

131. ZHAO, Xihui et al. Microwave-assisted synthesis of silver nanoparticles using sodium alginate and their antibacterial activity. *Colloids and Surfaces A: Physicochemical and Engineering Aspects*. 2014, vol. 444, no. 0, s. 180-188. ISSN 0927-7757.

132. WANG, Ming et al. Effect of pentaerythritol and organic tin with calcium/zinc stearates on the stabilization of poly(vinyl chloride). *Polymer Degradation and Stability*. 2006, vol. 91, no. 9, s. 2101-2109. ISSN 0141-3910.

133. ROSA, D. S. et al. Mechanical, thermal and morphological characterization of polypropylene/biodegradable polyester blends with additives. *Polymer Testing*. 2009, vol. 28, no. 8, s. 836-842. ISSN 0142-9418.

134. FARAH, Shady, Daniel G. ANDERSON and Robert LANGER. Physical and mechanical properties of PLA, and their functions in widespread applications — A comprehensive review. *Advanced Drug Delivery Reviews*. . ISSN 0169-409X.

135. AURAS, R. A. et al. *Poly(lactic acid): Synthesis, Structures, Properties, Processing, and Applications*.Wiley, 2011. ISBN 9781118088135.

136. TANT, M. R., K. A. MAURITZ and G. L. WILKES. *Ionomers: Synthesis, structure, properties and applications*. Springer Netherlands, 2012. ISBN 9789400914612.

137. SILVERAJAH, V. S. G. et al. *Mechanical, thermal and morphological properties of poly(lactic acid)/epoxidized palm olein blend*. 2012. ISBN 1420-3049.

138. YU, Hou-Yong et al. Fabrication of multifunctional cellulose nanocrystals/poly(lactic acid) nanocomposites with silver nanoparticles by spraying method. *Carbohydrate Polymers*. 2016, vol. 140, s. 209-219. ISSN 0144-8617..

139. SHANKAR, Shiv and Jong-Whan RHIM. Tocopherol-mediated synthesis of silver nanoparticles and preparation of antimicrobial PBAT/silver nanoparticles composite films. *LWT - Food Science and Technology*. 2016, vol. 72, s. 149-156. ISSN 0023-6438.

140. EGGER, Salome et al. Antimicrobial Properties of a Novel Silver-Silica Nanocomposite Material. *Applied and Environmental Microbiology*. 2009, vol. 75, no. 9, s. 2973-2976. ISSN 0099-2240; 1098-5336.

141. PLUTA, M., J. K. JESZKA and G. BOITEUX. Polylactide/montmorillonite nanocomposites: Structure, dielectric, viscoelastic and thermal properties. *European Polymer Journal*. 2007, vol. 43, no. 7, s. 2819-2835. ISSN 0014-3057.

142. SCHLOSSER, E. and A. SCHANHALS. Recent development in dielectric relaxation spectroscopy of polymers. *Colloid and Polymer Science*. 1989, vol. 267, no. 11, s. 963-969. ISSN 1435-1536.

143. REN, Jindong and Keiichiro ADACHI. Dielectric Relaxation in Blends of Amorphous Poly(dl-lactic acid) and Semicrystalline Poly(l-lactic acid). *Macromolecules*. 2003, vol. 36, no. 14, s. 5180-5186. ISSN 0024-9297.

144. SANTANGELO, P. G. and C. M. ROLAND. Molecular Weight Dependence of Fragility in Polystyrene. *Macromolecules*. 1998, vol. 31, no. 14, s. 4581-4585. ISSN 0024-9297.

CURRICULUM VITAE

Name:	**Gabriela Jandíková**
Date of birth:	19th September 1987
Address:	Luční 1155
	75701 Valašské Meziříčí
Nationality:	Czech
Contact:	jandikova@ft.utb.cz
Education:	2012 – to date

Doctoral degree studies
Tomas Bata University in Zlin. Faculty of technology
Chemistry and material technology

2010 – 2012
Master´s degree
Tomas Bata University in Zlin. Faculty of technology
Chemistry and material technology
Polymer engineering

2007 – 2010
Bachelor´s degree
Tomas Bata University in Zlin. Faculty of technology
Chemistry and material technology

Training
abroad:

1.9. – 30.11. 2013
Chalmers University of Technology. Materials and
Manufacturing Technology department. Gothenburg.
Sweden

Work on
projects:

2016
GJ15-08287Y Immobilization of specific bioactive natural
substances in functionalized biodegradable polymer
matrices (2015-2017)
Member of research team

2014 – 2016
TE02000006 Centre for alternative environment friendly

high effective polymer antimicrobial agents for industrial applications (2014-2019)
Member of research team

2012 – 2015
LE12002 The support centre for international cooperation in research and development in technical fields (2012-2015)

IGA/CPS/2016/004 Preparation and characterization of bioactive polymeric systems (2016)
Member of research team

IGA/CPS/2015/003 Development of advance biodegradable and antimicrobial polymer systems (2015)
Member of research team

IGA/FT/2014/012 Research of antimicrobial biodegradable polymer systems (2014)
Member of research team

IGA/FT/2013/004 Preparation and characterization of novel biologically active polymeric systems based on natural substances (2013)
Principal investigator

LIST OF PUBLICATIONS

Journal articles:
1. JANDIKOVA. G., KUCHARCZYK. P., MISKOLCZI. N., PAVELKOVA. A., GREGOROVA. A., SEDLARIK. V. Natural fibre reinforced polyester urethane copolymer: Effect of interfacial adhesion modification on physico-chemical properties. Journal of Polymer Engineering. 2016. vol. 36. 2. pp. 189-197. DOI: 10.1515/polyeng-2015-0077.

2. JANDIKOVA. G., HOLCAPKOVA. P., HRABALIKOVA. M., MACHOVSKY. M., SEDLARIK. V. Antimicrobial Modification of Polypropylene with Silver Nanoparticles Immobilized on Zinc Stearate. Accepted Manuscript (December 2015). Materials and Technology

3. STLOUKAL. P., JANDIKOVA. G., KOUTNY. M., SEDLARIK. V. Carbodiimide additive to control hydrolytic stability and biodegradability of PLA. Polymer Testing. 2016. In press. Available online. DOI:10.1016/j.polymertesting.2016.06.007

Conference proceedings:
1. JANDIKOVA. G., HOLCAPKOVA. P., HRABALIKOVA. M., MACHOVSKY. M., SEDLARIK. V. Antimicrobial Modification of Polypropylene with Silver Nanoparticles Immobilized on Zinc Stearate. 23rd International conference on materials and technology. Portorož. 2015. Slovenia

2. JANDIKOVA. G., MACHOVSKY. M., RIGDAHL. M., SEDLARIK. V. Biodegradable polylactide-based composites containing nanostructured. Plastko 2014. Zlín. Czech Republic

3. JANDIKOVA, G., KUCHARCZYK, P., HOLCAPKOVA, P., HRABALIKOVA, M., MACHOVSKY, M., SEDLARIK., V. Polymerní nanokompozit na bázi polypropylénu a nanočástic stříbra imobilizovaných na stearanu zinečnatém, Plastko 2016, Zlín, Czech Republic